TECHNISCHE UNIVERSITÄT WIEN
Vienna University of Technology

Vienna Doctoral Programme on
Water Resource Systems
www.waterresources.at

Doctoral Thesis

Spatial patterns of evaporation in a small catchment

submitted in satisfaction of the requirements for the degree of

Doctor of Science

of the Vienna University of Technology, Faculty of Civil Engineering

as part of the

Vienna Doctoral Programme on Water Resource Systems

by

Patrick Hogan, MSc.

Student registration number: 01228534

Brantropstraße 78, Bochum, Germany

Under the supervision of:

Univ. Prof. Dr. Günter Blöschl

Institute of Hydraulic Engineering and Water Resources Management, Department of Civil Engineering, Vienna University of Technology

Die approbierte gedruckte Originalversion dieser Dissertation ist an der TU Wien Bibliothek verfügbar.
The approved original version of this doctoral thesis is available in print at TU Wien Bibliothek.

TU Bibliothek Your knowledge hub WIEN

Die approbierte gedruckte Originalversion dieser Dissertation ist an der TU Wien Bibliothek verfügbar.
The approved original version of this doctoral thesis is available in print at TU Wien Bibliothek.

Dissertation

Räumliche Verdunstungsmuster in einem kleinen Einzugsgebiet

ausgeführt zum Zwecke der Erlangung des akademischen Grades eines Doktors der technischen Wissenschaft

eingereicht an der Technischen Universität Wien Fakultät für Bauingenieurwesen von

Patrick Hogan, MSc.

Matrikelnummer: 01228534

Brantropstraße 78, Bochum, Germany

unter der Leitung von:

Univ. Prof. Dr. Günter Blöschl

Institut für Wasserbau und Ingenieurhydrologie, Fakultät für Bauingenieurwesen, Technische Universität Wien

Examiners

Univ. Prof. Dr. Günter Blöschl
Institute of Hydraulic Engineering and Water Resources Management, Department of Civil Engineering, Vienna University of Technology
Karlsplatz 13/222/2, 1040 Vienna, Austria

Prof. Dr. Zoltán Gribovszki
Institute of Geomatics and Civil Engineering, Faculty of Forestry, University of Sopron
Bajcsy-Zsilinszky u. 4, Sopron, 9400, Hungary

Univ. Prof. Dr. Wolfgang Schöner
Institute of Geography and Regional Science, University of Graz
Heinrichstraße 36, 8010 Graz, Austria

Die approbierte gedruckte Originalversion dieser Dissertation ist an der TU Wien Bibliothek verfügbar.
The approved original version of this doctoral thesis is available in print at TU Wien Bibliothek.

Gutachter

Univ. Prof. Dr. Günter Blöschl
Institut für Wasserbau und Ingenieurhydrologie, Fakultät für Bauingenieurwesen, Technische Universität Wien
Karlsplatz 13/222/2, 1040 Wien, Österreich

Prof. Dr. Zoltán Gribovszki
Institut für Geomatik und Bauingenieurwesen, Fakultät für Forstwirtschaft, Universität Sopron
University of Sopron
Bajcsy-Zsilinszky u. 4, Sopron, 9400, Ungarn

Univ. Prof. Dr. Wolfgang Schöner
Institut für Geographie und Raumforschung, Universität Graz
Heinrichstraße 36, 8010 Graz, Austria

Die approbierte gedruckte Originalversion dieser Dissertation ist an der TU Wien Bibliothek verfügbar.
The approved original version of this doctoral thesis is available in print at TU Wien Bibliothek.

Abstract

Accurate knowledge of evaporation and its components is of great importance for reliable predictions of land-atmosphere interactions, for assessing the impact of human activities on climate change, as well as for water and land management. The objective of this thesis is to investigate the spatial patterns of evaporation in a small agricultural catchment, focusing on how these patterns are formed and what their environmental drivers are, how they change in time, and if we can further our understanding of these patterns by partitioning the evaporation into components, transpiration and soil evaporation.

This thesis is organised into 5 chapters, with Chapter 1 providing an introduction and outlining the objectives and research questions of the thesis. The aim of Chapter 2 is to partition evaporation in a growing maize field to test if the stable isotope method can be used in these conditions and to study how the evaporation partitioning ratio changes on a daily time scale. This experiment was the first study to focus on using the stable isotope method for the more complex canopy structure of maize during the growth stage between seedling and adult, where the canopy closes as the plant grows. Using sap flow sensors installed concurrently in the field as a control, the method is shown to also be appropriate for maize. During the experiment the amount of soil evaporation and transpiration is dependent on the availability of soil water in the upper layer of the soil, with a general pattern of a large decrease in the ratio of transpiration to soil evaporation following a precipitation event, followed by an increase, due to the drying out of the upper layer of the soil. The diurnal patterns of both evaporation and transpiration are much better correlated with solar radiation than with vapor pressure deficit.

Chapter 3 went further into evaporation partitioning comparing the different methods of Lagrangian dispersion analysis and stable isotopes. While most isotope partitioning methods require some sampling of the soil or plants, and are therefore less reliable in heterogenous conditions, the Lagrangian dispersion analysis method offers the possibility of partitioning evaporation using just sampling of the water vapour within the canopy. The study shows that the two methods give similar results, however, the stable isotope method returns a much larger amount of useable data, as well as having a lower within-day variance. This is offset by the need for more additional measurements and analysis, as well the uncertainty due to the need for the Isotopic Steady State assumption.

Chapter 4 investigates the spatial patterns of evaporation in the Hydrological Open Air Laboratory (HOAL) using spatially distributed eddy covariance stations and subcatchment water balances. Previous research has tended to be of a short duration, this study however was conducted over eight years. The results show that the daily and seasonal patterns of evaporation in the agricultural area of the catchment are strongly linked to the crop cycle while at the yearly timescale, the patterns tend to be averaged out. When the riparian zone is included however the influence of permanent vegetation results in yearly patterns between the hydrological subcatchments. Year to year variability in monthly evaporation measured by the eddy covariance stations is driven primarily by net radiation and air temperature. The different catchment evaporation estimation methods are consistent during years with above average precipitation, only when water storage and leakage are included.

In Chapter 5 a summary of the individual chapters as well the entire thesis is provided, along with a discussion of the wider implications of this research for evaporation measurements and modelling. This thesis has advanced our knowledge of evaporation and its role in the water cycle, its spatial patterns, and its components in small agricultural catchments. The work has provided one of the first long term analyses of spatial evaporation at this scale, showing the importance of detailed landuse information when agricultural catchments are to be studied or modelled. The results also show the importance of, and provide a method for, testing the water balance method for non-closure, by measuring and upscaling the evaporation using the eddy covariance method and vegetation. Two different methods of evaporation partitioning have been evaluated, providing direct insight into how the transpiration ratio changes in response to the environmental conditions and how detailed knowledge of the crop growing

Die approbierte gedruckte Originalversion dieser Dissertation ist an der TU Wien Bibliothek verfügbar.
The approved original version of this doctoral thesis is available in print at TU Wien Bibliothek.
TU Bibliothek Your knowledge hub WIEN

stage, soil moisture and precipitation intensities are needed when estimating the transpiration through modelling in order to correctly capture its dynamics.

Die approbierte gedruckte Originalversion dieser Dissertation ist an der TU Wien Bibliothek verfügbar.
The approved original version of this doctoral thesis is available in print at TU Wien Bibliothek.

Kurzfassung

Eine genaue Kenntnis der Verdunstung und ihrer Komponenten ist von großer Bedeutung für zuverlässige Vorhersagen der Land-Atmosphäre Interaktionen, für die Bewertung des Einflusses menschlicher Tätigkeiten auf den Klimawandel, sowie für Wasserwirtschaft und Landmanagement. Ziel dieser Arbeit war es, die räumlichen Muster der Verdunstung in einem kleinen landwirtschaftlich genutzten Einzugsgebiet zu untersuchen. Der Fokus lag darauf, wie diese Muster entstehen, welche Umweltfaktoren für sie relevant sind, wie sie sich mit der Zeit verändern und ob eine Unterscheidung von pflanzlicher Transpiration und Bodenverdunstung zum Verständnis der Muster beiträgt.

Diese Arbeit ist in fünf Kapitel gegliedert. Kapitel 1 führt in die Ziele und Forschungsfragen der Arbeit ein. In Kapitel 2 wird die Verdunstung in einem Maisfeld in der Wachstumsphase mittels stabiler Isotopen in ihre Komponenten aufgeteilt, um die Anwendbarkeit stabiler Isotope für diese Situation zu testen, und die Veränderung des Verhältnisses der Verdunstungskomponenten im Verlauf eines Tages besser zu verstehen. Es handelt sich dabei um das erste derartige Experiment, das Isotope verwendet für eine komplexen Kronenstruktur von Mais während der Wachstumsphase zwischen Keimling und adulter Pflanze verwendet, bei der sich die Krone vollständig schließt. Durch den zeitgleich als Kontrolle gemessenen Saftstrom, konnte gezeigt werden, dass sich die Isotopenmethode auch für Mais eignet. Während des Experiments hingen die Transpiration und die Bodenverdunstung von der Verfügbarkeit des Bodenwassers in der obersten Bodenschicht ab. Nach einem Niederschlagsereignis verringerte sich ihr Verhältnis stark, gefolgt von einem Anstieg während des Austrocknens der obersten Bodenschicht. Der tägliche Verlauf von Verdunstung und Transpiration ist insgesamt deutlich besser mit der Sonneneinstrahlung korreliert als mit dem Wasserdampfdruckdefizit.

Kapitel 3 geht weiter auf die Verdunstungskomponenten ein und vergleicht verschiedene Methoden der Lagrangeschen Dispersionsanalyse und stabiler Isotopen. Während die meisten Isotopenmethoden zur Verdunstungsaufteilung eine Beprobung des Bodens oder der Pflanzen erfordern, und daher unter heterogenen Bedingungen weniger zuverlässig sind, erlaubt die Lagrangesche Dispersionsanalyse eine Aufteilung der Verdunstung alleine auf Basis von Proben des Wasserdampfes in der Krone. Die vorliegende Untersuchung zeigt, dass mit beiden Methoden ähnliche Ergebnisse erzielen, doch liefert die Methode der stabilen Isotope eine größere Menge nutzbarer Daten, und die Varianzen sind geringer. Diesen Vorteilen stehen jedoch die Notwendigkeit zusätzlicher Messungen und Analysen, sowie die sich aus der erforderlichen Stationaritätsannahme ergebenden Unsicherheiten gegenüber.

Kapitel 4 untersucht die räumlichen Verdunstungsmuster im Hydrological Open Air Laboratory (HOAL; Hydrologisches Freiluftlabor) in Niederösterreich unter Verwendung räumlich verteilter Eddy Covarianz Stationen und Messungen zur Berechnung der Wasserbilanz von Teileinzugsgebieten. Vorhergehende Forschungsarbeiten waren zumeist auf kurze Zeiträume begrenzt, während diese Arbeit die Ergebnisse aus einer achtjährigen Forschungstätigkeit enthält. Die Ergebnisse zeigen, dass die täglichen und saisonalen Verdunstungsmuster im landwirtschaftlich bewirtschafteten Teil des Einzugsgebiets stark an die Fruchtfolge gekoppelt sind, während sich ihr Einfluss über das Jahr gesehen herausmittelt. Wenn die Gewässerrandstreifen in die Betrachtung einbezogen werden, dann führt deren dauerhafte Vegetation zu jährlichen Mustern der Teileinzugsgebiete. Die jährlichen Schwankungen der mittels der Eddy Covarianz Stationen gemessenen monatlichen Verdunstung werden hauptsächlich von der Nettostrahlung und der Lufttemperatur beeinflusst. Die unterschiedlichen Verfahren zur Bestimmung der Verdunstung des gesamten Einzugsgebiets sind in Jahren mit überdurchschnittlichen Niederschlägen nur dann konsistent, wenn Wasserspeicherung und Wasserverlust in den regionalen Aquifer berücksichtigt werden.

Diese Arbeit erweitert unsere Kenntnisse über die Verdunstung und deren Rolle im Wasserkreislauf in kleinen landwirtschaftlich genutzten Einzugsgebieten. Sie ist eine der ersten Langzeitanalysen der räumlichen Verdunstung auf dieser räumlichen Skala und zeigt die Bedeutung genauer Informationen

Die approbierte gedruckte Originalversion dieser Dissertation ist an der TU Wien Bibliothek verfügbar.
The approved original version of this doctoral thesis is available in print at TU Wien Bibliothek.
TU Bibliothek Your knowledge hub WIEN

über die Landnutzung für die Untersuchung und Modellierung vornehmlich landwirtschaftlich genutzter Einzugsgebiete.

Die Ergebnisse zeigen wie wichtig es ist, die Wasserbilanz-Methode zu überprüfen in Hinblick darauf ob die Bilanz geschlossen werden kann. Für die Überprüfung wird eine Methode vorgestellt, bei der die mit Eddy Covarianz gemessene Verdunstung mittels Vegetationdaten auf die Gebietsebene skaliert wird. Zwei Methoden der Verdunstungsaufteilung wurden evaluiert, die einen direkten Einblick geben, wie sich das Transpirationsverhältnis als Reaktion auf die Umweltbedingungen ändert und wie eine detaillierte Kenntnisse des Pflanzenwachstumsstadiums, der Bodenfeuchte und der Niederschlagsintensität verwendet werden kann, um die Transpiration zu modellieren und ihre Dynamik richtig zu erfassen.

Die approbierte gedruckte Originalversion dieser Dissertation ist an der TU Wien Bibliothek verfügbar.
The approved original version of this doctoral thesis is available in print at TU Wien Bibliothek.

Funding information, published articles and author's contributions
This work has been conducted as part of the following research project:
Vienna Doctoral Programme on Water Resource Systems (DK W1219-N28) of the Austrian Science Funds (FWF).

The results of this doctoral thesis have been published in (or submitted to) peer reviewed scientific journals in the form of the following three articles:

Hogan, P., Parajka, J., Oismüller, M., Heng, L., Strauss, P., & Blöschl, G. (2020). High-Frequency Stable-Isotope Measurements of Evapotranspiration Partitioning in a Maize Field. *Water*, 12(11), 3048.

Hogan, P., Parajka, J., Heng, L., Strauss, P., & Blöschl, G. (2020). Partitioning evapotranspiration using stable isotopes and Lagrangian dispersion analysis in a small agricultural catchment. *Journal of Hydrology and Hydromechanics*, 68, 134-143.

Hogan, P., Szeles, B., Rab, G., Oismueller, M., Pavlin, L., Parajka, J., Strauss, P., & Blöschl, G. (2022). *Hydrological Sciences Journal*. Under review.

Author's contributions:
In all three papers formal analysis, investigation, visualisation and writing - original draft preparation were undertaken by the author of the present thesis.
Conceptualisation, methodology, data curation and writing - review and editing were performed in cooperation with the respective co-authors.

Die approbierte gedruckte Originalversion dieser Dissertation ist an der TU Wien Bibliothek verfügbar.
The approved original version of this doctoral thesis is available in print at TU Wien Bibliothek.
TU Bibliothek Your knowledge hub WIEN

Acknowledgements
I would very much like to thank Professor Günter Blöschl for giving me the opportunity to work on this topic and for his guidance and support throughout the years of my study, as well as for supervising this thesis. I would also like to thank Professor Juraj Parajka for his advice and suggestions, which helped me to improve my research.

I would like to express my gratitude to Professor Gribovszki and Professor Schöner for taking the time to review this thesis.

I wish to thank all my friends and colleagues who helped me, particularly those from the Institute of Hydraulic Engineering and Water Resources Management, particularly Bori and Markus, from the Doctoral Programme on Water Resource System, and the IKT at Petzenkirchen.

Finally, I would like to thank my mother Mary and my partner Elisabeth, for all your support throughout the years.

Die approbierte gedruckte Originalversion dieser Dissertation ist an der TU Wien Bibliothek verfügbar.
The approved original version of this doctoral thesis is available in print at TU Wien Bibliothek.

Contents

Examiners 3
Gutachter 4
Abstract 5
Kurzfassung 7
Funding Information 9
Acknowledgements 10
Contents 11
1. Introduction 13
2. High frequency stable isotope measurements of evapotranspiration partitioning in a maize field 16
2.1 General 16
2.2 Key points 16
2.3 Abstract 16
2.4 Introduction 17
2.5 Materials and Methods 18
2.6 Results 21
2.7 Discussion 26
2.8 Conclusions 28
3. Partitioning evapotranspiration using stable isotopes and Lagrangian dispersion analysis in a small agricultural catchment 29
3.1 General 29
3.2 Key points 29
3.3 Abstract 29
3.4 Introduction 30
3.5 Theory and methods 31
3.6 Results 35
3.7 Discussion 38
3.8 Conclusions 39
4. Spatial patterns of evaporation in a small catchment 40
4.1 General 40
4.2 Key Points 40
4.3 Abstract 40
4.4 Introduction 42
4.5 Materials and Methods 43
4.6 Results 49
4.7 Discussion 61
4.8 Conclusions 62

Die approbierte gedruckte Originalversion dieser Dissertation ist an der TU Wien Bibliothek verfügbar.
The approved original version of this doctoral thesis is available in print at TU Wien Bibliothek.

5. Summary and conclusions..... 63
6. References..... 66

Die approbierte gedruckte Originalversion dieser Dissertation ist an der TU Wien Bibliothek verfügbar.
The approved original version of this doctoral thesis is available in print at TU Wien Bibliothek.

1. Introduction

Evaporation is an important part of both the terrestrial water cycle and the surface energy balance, accounting for over 60% of precipitation that falls on the land surface (Shiklomanov, 1998). It links the earth's surface and atmosphere as the process by which water moves from a liquid to a gaseous state. Terrestrial evaporation is composed of water from a number of different sources, with evaporation from plant stomata (transpiration) being the largest with smaller contributions from water evaporated from the soil, open water surfaces and plant surfaces (interception). Accurate knowledge of evaporation and its components is important for improving our knowledge of water-atmosphere interactions and water and landuse management, as well as the effects of human activities and climate change on them (Allen et al., 1998; Haddeland et al., 2014; Dai, 2013; Dai et al., 2018).

Measurement of evaporation remains a challenge, due to the turbulent nature of the water vapour flux, particularly over heterogeneous surfaces. Estimating the spatial distributions of evaporation with different model approaches is also a complex process with large amounts of information needed to account for the factors that influence the rate of evaporation e.g., net solar radiation, precipitation, vegetation and soil texture. Land-atmosphere feedbacks can also affect evaporation estimates at every scale, requiring coupled models that add another layer of complexity (Overgaard et al., 2005).

As part of a community initiative to identify the major unsolved problems in hydrology, Blöschl et al. (2019) identified two major questions relating to the fundamental hydrological process of evaporation: (1) what are the impacts of land cover change on water and energy fluxes at the land surface and (2) what causes spatial heterogeneity and homogeneity in evaporation, and in its sensitivity to its controls. In addressing these questions it is important to consider whether the processes that dominate the hydrological response of the quantity of interest change as we change scale, and then how to identify and represent the dominant processes at different scales (Grayson and Blöschl, 2000).

At the global and regional scales much work has been done to measure and model evaporation, using remotely sensed data (Kustas and Norman, 1996; Mu et al., 2011; Ruhoff et al., 2013; Tasumi et al., 2005; Vinokullu et al., 2011) or a combination of point measurements, catchment water balances, climate reanalysis and spatial maps of landuse and soil properties (Brutsaert et al., 2020; Walker and Venturini, 2019). At this scale global radiation, topography, and aridity play important roles in shaping the spatial patterns of evaporation. At the small catchment scale, i.e., greater than the field scale but smaller than the meso-scale where convective precipitation plays a major role in the formation of hydrological patterns, more work is needed to identify the spatial patterns of evaporation and how they change in time. While certain meteorological quantities can be treated as constant at this scale, e.g., global radiation, over non-uniform surfaces the variations and resulting interactions between the vegetation, soil, topography as well as the temperature and humidity need to be taken into account and nonlinear processes may become important (Grayson and Blöschl, 2000). Most research so far has tended to focus on using measurements from a measurement station combined with remote sensing products such as the SMACEX and BEAREX08 experiments (Kustas et al. 2005; Anderson et al., 2012), or upscaling multi-site measurements with relatively large footprints, typically from eddy covariance or scintillometer systems, such as in Liu et al. (2016). Satellite based monitoring tends to be limited by the frequency of the overpass as well as the pixel size and cloud cover with Castelli et al. (2018) reporting large model-measurement differences between coarse satellite imagery based evaporation estimates and eddy covariance measurements for an alpine grassland. Multi-site measurement campaigns are usually of a limited duration (< 1 year) due to the high level of instrumentation required. Long term studies of the spatial differences in evaporation at the small catchment scale are however lacking. The water balance method of estimating evaporation, provides relatively simple and effective estimates if accurate discharge gauging and precipitation measurements are made, with many catchments having long time series of data. At the small catchment scale, Seneviratne et al., (2012) and Hirschi et al., (2017) found that for a 3.3 km^2 alpine catchment with homogenous landuse there was a good agreement between lysimeter and eddy covariance evaporation

Die approbierte gedruckte Originalversion dieser Dissertation ist an der TU Wien Bibliothek verfügbar.
The approved original version of this doctoral thesis is available in print at TU Wien Bibliothek.
TU Bibliothek Your knowledge hub WIEN

measurements made at a single location and the catchment averaged water balance estimate, at the annual time scale. Here the water balance was evaluated over the entire catchment area by measuring at the catchment outlet; in a similar sized catchment with heterogeneous landuse and different runoff regimes, by gauging all the individual subcatchments spatial information on the variability of evaporation could be provided. The temporal resolution of the method however is often limited to the annual timescale, to neglect storage changes in the catchment which can bias the evaporation estimate.

As transpiration is related to biomass production while evaporation from the soil and interception are not, accurately partitioning the total evaporation measured using an above-canopy method such as eddy covariance provides valuable information which can be used to increase 'water productivity' (the crop yield per volume of water used) by reducing the unproductive components. In water limited regions of the world rainfed crop production is not possible and additional water must be provided through irrigation placing stress on water supplies available for other human needs (Guerra et al., 1998), therefore reducing unproductive soil evaporation is of great importance. While efforts to separately measure soil evaporation and transpiration began in the 1970s and 1980s with the development of micro-lysimeters (Ritchie, 1972; Walker 1983) and sap flow sensors (Čermák et al., 1973; Granier 1985). In homogenous conditions modern weighing lysimeters can provide highly accurate estimates of evaporation, and also allow for testing the response of vegetation to climate change induced temperature and CO_2 increases (Forstner et al., 2020) or determining of the contribution of dew to the water budget (Groh et al., 2020). These methods require considerable care in their application in non-homogenous conditions, as due to their small footprint upscaling of the individual measurements is always required. In recent years methods based around measurements of canopy water vapour have been developed, allowing for a larger and more representative measurement footprint. Measurements of the isotopic composition of water vapour from within and above the canopy, coupled with samples of plant and soil water allow for the partitioning of total evaporation measured above the canopy, although here the soil and plant sampling still limits the spatial representativity of the method (Williams et al., 2004; Yepez et al., 2003; Rothfuss et al., 2010). The Lagrangian dispersion analysis method uses an inverse modelling approach, where the source/sink distribution of a scalar is related to a concentration profile of the scalar within a canopy ecosystem through a turbulent dispersion field (Raupach 1989a; Warland and Thurtell, 2000; Haverd et al., 2011). In addition to the concentration measurements, this method only requires basic meteorological data to parameterise the canopy turbulence profile, greatly simplifying the instrumentation and sampling requirements. Several questions and challenges relating to the application of these methods need to be addressed however, before they can be reliably applied for making long term measurements. As different crops have different planting and growing patterns, these methods must be controlled for the differing canopy structures of these crops, particularly for crops with denser canopies which can affect the turbulent exchange of the air.

In order to identify the factors that dominate the spatial patterns of evaporation at the appropriate spatial and temporal scales for a small catchment, an appropriate research catchment or observatory is required. The Hydrological Open Air Laboratory (HOAL) (Blöschl et al., 2016) located in Petzenkirchen, Lower Austria provides an aptly sized catchment (66 ha), with a densely equipped, hydrological monitoring network. Here, state of the art measurement techniques are combined with traditional observational methods to make long-term observations of evaporation, soil moisture, the meteorological conditions as well as all the components of the water cycle. To assess as much of the catchment as possible, evaporation is measured using three eddy covariance stations located in different fields throughout the catchment. The eddy covariance method (EC) is generally regarded as one of the most accurate ways to measure evaporation (Aubinet 2012; Rana and Katerji, 2000; Baldocchi, 2003). Evaporation is also estimated for the entire catchment and six subcatchments using the water balance, by measuring the precipitation and discharge. The catchment also offers the possibility of conducting short term experiments at a finer spatial or temporal resolution. By running field campaigns during the agricultural

Die approbierte gedruckte Originalversion dieser Dissertation ist an der TU Wien Bibliothek verfügbar.
The approved original version of this doctoral thesis is available in print at TU Wien Bibliothek.
TU Bibliothek Your knowledge hub WIEN

growing season evaporation partitioning methods can be tested, allowing us to improve our insight understanding of the ratio of transpiration to evaporation and its controls.

The objective of this thesis is to investigate the spatial patterns of evaporation in a small agricultural catchment, focusing on how these patterns are formed and what their environmental controls are, how they change in time, and if we can further understand these patterns and controls by partitioning the evaporation into transpiration and soil evaporation. The following chapters (2-4) contain the research section of this thesis. Chapter 2 tests if the stable isotope method can be used to partition evaporation in a maize field and how the ratio of evaporation to transpiration changes in response to the environmental conditions on a daily time scale. Chapter 3 further explores evaporation partitioning, comparing two different methods: Lagrangian dispersion analysis and stable isotopes, and using the results to investigate how evaporation partitioning changes in response to precipitation events. Chapter 4 investigates what the spatial patterns of evaporation are in the Hydrological Open Air Laboratory (HOAL) using a combination of spatially distributed eddy covariance evaporation measurements and subcatchment water balances. Chapter 5 provides a summary and conclusion of the key findings of this research, with a view to potential future research on this topic. As a general note, the use of the terms *evapotranspiration* and *evaporation* is a topic of discussion within the hydrological community (Miralles et al., 2020). As the focus of the research in Chapters 2 and 3 is on partitioning the total amount of vaporised water between water vaporised from the soil and from plants, the term evapotranspiration is used to avoid confusion between total evaporation and soil evaporation. As Chapter 4 is focused on the total amounts of water vaporised per field and for the entire catchment regardless of source, the term evaporation is used.

Die approbierte gedruckte Originalversion dieser Dissertation ist an der TU Wien Bibliothek verfügbar.
The approved original version of this doctoral thesis is available in print at TU Wien Bibliothek.

2. High frequency stable isotope measurements of evapotranspiration partitioning in a maize field

2.1 General

This chapter discusses a short-term experiment (9 days) using high frequency measurements of the isotopic composition of the atmospheric water vapor inside a growing maize canopy. The aim of the experiment was to test if the stable isotope method can be used in these changing conditions and to study the variation of soil evaporation and transpiration in response to precipitation events.

The present chapter is based on the following scientific publication:

Hogan, P., Parajka, J., Oismüller, M., Heng, L., Strauss, P., & Blöschl, G. (2020). High-Frequency Stable-Isotope Measurements of Evapotranspiration Partitioning in a Maize Field. *Water*, 12(11), 3048.

In the original publication the term *evapotranspiration* was used instead of *evaporation*, as the emphasis of this research was on partitioning.

2.2 Key points

Stable isotopes of oxygen-18 (^{18}O) can be used to partition ET during the growing stage of maize. Results from the Keeling plots on soil evaporation and transpiration partitioning compare well with sap flow measurements.

During the experiment the amount of soil evaporation and transpiration was dependent on the availability of soil water in the upper layer of the soil, with a general pattern of a large decrease following a precipitation event followed by a period of increasing.

Soil evaporation and transpiration were much better correlated with solar radiation than with vapor pressure deficit.

2.3 Abstract

Knowledge of the soil evaporation (*E*) and transpiration (*T*) components of evapotranspiration (*ET*) is important for ecohydrological modelling and agricultural productivity. The stable isotope method offers the possibility to partition *E* and *T* due to the distinct differences in the isotopic signals of the sources. In this study the concentration and isotopic ratios of oxygen-18 (^{18}O) of water vapor in the ecosystem boundary layer of a growing maize field at the HOAL catchment in Austria were measured using a high frequency field sampling device and in conjunction with isotope samples from the soil and maize plants, these data were used to partition *ET* using the Keeling plot technique. Eddy covariance and sap flow measurements were used to provide a comparison to test the stable isotope method. The fraction of transpiration (*Ft*) calculated with the stable isotope method showed good agreement with the sap flow method. Overall daily average values of Ft were in a range from 43.0 to 88.5% with transpiration accounting for an average value of 67.5% of the evapotranspiration over the 9 days of the experimental period. Following a precipitation event of 9.7mm *Ft* increased from 63.4 to 88.5% over the next 4 days as the upper layer of the soil dried out while the plants accessed deeper soil water.

Die approbierte gedruckte Originalversion dieser Dissertation ist an der TU Wien Bibliothek verfügbar.
The approved original version of this doctoral thesis is available in print at TU Wien Bibliothek.

2.4 Introduction

Evapotranspiration (*ET*) is one of the most important processes in describing land surface - atmosphere interactions as it connects the energy and water balances (Bastiaanssen et al., 1998) Furthermore, knowledge of the individual components of evapotranspiration is important for ecohydrological modelling and agriculture, particularly for irrigation efficiency and crop productivity. In arid and semiarid regions agricultural productivity is directly linked to water availability, resulting in a competition for water resources in regions where there is also a high human population density, (Zhang et al., 2011). To reduce the stress placed on the water supply it is of great importance to achieve a high level of irrigation efficiency, this ensures that water supplied to the crops has less loses via evaporation from the soil.

Common methods for making measurements of transpiration (*T*) and soil evaporation (*E*) such as sap flow sensors (Kelliher et al., 1992; Klimešová et al., 2014; Zhou et al., 2017) and lysimeters (Liu et al., 2002; Kang et al., 2003) are limited to individual plants or small footprints, which can lead to difficulties in upscaling in heterogeneous environments (Ehleringer and Field, 1993). Methods which make an integrated measurement with a much larger footprint at the field scale such as eddy covariance, Bowen ratio or scintillometry are only able to measure the total *ET* and provide only implicit information on *E* and *T*. These methods are also generally unsuitable for use inside plant canopies as they need to be a minimum height above the surface (Moore, 1986) and require minimum levels of turbulent intensity which is strongly reduced within a closed canopy. Hence a second method must be used in conjunction with the field scale measurement to partition the *ET*. Different types of methods have been developed such as Lagrangian dispersion analysis (Raupach, 1989), flux variance similarity partitioning (Good et al., 2014), and stable isotope partitioning (Yepez et al., 2003; Williams et al., 2004; Wang et al., 2013; Sutanto et al., 2012).

Stable isotopes of oxygen from soil water and plant stomata allow for the possibility to partition the evapotranspiration measured at the field scale. Water vapor evaporated from a macropore in the soil will have a lower ratio of heavy to light isotopes than the water it evaporated from, as lighter isotopes evaporate faster. For a plant at isotopic steady state (ISS), it is assumed the water transpired from the stomata is equal to that of the source water taken up by the plant's roots, with no fractionation occurring during evaporation due to the small pore size of the stomata (Flanagan et al, 1991; Roden and Ehleringer, 1999; Yakir and Sternberg, 2000). This results in the water vapor transpired by the plant having a distinctly different isotopic signal to the water evaporated from the soil. This has allowed for the determination of the transpiration-evaporation ratio using the Keeling Plot approach based on a mass balance equation for the ecosystem (Yepez et al., 2003; Wiliams et al., 2004; Moreira et al., 1997). In recent years, non-steady state conditions have been reported in several studies, especially under short time scales (Yepez et al., 2005; Wang et al., 2013). However, most of these studies showed that the steady state conditions can still be met in the afternoon (Yepez et al., 2005; Lai et al., 2006; Zhang et al., 2010). As this current study is based on data collected in the late morning and afternoon, the steady state is being assumed.

Technological advances in recent years with the development of continuous, high frequency, in-situ measurement devices have allowed for further testing and application of stable isotope methods in a wider variety of conditions; grassland (Hu et al., 2014; Good et al., 2014; Wang et al., 2013), wheat (Zhang et al., 2011), fescue (Rothfuss et al., 2010), rice (Wei et al., 2015), soybean (Welp et al., 2015) and woodland (Dubbert et al., 2013). These studies showed the applicability of the stable isotope method, while highlighting the effects of ecosystem conditions on the measurement principle. Maize is a major crop in many regions of the world and correct determination of its (*T*/*ET*) ratio is of great importance in regions with low precipitation and/or high evapotranspiration rates in order to achieve a high crop water uptake. During its growing period, the characteristics of the maize ecosystem change from an open to a closed canopy as leaf area index (LAI) increases, however its physiology and row

Die approbierte gedruckte Originalversion dieser Dissertation ist an der TU Wien Bibliothek verfügbar.
The approved original version of this doctoral thesis is available in print at TU Wien Bibliothek.
TU Bibliothek Your knowledge hub WIEN

structure results in a different canopy architecture than other crops, with a high variability in surface soil moisture and evaporation (Hupet and Vanclooster, 2005).

The goals of this paper are (1) to test the stable isotope method for maize during its vegetative stage using sap flow measurements and (2) to investigate the changes in (*T*/*ET*) during the course of the experiment due to the environmental controls, and (3) to test if the isotope approach for estimating the transpiration fraction performs better than the sapflow method during the vegetative growing stage. In this experiment, we made high frequency measurements of the isotopic composition of the atmospheric water vapor inside a maize canopy to study the variation of (*E*) and (*T*) during the vegetative growing stage of the maize crop in response to precipitation events.

2.5 Materials and Methods

2.5.1 Stable Isotope Method

All isotope measurements in this work are expressed as the ratio of heavy to light isotopes relative to the international standard and written in (δ) notation in per mil (‰)

$$\boldsymbol{\delta = \frac{R_{sample} - R_{standard}}{R_{standard}} \times 1000} \tag{2.1}$$

where R_{sample} is the molar ratio of the sample and $R_{standard}$ is the Vienna Standard Mean Ocean Water (V-SMOW). The division of the bulk evapotranspiration as measured by the eddy covariance method is calculated by (Yakir and Sternberg, 2000)

$$\mathrm{Ft}(\%) = \frac{\delta_{ET} - \delta_E}{\delta_T - \delta_E} \tag{2.2}$$

where *Ft* (%) is the fraction of the evapotranspiration due to transpiration (T/ET x 100), δ_{ET} is the isotopic composition of the evapotranspiration water vapor, δ_E is the isotopic composition of the evaporated soil water and δ_T is the isotopic composition of the transpired water vapor. δ_E and δ_T can be estimated by sampling the soil and vegetation while δ_{ET} is determined using a Keeling mixing model approach (Keeling, 1958), which is based on a mass balance equation for the ecosystem

$$\boldsymbol{\delta_{EBL} = C_a\left((\delta_a - \delta_{ET})\left(\frac{1}{Cebl}\right) + \delta_{ET}\right)} \tag{2.3}$$

where δ_{ebl} is the isotopic composition of the ecosystem boundary layer water vapor, C_a the concentration of water vapor in the atmosphere, δ_a the isotopic composition of the atmospheric water vapor and C_{ebl} is the concentration of the water vapor in the ecosystem boundary layer. As this is a linear relationship, if we measure the isotope ratio and concentration of the air at different heights within the canopy and then plot the isotope ratio versus the inverse of the concentration, the resulting y-intercept is an estimate of δ_{ET} (Yakir and Sternberg, 2000; Yepez et al., 2003). T_{iso} (transpiration calculated using the stable isotope method) and E_{iso} (soil evaporation calculated using the stable isotope method) can then be calculated using *Ft* from Eq. (2.2) if the *ET* is also measured.

Due to the difficulty in directly measuring δ_E, the Craig-Gordon model (Craig and Gordon, 1965) can be used instead to estimate the effects of kinetic and equilibrium fractionations on liquid water samples from the soil as it evaporates (see section 2.5.3)

$$\boldsymbol{R_E = (1/\alpha_K)\frac{(R_s/\alpha^*) - R_a h}{1-h}} \tag{2.4}$$

where R_E is the molar ratio of heavy to light isotopes of the evaporated water, α_K is the kinetic fraction rate, taken to be 1.0189 ‰ (Flanagan et al., 1991), R_s is the ratio of liquid water sampled in the soil at

Die approbierte gedruckte Originalversion dieser Dissertation ist an der TU Wien Bibliothek verfügbar.
The approved original version of this doctoral thesis is available in print at TU Wien Bibliothek.
TU Bibliothek Your knowledge hub WIEN

the evaporating front, R_a is the ratio of atmospheric air from near the surface, h is the relative humidity normalised by the saturation pressure at the surface and α^* is the equilibrium fractionation factor calculated as a function of soil temperature Ts (K) (Majoube, 1971).

$$\alpha^* = \left(\frac{1.137 \times 10^6}{Ts^2} - \frac{0.4156 \times 10^3}{Ts} - 2.0667\right) \quad (2.5)$$

2.5.2 Experimental Site

The experiment was performed at the 66 ha Hydrological Open Air Laboratory (HOAL) research catchment located at Petzenkirchen, Austria (Blöschl et al., 2016). The site has a mean annual air temperature of 9.5 °C and receives on average 823 mm of precipitation per year. The evapotranspiration measured using an eddy covariance device over grassland at the center of the catchment from 2013 - 2016 for the month of June ranged from 64.9 – 72.5 mm, with an average of 69.1 mm. Average total net radiation at the weather station for the month of June was 192 kW/m^2. An eddy covariance (EC) system and a stable isotope analyser along with supporting meteorological sensors were installed within a 4.8 ha maize field from June 24th - July 2nd, 2014 (Figure 2.1). On account of the size of the maize field and the limited fetch, the devices were installed to take advantage of the westerly prevailing wind, giving a minimum fetch of 100 m except in the southeast quadrant. At the beginning of the experiment the maize was approximately at stage V7 in its development, progressing to V11/V12.This is a period of rapid growth for maize. The maize had an average height of 0.95 m at the beginning of the experiment and during the course of the experiment this increased to 1.40 m. The average leaf area index was approximately 1.8 based on canopy cover taken above the maize canopy, growing from 1.2 to 2.4 over the period of the experiment.

2.5.3 Isotope Measurements

This section describes how to determine values for δ_{ET}, δ_T and δ_E in order to calculate Ft using Eq (2.2). In order to obtain a value for δ_{ET} using Eq. (2.3), a profile of the concentration and stable isotope ratio of ^{18}O of the water vapor within and above the plant canopy was measured. δ_{ebl} and C_{ebl} were sampled at 4 heights within the canopy (0.1, 0.2, 0.5 and 1.0 m), and 2 additional sample intakes were located above the canopy (1.7 and 2.4 m). The ports at heights 0.5 and 1.0 m were later increased to 0.8 and 1.2 m on the 1st July due to the increase in canopy height. Air was sampled through the intakes consecutively using a pump connected to a 6-port valve and analysed at 1 Hz using a L2130-i analyser (Picarro) installed nearby. The sensor requires an averaging time of at least 100 seconds to achieve a precision of 0.02 ‰, which resulted in an average cycling period of 20 minutes between the 6 ports for this experiment, and a 20-minute resolution in estimates of δ_{ET}.

δ_T can be measured directly using a leaf chamber, however as one was not available for this experiment, δ_T was estimated from xylem water taken from 4 maize plants, sampled between 11-14 h on each day of the experiment. This limits the application of the stable isotope method to times when the ISS assumption is valid i.e., late morning - afternoon. As a large number of soil gas chambers are required to obtain a directly measure and obtain a spatially averaged value of δ_E, it was instead estimated using Eq (2.4). Soil samples were taken daily at 4 locations near the air intake, at depths of 0-2, 2-5 and 5-10 cm in order to correctly identify the evaporation front according to Rothfuss et al. (2010). All soil and plant samples were sealed in glass vials, frozen and then transported to the laboratory for extraction. The samples were first chilled using a commercial immersion cooler and Dewar container to prevent water losses and then heated to 100°C and distilled in batches of 15 samples using a heating block for two hours before being transferred to a collection vial using an evacuation pump and analysed with the L2130-i analyser. Standard deviations of the 20-minute values for δ_E and δ_{ET} were calculated from the range of measurements for each day, to check for the effects of changes in the water vapor composition.

Die approbierte gedruckte Originalversion dieser Dissertation ist an der TU Wien Bibliothek verfügbar.
The approved original version of this doctoral thesis is available in print at TU Wien Bibliothek.

2.5.4 Micro-meteorological Instrumentation

Evapotranspiration over the field was measured using an integrated open path eddy covariance sensor (IRGASON, Campbell Scientific). The device was installed in the middle of the maize field to the north of the weather station tower on a tripod at a height of 2.20 m before the experiment and it was later moved to a height of 2.80 m during the early morning of the 1st to stay above the minimum height limit described by (Aubinet et al., 2012), while keeping the sensor footprint as small as possible.

The sensor was oriented facing down a slight slope at an angle of 260° from true north to point into the prevailing wind direction. Raw data measurements of the three-dimensional wind speed and water vapor density were acquired at 20 Hz and stored on a CR3000 datalogger (Campbell Scientific). The latent and sensible heat fluxes were calculated offline using the TK3 software from Bayreuth University (Mauder and Foken, 2015). A coordinate rotation and a number of corrections were applied to the raw covariances as part of the processing procedure to account for limitations of the instrumentation: (i) a double rotation of the coordinate system, this was preferred to the planar fit method because of the rapid growth of the maize crop, (ii) the sensible heat flux was corrected for the sonic air temperature, (iii) the WPL correction for density fluctuations (Webb et al., 1980) and (iv) the Moore correction for frequency response (Moore, 1986). The results were quality controlled using a routine implemented in the TK3 and low-quality data for the sensible and latent heat flux were removed. No gap filling of missing data was performed due to the relatively short nature of the experiment and as the majority of missing data values for the latent heat flux occurred at night-time or during precipitation events.

The incoming shortwave solar radiation and the net radiation were measured using a CNR4-net radiometer (Kipp and Zonen). Measurements were made every 5 seconds and averaged over a period of 30 minutes for comparison with the eddy covariance data. A soil moisture station (Spade-TDT, Jülich) was located in the maize field to measure the soil temperature and water content at depths of 0.05, 0.10, 0.20 and 0.30 m.

Figure 2.1: Experimental setup for the field campaign, showing the location of the measurement profile pole (blue arrow), the Picarro isotope analyzer (orange arrow, under blue tarp) and the eddy covariance station (green arrow).

2.5.5 Sap Flow Measurements

In order to have a control for Ft calculated using the stable isotope method and eddy covariance device, the sap flow of ten maize plants was measured and then upscaled. The sap flow was measured using EMS 62 (EMS Brno) sensors based on the stem heat balance method with external heating and internal

Die approbierte gedruckte Originalversion dieser Dissertation ist an der TU Wien Bibliothek verfügbar.
The approved original version of this doctoral thesis is available in print at TU Wien Bibliothek.
TU Bibliothek Your knowledge hub WIEN

temperature sensing (Lindroth et al., 1995; Čermák et al., 2004). Two thermocouples were inserted into the stem in the radial direction 15 cm apart and a system of linear heating elements were installed just below the upper thermocouple to supply heat to the water travelling up the stem (Figure 2.2). The temperature difference between the heated and non-heated thermocouples was then maintained at 4 K using the feedback loop of the EMS 62 module. This resulted in the input power supplied being directly proportional to the amount of water passing the sensor. The sap flow rate was then calculated using

$$\boldsymbol{P = QdTc_w + dTz} \tag{2.6}$$

where P is the supplied power (W), Q is the sap flow rate (kg / s), dT is the temperature difference, c_w is the specific heat of water (J/ kgK) and z is a coefficient representing heat losses from the sensor (W/ K). The heat losses were calculated and removed by analysing the base line measurement of the device during periods where there was no sap flow, e.g., a precipitation event or at night and subtracting this from the measurement. Measurements were made every minute and ten minute averages were saved by the datalogger. The sap flow rates were then upscaled to transpiration values. The upscaling method is based on discussion with Jiri Kucera (private communication). By sampling the plants in the field, we can estimate the representative plant stem diameter for the field, and then calculate the representative plant transpiration rate. The upscaled field transpiration is then calculated by multiplying the rep. plant transpiration by the plant density. Owing to the rapid growth of the plants during this period some of the thermocouples became dislodged affecting the quality of the measurements, therefore these sensors were not included leaving 4 sensors for the final analysis.

Figure 2.2: Example of sap flow system EMS 62**.** The thermocouples are inserted 15cm apart, with the heating elements installed at the upper section.

2.6 Results

2.6.1 Environmental Conditions

The experiment was performed over a 9-day period at the beginning of the summer season. Figure 2.3 and Figure 2.4 show the environmental conditions over the course of the experiment. Wind speeds were generally low ranging from close to zero at night to a maximum of 3.6 ms^{-1}. Precipitation was recorded on 4 days of the experiment. A significant event (9.7 mm) occurred on the afternoon of the 25th followed by a drying period until the 30th. During this dry period the vapor pressure deficit (*VPD*) increased to a maximum of 2400 Pa on the 28th June. The precipitation event on the 30th (14.3 mm) was preceded by a change in air mass resulting in a significant decrease in temperature and *VPD*. After the event the temperature and *VPD* increased again resulting in similar conditions to the previous days. The event on the 30th lead to an increase in soil moisture at 5 cm depth from 17.2 % to 22.6 %, while the event on the 25th resulted in an increase from 17.9 % to 19.0 %. Mean daily air temperatures during the experiment varied between 14.2 – 20.0 °C. Average mean daily air temperature for this growing period for maize (14th June - 14th July) at the catchment is 18.9°C. Daily totals of *ET*, converted from

Die approbierte gedruckte Originalversion dieser Dissertation ist an der TU Wien Bibliothek verfügbar.
The approved original version of this doctoral thesis is available in print at TU Wien Bibliothek.

the latent heat flux, ranged from 1.6 to 3.4 mm with a total amount of 23.2 mm measured during the experimental period.

Daily values of *ET* are closely related to solar radiation (*Rs*) and *VPD*, with the largest values of *ET* corresponding to the days with the greatest amounts of R_s and highest *VPD*.

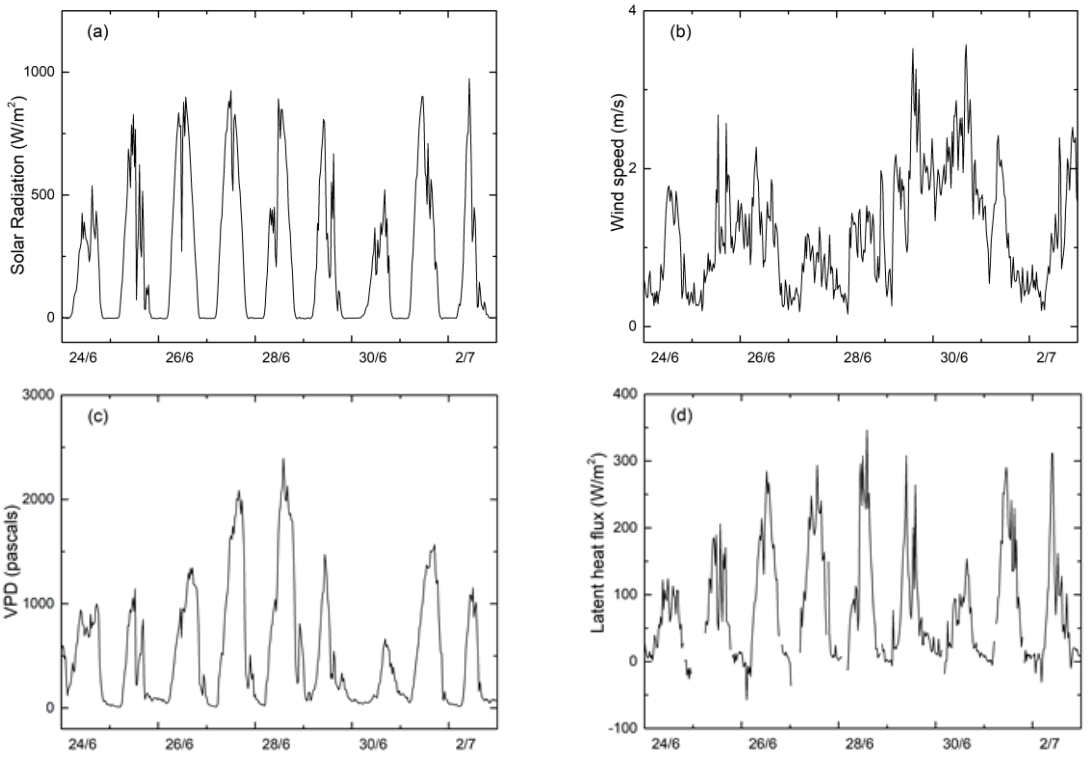

Figure 2.3: Half hourly plots of (a) solar radiation (b) wind speed, (c) vapor pressure deficit and (d) latent heat flux for June 24th - July 2nd, 2014.

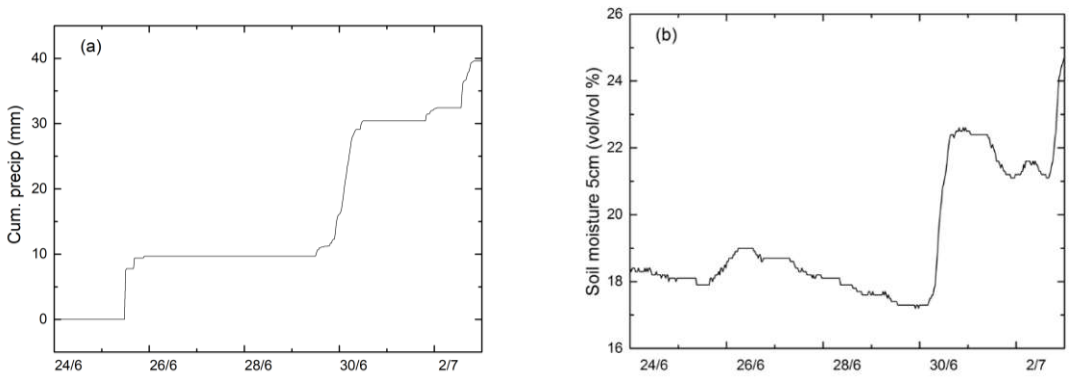

Figure 2.4: (a) cumulative precipitation and (b) half hourly soil moisture at 5cm depth for the period June 24th - July 2nd 2014.

Die approbierte gedruckte Originalversion dieser Dissertation ist an der TU Wien Bibliothek verfügbar.
The approved original version of this doctoral thesis is available in print at TU Wien Bibliothek.

2.6.2 Isotope Results

The $\delta^{18}O$ composition (black line) as well as the concentration of the water vapor (blue line) over the whole experimental period is shown in Figure 2.5. Distinct differences in average daily isotopic composition can be seen between δ_E and δ_T with δ_E being substantially more depleted in heavy isotopes compared to δ_T (Figure 2.6). δ_T showed little change during the experimental period, varying between -9.1 and -10.3 ‰. The precipitation events on the 25th and 30th had $\delta^{18}O$ values of -11.1 and -13.7 ‰ respectively and may be responsible for a slight decrease of approximately 1 ‰ in δ_T for the following day. The average daily value of δ_{ET} decreased to -18.7 ‰ following the precipitation event on the 25th due to the addition of the rainwater and then steadily increased over the next days to -13.2 ‰ on the 29th. Large values of the standard deviation are observed on the 25th and 2nd where a rain shower occurred during the afternoon measuring period. Measurements from, and directly after precipitation events were excluded from the analysis to exclude the effects of interception evaporation. One the afternoon of the 29th there is a large decrease in the value of $\delta^{18}O$ resulting from the movement of an atmospheric air mass. As the Keeling Plot requires any changes in isotopic ratio to be caused by sources within the system, data from this time period may not be used. The large gradients in the profiles of atmospheric water vapor concentration and isotope ratio allow the application of the Keeling Plot method on each day of the experimental period, with the exception of the 30th, because of the sustained precipitation event.

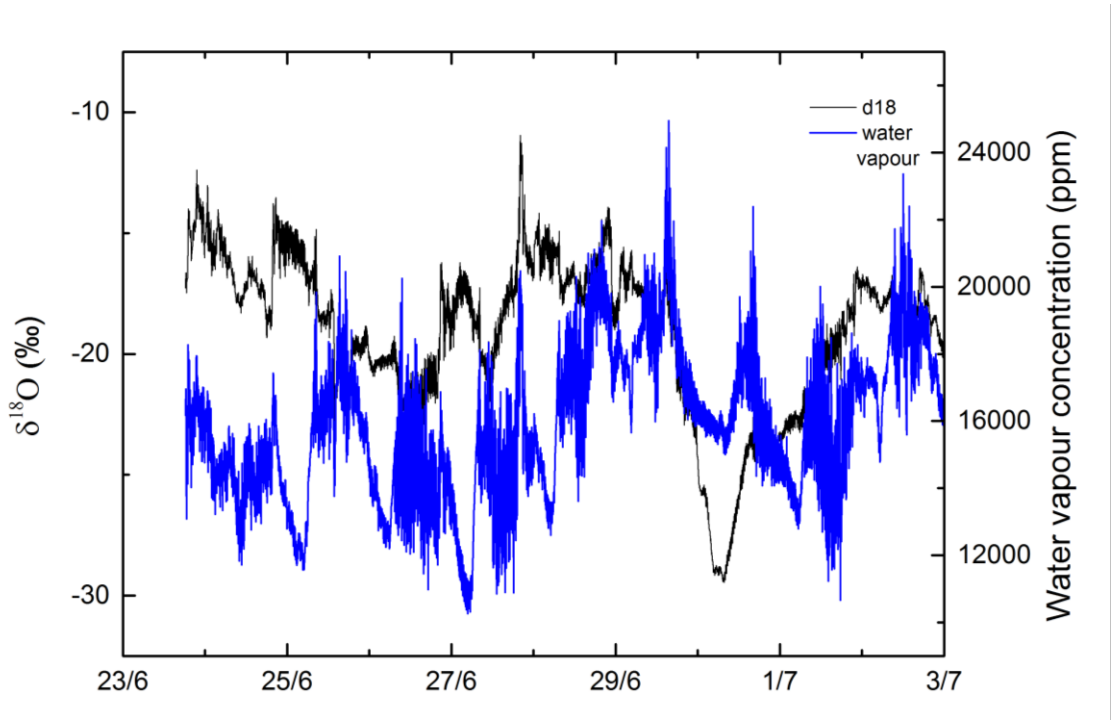

Figure 2.5: Time series (~4minute interval) of the $\delta^{18}O$ composition (black line) and the concentration (blue line) of the water vapour of the air at 2.4m in height.

Die approbierte gedruckte Originalversion dieser Dissertation ist an der TU Wien Bibliothek verfügbar.
The approved original version of this doctoral thesis is available in print at TU Wien Bibliothek.

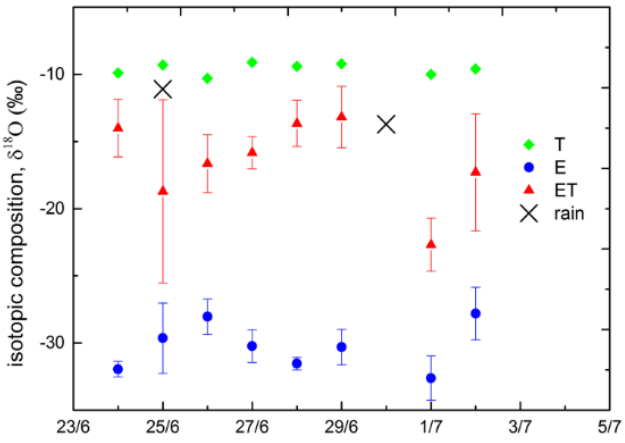

Figure 2.6: Daily averages of the isotopic composition of the precipitation (black cross) evapotranspiration flux, δ_{ET} (red triangles), soil evaporation flux, δ_E (blue circles), and transpiration flux δ_T (green diamonds). Error bars depict one standard deviation of measurement.

Twenty-minute values of *Ft* were calculated for late morning (to allow the plant to reach ISS) - afternoon times periods (Figure 2.7). *Ft* values follow a trend of decreasing to a minimum value following a precipitation event, followed by an increase in *Ft* over the following days. The daily average value of *Ft* was 67.5 % for this period. It is possible to split the experiment into two periods showing a similar pattern of increasing *Ft*, demarcated by the two large precipitation events on the 25th and 30th. During these periods, *Ft* follows an inverse relationship with the soil moisture measured at 5 cm in depth, as the soil moisture increases *Ft* decreases and vice versa, as the amount of water available to be evaporated in the soil decreases.

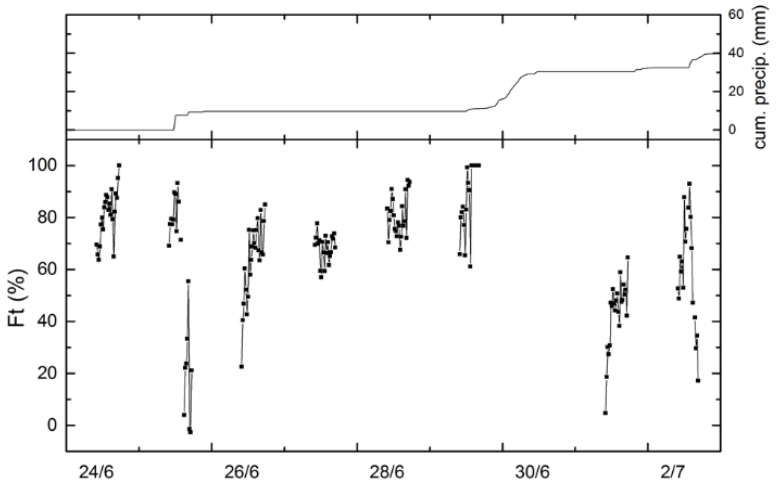

Figure 2.7: Twenty-minute values of *Ft* using the isotope method for the entire experimental period (bottom) and cumulative precipitation (top).

2.6.3 Technique comparison and environmental controls

Owing to the need for at least 30 cm of stem to install the sap flow sensors, the devices were installed close to the ground leading to an overestimation in the measured sap flow because of the presence of a strong temperature gradient near the surface on certain days. By comparing near surface temperature

Die approbierte gedruckte Originalversion dieser Dissertation ist an der TU Wien Bibliothek verfügbar.
The approved original version of this doctoral thesis is available in print at TU Wien Bibliothek.
TU Bibliothek Your knowledge hub WIEN

measurements of the soil (2cm depth) made as part of the soil moisture measurement and an air temperature reading inside the canopy as part of the sap flow system (~30cms), differences of up to 10°C (versus 6°C on the 'acceptable' days) were found on the days where the sap flow transpiration also appeared to be overestimated. As this leads to an overestimation in calculated transpiration, two days, the 26th June and 2nd July where this effect was not noticed were chosen for a comparison with the stable isotope data. The uncertainty on the T_{iso} estimates was calculated using the single isotope, two source mixing model of (Philips and Gregg, 2001), an estimate for the uncertainty of the eddy covariance measurement based on the net radiation (Hollinger and Richardson, 2005) and Eq. (2.2), while the uncertainty of T_{sap} is the standard error of the devices. The results show that the two methods compare favourably, with both T_{iso} and T_{sap} showing a similar pattern on both days (Figure 2.8) and R^2 values of 0.80 for the 26th and 0.72 for the 2nd.

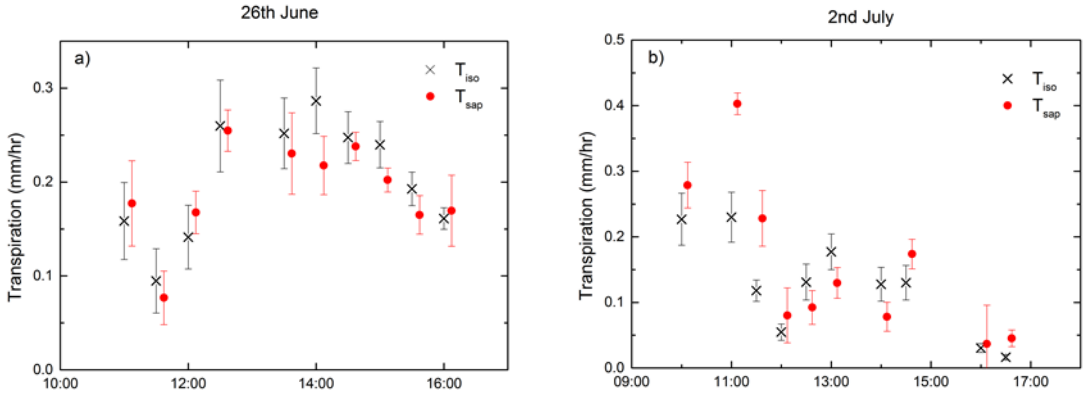

Figure 2.8: Comparison of isotope and sap flow estimates of *T* for (a) 26th June and (b) 2nd July. Error bars depict standard error.

On the 26th, the value of T_{iso} increased steadily during the late morning period with *Ft* increasing from 29 % to an almost constant value of 70% in the later afternoon. Both T_{iso} and E_{iso} were driven by R_s (Figure 2.9a) with T_{iso} showing little influence from *VPD* (Figure 2.9b). On the 2nd temperatures were in the range of 12.0 - 22.9 °C. The incoming R_s was heavily affected by the presence of clouds in the late afternoon, with a peak value of 973 Wm^{-2} measured around 10:30 before reducing to 50 - 100 Wm^{-2} after 15:00. T_{iso} follows a similar pattern on the late morning and early afternoon of the 2nd, however in the late afternoon it starts to decrease because of the effect of a small rain shower increasing the amount of water available for soil evaporation and a decrease in solar energy due to clouding, with Ft_{iso} decreasing from 92.9 - 17.1 % during this period.

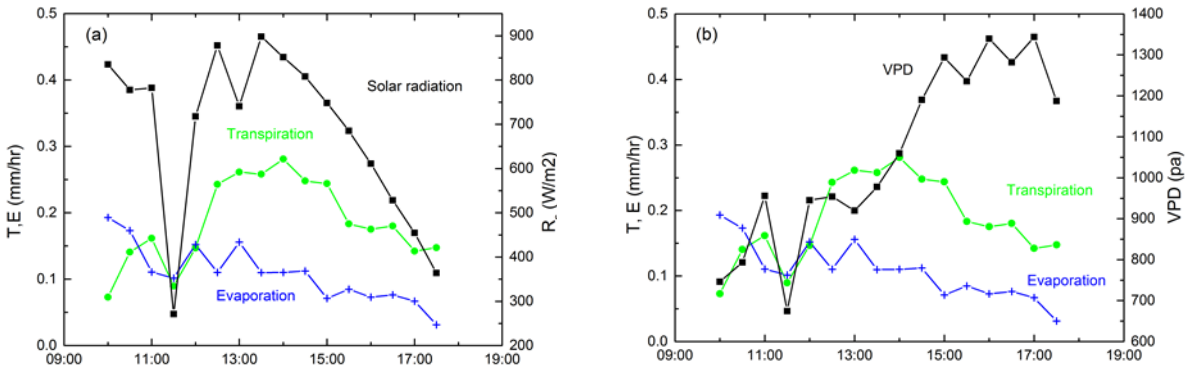

Figure 2.9: Half hourly plots of soil evaporation (*E*), transpiration (*T*), and (a) incoming solar radiation (R_s) and (b) vapor pressure deficit (*VPD*) on 26th June.

Die approbierte gedruckte Originalversion dieser Dissertation ist an der TU Wien Bibliothek verfügbar.
The approved original version of this doctoral thesis is available in print at TU Wien Bibliothek.
TU Bibliothek Your knowledge hub WIEN

Figure 2.10 shows the comparison between E and T calculated from the isotope method versus R_s and VPD for the entire experimental period. T shows a moderate correlation with R_s and VPD while E shows a moderate correlation only with R_s and no correlation with VPD.

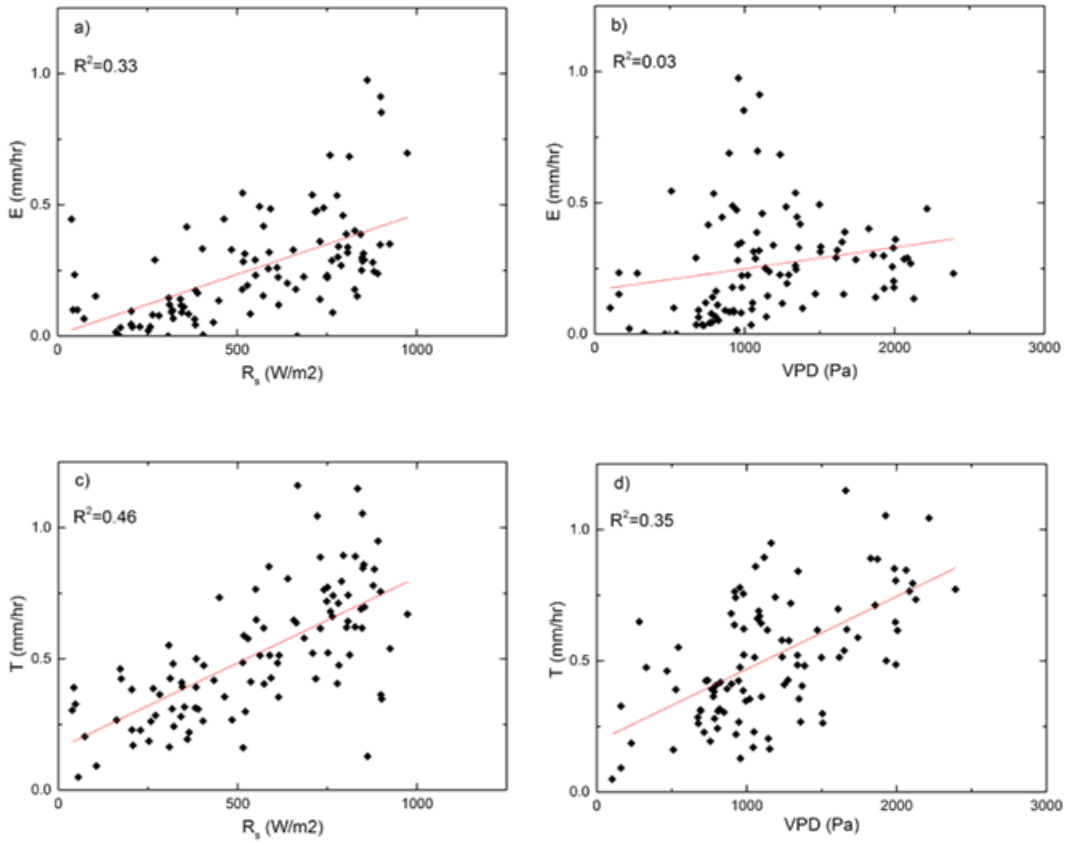

Figure 2.10: Scatterplots of half-hourly values for the entire experimental period (10:00 - 17:30). Top two figures show the comparison between soil evaporation (E) and (a) solar radiation (R_s) and (b) vapor pressure deficit (VPD), while the bottom figures compare transpiration (T) with (c) solar radiation and (d) vapor pressure deficit.

2.7 Discussion

Using high frequency isotope measurements and sap flow devices we were able to test the ability of the stable isotope method to partition the field scale evapotranspiration measured from a maize crop by the eddy covariance method. In general, the results shown here indicate that the method can be applied to maize crops, with similar estimates of Ft being made by the stable isotope method in comparison with the sap flow method. Due to the higher time resolution afforded by the use of high frequency measurements we are able to see the change in Ft throughout the day and the response of Ft to the environmental conditions. This also allows for a more detailed comparison between the two methods as compared to the previous sap flow comparison made by Williams (2004) for an olive orchard where it was only possible to get two values for Ft per day. While the results showed good agreement between the methods, the sap flow method suffered from a number of limitations because of the growth of the maize. Many sensors were disturbed as the rapid growth of the maize plants proved an issue with these particular sensors, as the lower part of the stem stretched disrupting the installation of the thermocouple needles. This reduced the amount of good quality data and leads to a larger uncertainty in $T_{sap.}$ In addition, the amount of stem required for installation means that the sensors cannot be installed for the full growing period of the crop.

Die approbierte gedruckte Originalversion dieser Dissertation ist an der TU Wien Bibliothek verfügbar.
The approved original version of this doctoral thesis is available in print at TU Wien Bibliothek.

The main assumptions of the stable isotope technique, that the plant's water is being transpired at isotopic steady state, that there is no loss of water due to condensation and that there are only two sources for the water vapor in the ecosystem mean that it is not possible to analyse *Ft* over the entire diurnal cycle as condensation was present every morning during the experimental period (Yakir and Sternberg, 2000). However, it can be seen from the eddy covariance and sap flow data that transpiration is minimal during the night and early morning. In Figure 2.8 we see quite good agreement on the 26th between the two methods throughout the day, while on the 2nd there are greater differences in *T*, particularly during the later parts of the morning. This might suggest that there was some fractionation occurring and the ISS assumption did not hold during this period. In future experiments direct measurements of δ_T and δ_E should be made using chamber methods to reduce the uncertainty and extend the available data period to the morning and evening. Interception is also neglected as it is difficult to estimate, which may affect the values of *Ft* on the 25th and the 2nd directly following the precipitation. As the canopy was observed to be effectively dry within one hour of the end of the intense rainfall event on the 25th, attributing all the measured evaporated water within this time period to interception would lead to a maximum estimate of 0.25 mm or 12.5 % of the daily sum of *ET*. For the other event the interception loss may be greater, due to the lower rainfall intensity. The method cannot be applied successfully during periods of precipitation as the presence of the rain drops results in large measured values of δ_{ebl} leading to values of *Ft* exceeding 1, also seen by Wei (2015) for a rice paddy field during periods of irrigation. By expanding the experimental set-up to include an additional intake port for sampling of precipitation it would be possible to directly determine the time periods where interception water is present and evaporating and exclude them from the full analysis to reduce the uncertainty in *Ft*. This would also be necessary for detecting the presence of dew or fog if the measuring period is extended beyond the late morning and afternoon using chamber devices. As the Keeling plot requires distinct differences in the isotopic signals of transpiration and soil evaporation, the applicability of the technique can be affected by the depth of root water uptake, if the plants have short root systems such as shrubs or herbs and/or the soil becomes very dry the difference in the signals may decrease, leading to regression plot slopes that are not significant (Yakir and Sternberg, 2000). As maize does not uptake water among all rooting depths equally but extracts a larger percentage of water from shallower roots, the use of the method may be limited during the early stages of growth. The sampled values of δ_T were however at least 2 ‰ more depleted than samples of the soil water, indicating the majority of the roots were accessing water below the soil evaporation front. As the air is sampled at different heights within the canopy, the Keeling Plot method spatially integrates the flux over different footprints. In canopies such as trees (Yepez et al., 2003) or grassland (Yepez et al., 2005) this allows the comparison of the point samples of plant and soil isotopic composition, to that of the evapotranspiration signal. Within a canopy with a regimented architecture such as maize, however, this may not be sufficient to allow, as Hupet and Vanclooster (2005) showed that the amount of rainfall that reaches the surface in maize is highly variable. During the experiment the average height of the crop increased from 0.95 m to 1.40 m, while the average leaf area index increased from 1.2 to 2.4. In a paper on the canopy architecture of maize Huang (2007) measured canopy openness in a field with a similar plant density as ~50% at the upper layer of the canopy at the silking stage, which is a later stage of development than when our experiment took place (15-20 days later) where the plants will have a height over 2 metres and a LAI greater than 4. The good level of agreement between the sap flow and isotope results though here indicates that the isotope method was successfully applied to maize.

The transpiration rate of maize has up until now been investigated using point measurement instruments that require upscaling to the field scale. Using lysimeters (Liu et al., 2002) and (Kang et al., 2003) reported values of 71 and 75 % for *Ft* for the entirety of the growing stage. The average value of *Ft* for this experimental period was 67.5%. As the experiment took place during a short time period within the vegetative stage (length of approximately 25 - 40 days) these differences will be partly due to the changing LAI and soil cover during this period, as well as differences in irrigation/precipitation. Our study provides information for when the soil in a maize crop field has been wetted and begins to dry

Die approbierte gedruckte Originalversion dieser Dissertation ist an der TU Wien Bibliothek verfügbar.
The approved original version of this doctoral thesis is available in print at TU Wien Bibliothek.
TU Bibliothek Your knowledge hub WIEN

out; while we only have 9 days there was a soil moisture cycle of dry – wet – dry – wet. *Ft* followed a pattern of decreasing following a rain event and then increasing over the following days as the top layer of the soil dries out reducing the amount of water available for further soil evaporation, consistent with the findings of (Yepez et al., 2003) and Jara et al., (1998) for mesquite and maize. Daily average values of *Ft* varied between 43.0 and 88.5% (Figure 2.7) indicating that there was a considerable effect due to the precipitation events. One of the main points of this experiment is to focus on the rapid-growth phase of maize, where the maize is rapidly changing. While the meteorological conditions remain representative, the transpiration dynamics at this distinct growth phase of the maize were captured for the case of wetted soil. During periods where meteorological conditions lead to high rates of *ET* without a wetting of the soil, transpiration can be expected to approach 90% and greater and care must be taken when using average values for *Ft* calculated over longer periods during the growing season.

Transpiration was correlated with solar radiation and vapour pressure deficit over the examined period, with correlation coefficients of 0.68 and 0.59 (Figure 2.10), respectively, however Klimešová et al. (2014) reported a much higher correlation of 0.88 with R_s for a potted maize experiment during a slightly later growing stage. This may be due to the relatively frequent precipitation events and lower amount of soil evaporation expected from a potted experiment, leading to more energy being available for transpiration and a higher correlation. During a 3-day intensive sampling period during that experiment, with soil moisture close to field capacity, the correlation with R_s was significantly lower and closer to the values measured here at 0.65. Other long-term studies on the sap flow rate of maize found for the entire growing season also ranked R_s as the most important meteorological variable affecting the rate of transpiration of maize (Zhao et al., 2016; Gao et al., 2010). The lack of a strong correlation of soil evaporation with *VPD* was unexpected, as a high correlation has been previously reported for both trees (Williams et al., 2004) and grassland (Hu et al., 2014) using stable isotope methods. However, for maize a lack of correlation has been observed before on certain days using lysimeters (Herbst et al., 1996). An explanation may be attributable to the spaced row structure of maize crops, which results in the fraction of radiation intercepted by the canopy having a 'U' shaped diurnal pattern with the minimum occurring around midday (Hossain et al., 2014). This will lead to the soil receiving more energy at this time resulting in higher values of soil evaporation than later in the afternoon, when *VPD* is highest.

2.8 Conclusions

In this experiment, we tested the application of the stable isotope method to a maize crop during the vegetative stage, using sap flow sensors as a comparison technique. Field scale *ET* was measured using an eddy covariance device and then partitioned using high frequency in-situ measurements of the isotopic signal of the canopy water vapor. Keeling plots were used to generate values of δ_{ET} and combined with estimates of δ_T obtained from plant samples assuming ISS and estimates of δ_E using soil samples and the Craig-Gordon equation. High correlation coefficient values were generally found between the two techniques, indicating the stable isotope method can successfully be applied in maize. While the method has previously been shown to work well for crops with simpler canopy structures such as rice and wheat, it appears that the more complex canopy structure of maize does not limit the accuracy of the method. During the experiment the amount of soil evaporation and transpiration was dependent on the availability of soil water in the upper layer of the soil, with a general pattern of a large decrease following a precipitation event followed by a period of increasing, due to the drying out of the upper layer of the soil. Daily average values of *Ft* varied between 43.0 and 88.5 % indicating that there was a considerable effect due to the precipitation events. The diurnals patterns of both soil evaporation and transpiration are much better correlated with solar radiation than with vapor pressure deficit.

With the extension of the measurement period, the stable isotope method can be used to test irrigation and soil management practices at the field scale over the entire growing season in maize and similar crops, leading to more efficient agricultural water use and water availability.

Die approbierte gedruckte Originalversion dieser Dissertation ist an der TU Wien Bibliothek verfügbar.
The approved original version of this doctoral thesis is available in print at TU Wien Bibliothek.
TU Bibliothek Your knowledge hub WIEN

3. Partitioning evapotranspiration using stable isotopes and Lagrangian dispersion analysis in a small agricultural catchment

3.1 General

This chapter compares the different methods of Lagrangian dispersion analysis (Lagrangian near field theory) and stable isotopes analysis and investigates how the evaporation partitioning changes in response to precipitation events. While most partitioning methods require some sampling of the soil or plants, and are therefore less reliable in heterogenous conditions, the Lagrangian dispersion analysis method offers the possibility of partitioning evaporation using just sampling of the water vapour within the canopy.

The present chapter is based on the following scientific publication:

Hogan, P., Parajka, J., Heng, L., Strauss, P., & Blöschl, G. (2020). Partitioning evapotranspiration using stable isotopes and Lagrangian dispersion analysis in a small agricultural catchment. *Journal of Hydrology and Hydromechanics*, 68, 134-143.

In the original publication the term *evapotranspiration* was used instead of *evaporation*, as the emphasis of this research was on partitioning.

3.2 Key points

The two methods give similar results, with the Lagrangian method giving a higher average and maximum estimate of transpiration.

The stable isotope method was found to return a much larger amount of useable data, as well as having a lower variance. This is offset by the need for more additional measurements and analysis.

Different levels of precipitation intensity give different soil evaporation responses, due to the changes in soil moisture.

3.3 Abstract

Measuring soil evaporation and transpiration at the field scale is complicated due to the heterogenity of the environment, with point measurements requiring upscaling and field measurements such as eddy covariance measuring only the evapotranspiration. During the summer of 2014 an eddy covariance device was used to measure the evapotranspiration of a growing maize field at the HOAL catchment. The stable isotope technique and a Lagrangian near field theory (LNF) were then utilized to partition the evapotranspiration into soil evaporation and transpiration, using the concentration and isotopic ratio of water vapour within the canopy. The stable isotope estimates of the daily averages of the fraction of evapotranspiration (*Ft*) ranged from 43.0 – 88.5 %, with an average value of 67.5 %, where slightly lower than the LNF method, where *Ft* was found to range from 52.3 – 91.5 % with an average value of 73.5 %. Two different parameterizations for the turbulent statistics were used, with both giving similar R^2 values, 0.65 and 0.63 for the Raupach and Leuning parameterizations, with the Raupach version performing slightly better. The stable isotope method demonstrated itself to be a more robust method, returning larger amounts of useable data, however this is limited by the requirement of much more additional data.

Die approbierte gedruckte Originalversion dieser Dissertation ist an der TU Wien Bibliothek verfügbar.
The approved original version of this doctoral thesis is available in print at TU Wien Bibliothek.

3.4 Introduction

Evapotranspiration (*ET*) forms an important part of the water balance across all spatial and temporal scales. For many applications however, further information on the partitioning of evapotranspiration into its constituent components of soil evaporation and transpiration is required, e.g., for irrigation management (Tong et al., 2009) and climate modelling (Lian et al., 2018).

At different spatial scales *ET* can be estimated using different methods and techniques such as water balance, remote sensing and energy balance modelling at global and regional scales (Vinukollu et al., 2011), or measured using eddy covariance or scintillometry at field scales. However, these methods provide little or no information on how the *ET* is partitioned into its components of soil evaporation (*E*) and transpiration (*T*). Other direct measurement techniques at the point scale, such as lysimeters for measuring soil evaporation (Heinlein et al., 2017; Rafi et al., 2019) or sap flow sensors for transpiration (Agam et al., 2012; Zhao et al., 2016) can be used to directly measure the individual components, however they have a very small footprint which requires upscaling to the field scale, which is strongly influenced by the heterogeneity of the surrounding area. For trees in the riparian zone, transpiration can be estimated from shallow groundwater diurnal fluctuations (Gribovszki et al., 2008), however this is not applicable for crops with their shallower root systems. Assumptions can be made in order to estimate *Ft*, such as when *E* or *T* could be assumed to be negligible, however these assumptions have been shown to not be applicable to every ecosystem (Stoy et al., 2019). An alternative approach is to partition the measured field scale *ET* using methods such as Lagrangian dispersion analysis (Raupach, 1989a; Warland and Thurtell 2000) or stable isotopes (Ma et al., 2018; Williams et al., 2004; Wang et al., 2013; Xiao et al., 2018; Yepez et al., 2003).

The Lagrangian dispersion analysis method an inverse modelling approach, where the source/sink distribution of a scalar is related to a concentration profile of the scalar within a canopy ecosystem through a turbulent dispersion field (Raupach 1989a; Santos et al., 2011; Warland and Thurtell, 2000). Within a plant canopy, the gradient - diffusion relationship cannot be used to calculate the flux of a trace gas due to the role of large turbulent eddies in the vertical transport of the scalar, resulting in the observation of counter-gradient fluxes (Denmead and Bradley, 1985). Instead Raupach (1989a, 1989b) developed a model in a Lagrangian framework where the trajectory of fluid particles released from a source is followed, thereby taking into account the history of the particles. Then the resulting concentration profile can be broken up into two regions, a near field region where the particles disperse linearly in time due to the persistence of the turbulent eddies, and a far field region where the particles disperse with the square root of time diffusively. The method has been used to calculate the flux of CO_2, H_2O and heat within coniferous (Styles et al., 2002) and eucalyptus forest canopies (Haverd et al., 2011). In addition, Haverd et al. (2009) applied the method in a eucalyptus forest along with a Soil-Vegetation-Atmospheric-Transfer model (SVAT) to improve the estimation of turbulent statistics in a forest canopy.

The Keeling Plot (Keeling, 1958) mass balance can be applied within a field ecosystem, to the isotopes of water evaporated from within the canopy. As water evaporated from the soil has a different ratio of light to heavy isotopes compared to water vapour evaporated from plant stomata, this difference in isotopic ratio allows for the estimation of the soil evaporation- transpiration ratio within the ecosystem. This method has been tested in a number of different vegetation and crop types such as an olive orchard (Williams et al., 2004), woodland (Dubbert et al., 2013), beets (Quade et al., 2019) and maize (Wu et al., 2016). Applying the method to determine the temporal variability of root water uptake depth of wheat plants, Zhang et al. (2011) estimated that up to 30% of water consumption during the irrigation season can be soil evaporation. Using deuterium isotopes in grassland over a short time period, Good et al. (2014) investigated the evolution of the soil evaporation/transpiration ratio during the growing phase of the grass crop. Wei et al. (2015) measured *Ft* over a rice field over the course of an entire growing season, with the estimated *Ft* ranging from 0.2 at the start of the growing season up to a near constant value between 0.8 - 1.0.

Die approbierte gedruckte Originalversion dieser Dissertation ist an der TU Wien Bibliothek verfügbar.
The approved original version of this doctoral thesis is available in print at TU Wien Bibliothek.
TU Bibliothek Your knowledge hub WIEN

The objective of this study is to estimate the components of evapotranspiration in a vegetative maize field and its response to precipitation events at a high temporal resolution. In this paper we use the stable isotope method and the localised near field theory of Lagrangian dispersion analysis. Both methods use measurements of water vapour concentration within the canopy and a mass balance approach as their basis, while the isotope method requires extra measurements and assumptions, this allows for an additional study of the robustness and effectiveness of the two methods.

3.5 Theory and methods

3.5.1 Lagrangian dispersion analysis

In order to partition the evapotranspiration inside a crop ecosystem between E and T using an inverse method we first divide the source distribution into m vertical layers, where the first layer is just above the surface to account for soil evaporation, and the subsequent layers extend from just above this layer to the top of the canopy for transpiration. The water vapour released from these layers results in a concentration profile, which can be measured at n different heights. The relationship between scalar source density $\varphi(z)$ and concentration $C(z)$ under steady conditions in a horizontally homogenous canopy can be written as

$$C_i - C_r = \sum_{j=1}^{m} D_{ij} \varphi_j \Delta z_j \tag{3.1}$$

Where C_i is the concentration at height z_i, C_r is the concentration at a reference height above the canopy z_r, D_{ij} is the dispersion matrix, with i rows for 1.. n measurement heights, and j columns for 1..m source layers , φ_j is the source strength in layer j, and Δz_j is the thickness of layer j. The inversion of this equation then allows for the estimation of the source strengths, in this case E and T. To calculate the dispersion matrix, the source strength in one layer j is set to be a steady unit source, S_j and set to zero in all other layers. This gives a partial concentration profile C_i, which defines the elements of D_{ij} for dispersion from layer j to the concentration at height z_i

$$D_{ij} = \frac{C_i - C_r}{S_j - \Delta z_j} \tag{3.2}$$

In a Lagrangian analysis of particle dispersion within a canopy, the trajectory of a particle is followed from its release from a source. The resulting concentration C_i is due to the influence of two different regions on this path, a near field and a far field region.

In the Localised Near Field (LNF) theory of Raupach (1989a, 1989b), the two regions are treated separately, with C_i equal to the sum of both regions

$$C_i = C_n + C_f \tag{3.3}$$

In the near field, local effects dominate the dispersion of the particles while in the far field, it is assumed that particles diffuse in accordance with gradient-diffusion theory. The near and far field components can be described using the turbulent statistics for the canopy, the vertical profile of the standard deviation of the vertical velocity (σ_w) and the Lagrangian time scale (T_L) according to Raupach (1989a) as

$$C_n(z) = \int_0^{\infty} \int \frac{S(z_s)}{\sigma_w(z_s)} \left\{ k_n \left[\frac{z - z_s}{\sigma_w(z_s) T_L(z_s)} \right] + k_n \left[\frac{z + z_s}{\sigma_w(z_s) T_L(z_s)} \right] \right\} dz_s \tag{3.4}$$

$$C_f(z) = C(z_{ref}) - C_n(z_{ref}) + \int_z^{z_{ref}} \frac{F(z')}{K_f(z')} dz' \tag{3.5}$$

where z' is the discrete height, z_s is the source height, k_n is a near field 'kernel', $F(z)$ is the flux density, and K_f is the far field diffusivity.

Die approbierte gedruckte Originalversion dieser Dissertation ist an der TU Wien Bibliothek verfügbar.
The approved original version of this doctoral thesis is available in print at TU Wien Bibliothek.
TU Bibliothek Your knowledge hub WIEN

$$k_n(\zeta) = -0.3989\ln(1-\exp(-|\zeta|)) - 0.1562\exp(-|\zeta|) \quad (3.6)$$

$$F(z) = -K_f(z)\frac{dc_f}{dz} \quad (3.7)$$

$$K_f = \sigma_w^2(z)T_L(z) \quad (3.8)$$

Where $\zeta = (z-z_0)/(\sigma_{w0}\,T_{L0})$. As T_L cannot be directly measured by fixed sensors as it is a Lagrangian quantity and due to the difficulty of making vertical wind measurements inside a canopy, the profiles of σ_w and T_L needed for the calculation of D_{ij} are normally calculated using turbulent statistical parameterisations. Based on the results of Santos et al (2011) the parameterisations suggested by Raupach (1989a) and Leuning (2000) were used in this study (Figure 3.1). Raupach (1989a) proposed that σ_w and T_L profiles could be approximated by the piecewise linear profiles

$$\frac{\sigma_w}{u^*} = f(x) = \begin{cases} a_0 + (a_1 - a_0)\times\frac{z}{h}, & z < h \\ a_1, & z \geq h \end{cases} \quad (3.9)$$

$$\frac{T_L u^*}{h} = max\left[c_0\,,\frac{k(z-d)}{a_1 h}\right] \quad (3.10)$$

where $a_1 = 1.25$, $a_0 = 0.25$, $c_0 = 0.3$, $d = 2/3{*}h$ is the displacement height, h is the canopy height, u^* is the friction velocity and $k = 0.41$ is the von Karman constant.

The parameterisations of Leuning are based on exponential and non- rectangular functions within and above the canopy

$$y = c_1 e^{c_2 z/h}\ for\ z < 0.8h$$

$$y = \frac{(ax+b)+d_1\sqrt{(ax+b)^2-4\theta abx}}{2\theta}\ for\ z \geq 0.8h \quad (3.11)$$

where $c_1 = 0.2$ and the other coefficients can be found in Table 3.1

These parameterisations were originally derived for near-neutral conditions and corrections functions have been suggested for use in non-neutral conditions (Leuning 2000). However, the performance of these corrections has been mixed, with Santos et al (2011) reporting an increase in the overestimation of the latent heat flux when the corrections were used.

Table 3.1: A list of the variables and parameters used for the determination of normalised profiles of the standard deviation of the vertical velocity, σ_w and the Lagrangian timescale, T_L. (Leuning 2000)

z/h	*x*	*y*	*θ*	*a*	*b*	*d*
≥0.8	z/h	σw/u*	0.98	0.850	1.25	-1
≥0.25	z/h-0.8	TLu*/h	0.98	0.256	0.40	+1
<0.25	4z/h	TLu*/h	0.98	0.850	0.41	-1

Die approbierte gedruckte Originalversion dieser Dissertation ist an der TU Wien Bibliothek verfügbar.
The approved original version of this doctoral thesis is available in print at TU Wien Bibliothek.

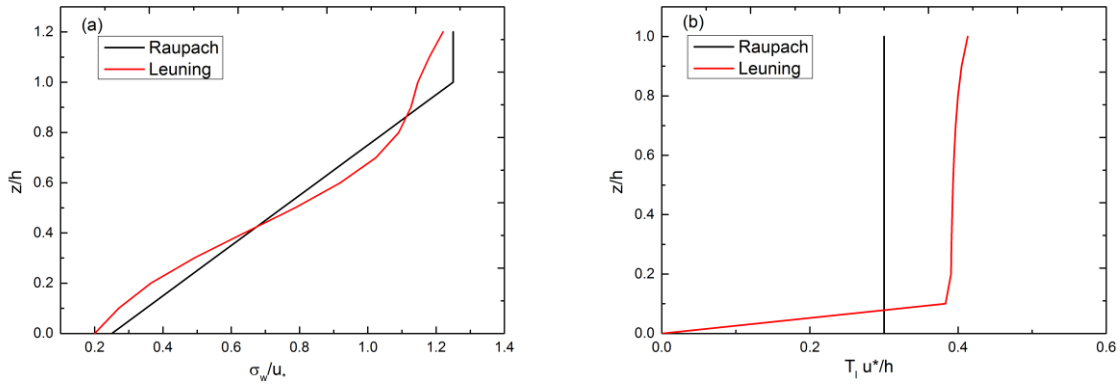

Figure 3.1: Normalised profiles of the standard deviation of (a) the vertical velocity, σ_w and (b) the Lagrangian time scale, T_L, according to Raupach (1989a) and Leuning (2000).

3.5.2 Study area

The experiment was performed from the 24th June – 2nd July 2014 at the Hydrological Open Air Laboratory (HOAL) at Petzenkirchen, Austria (48°9' N, 15°9' E) (Blöschl et al., 2016) (Figure 3.2). The catchment has an area of 66 ha, elevation ranges from 268 – 323 m above sea level, with a mean slope of 8%. Land use comprises of 87 % agricultural crops, 5 % grassland pasture, 6 % forest and 2 % paved surfaces. The local climate can be described as humid, with a mean annual precipitation of 823

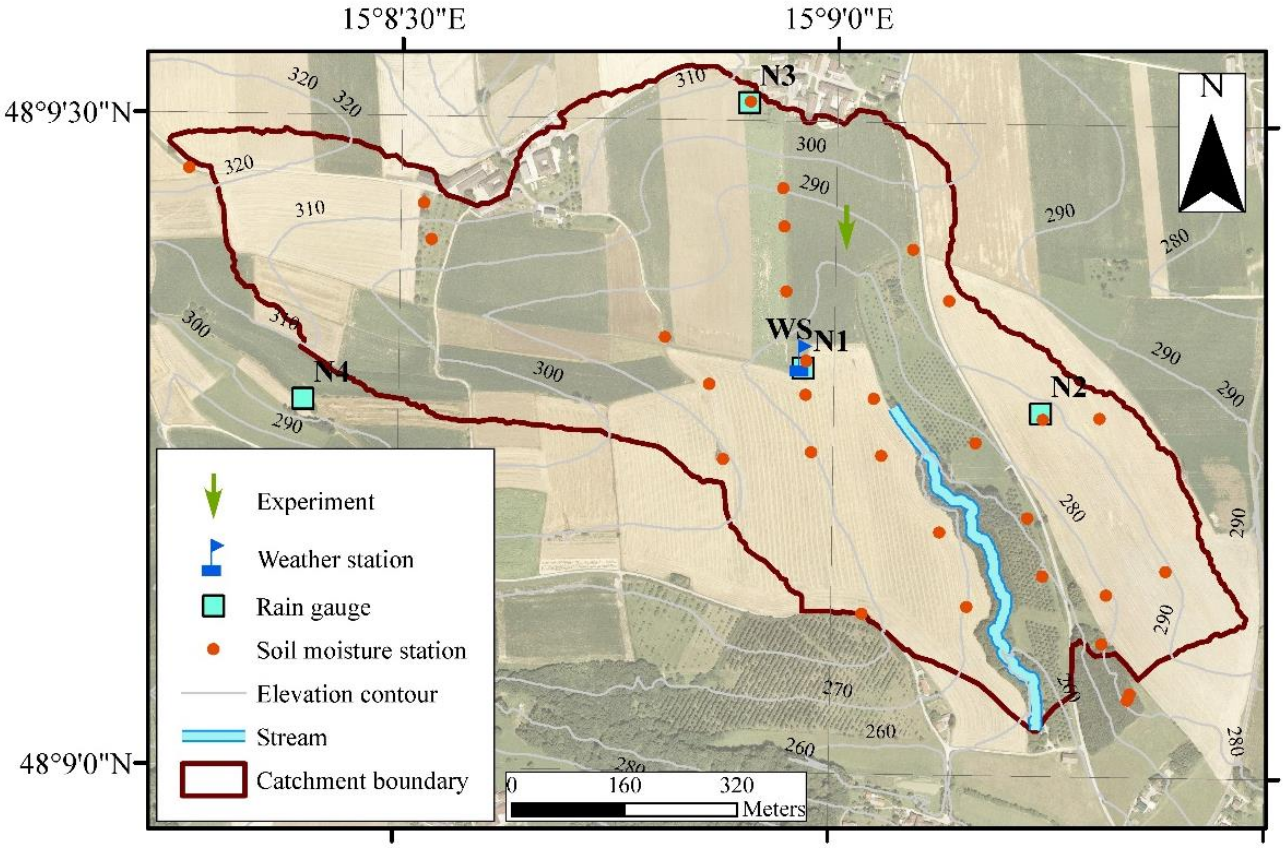

Figure 3.2: The experimental catchment showing the location of the measurement devices and the study field (green arrow).

Die approbierte gedruckte Originalversion dieser Dissertation ist an der TU Wien Bibliothek verfügbar.
The approved original version of this doctoral thesis is available in print at TU Wien Bibliothek.

mm/yr, with larger amounts of precipitation in summer than in winter. The mean annual temperature is 9.5 °C. Evapotranspiration in the years from 2013 – 2017 ranged from 442 – 518 mm/yr. As the experiment was planned for early summer and a limited time period, a 4.8 ha maize field was selected as the early growing stage and wider spacing between crops would allow for assumptions of turbulent mixing within the ecosystem to be fulfilled. The average height of the plants increased from 0.95 m to 1.40 m with the Leaf Area Index (LAI) progressing from 1.2 to 2.4 during this period.

3.5.3 Instrumentation

To measure the profiles of water vapour concentration and isotopic ratio (O_{18}/O_{16}) within the canopy a L2130-i analyser (Picarro) was installed within the maize field (Figure 3.3). Air was sampled within the canopy and above, using a 6-port intake valve connected to a pump and sampled using the analyser at 1 Hz. To achieve a precision of 0.02 ‰ an averaging time of at least 100 seconds was required for each individual ports and gave an overall resolution of 20 minutes for δ_{ET} and C across the 6 ports. δ_{ebl} and C_{ebl} were sampled at 4 heights within the canopy (0.1, 0.2, 0.5 and 1.0 m), and 2 additional sample intakes were located above the canopy (1.7 and 2.4 m). The ports at heights 0.5 and 1.0 m were later increased to 0.8 and 1.2 m on the 1st July due to the increase in canopy height. δ_T was estimated from xylem water taken from 4 maize plants, sampled between 11-14 h on each day of the experiment. This assumes that the xylem water is at isotopic steady state which is normally valid between late morning and early afternoon. To estimate δ_E using Eq. (2.4), soil samples were taken daily at 4 locations near the air intake, at depths of 0-2, 2-5 and 5-10 cm to correctly identify the evaporation front according to Rothfuss et al. (2010). All soil and plant samples were sealed in glass vials, frozen and then transported to the laboratory for extraction, according to the guidelines of Mayr et al. (2016).

Figure 3.3: The experimental area, showing the location of the eddy covariance system (orange arrow) and the picaro device (green arrow).

Evapotranspiration was measured using an open path eddy covariance sensor (IRGASON, Campbell Scientific). The device was installed in the middle of the maize field at a height of 2.20 m before the experiment and moved to a height of 2.80 m during the early morning of the 1st to stay above the minimum height limit described by (Aubinet et al., 2012). The TK3 software was used to calculate the latent heat flux from the raw measurements of the wind speed and water vapour (Mauder and Foken, 2015). As part of the processing procedure a number of corrections must be applied to the raw data: (i) a double rotation of the coordinate system, this was used rather than the planar fit method due to the rapid growth of the maize crop and short time period of the experiment, (ii) the Moore correction for high frequency loss (Moore, 1986), (iii) a sonic air temperature for the sensible heat flux, and (iv) the WPL correction to account for density fluctuations (Webb et al., 1980). The TK3 software includes a quality control analysis and sensible and latent heat flux data of a low quality were removed. Air

Die approbierte gedruckte Originalversion dieser Dissertation ist an der TU Wien Bibliothek verfügbar.
The approved original version of this doctoral thesis is available in print at TU Wien Bibliothek.
TU Bibliothek Your knowledge hub WIEN

temperature and humidity were measured at the eddy covariance station using a HMP155 probe. Precipitation was measured across the catchment using 4 weighing balance gauges (OTT Pluvio). For this experiment the data from the closest rain gauge, located at the nearby weather station was used. The catchment is instrumented with a network of soil moisture stations utilising Time Domain Transmission (TDT) probes. A station was located in the maize field to measure the near surface soil temperature and water content at depths of 0.05 and 0.1 m.

3.6 Results

3.6.1 Environmental conditions

Figure 3.4 shows the environmental conditions over the time period of the experiment. Weather conditions were mixed over the course of the experiment, with most days experiencing periods of sunshine and cloud, except for the 30th where the passage of a frontal system resulted in overcast conditions and persistent rain until late afternoon. In total four precipitation events were recorded, with three of them having a major effect on the near surface soil moisture level. The duration of the event on the 30th meant that it was not possible to use the data from this day, however the shorter nature of the other events meant less loss of data on those days. The average daily mean temperatures ranged from 14.2 – 20.0 °C with maximum daily temperatures between 17.8 - 27.5 °C. Daily evapotranspiration was strongly related to temperature, VPD and net radiation, with a total of 23.2 mm recorded over the

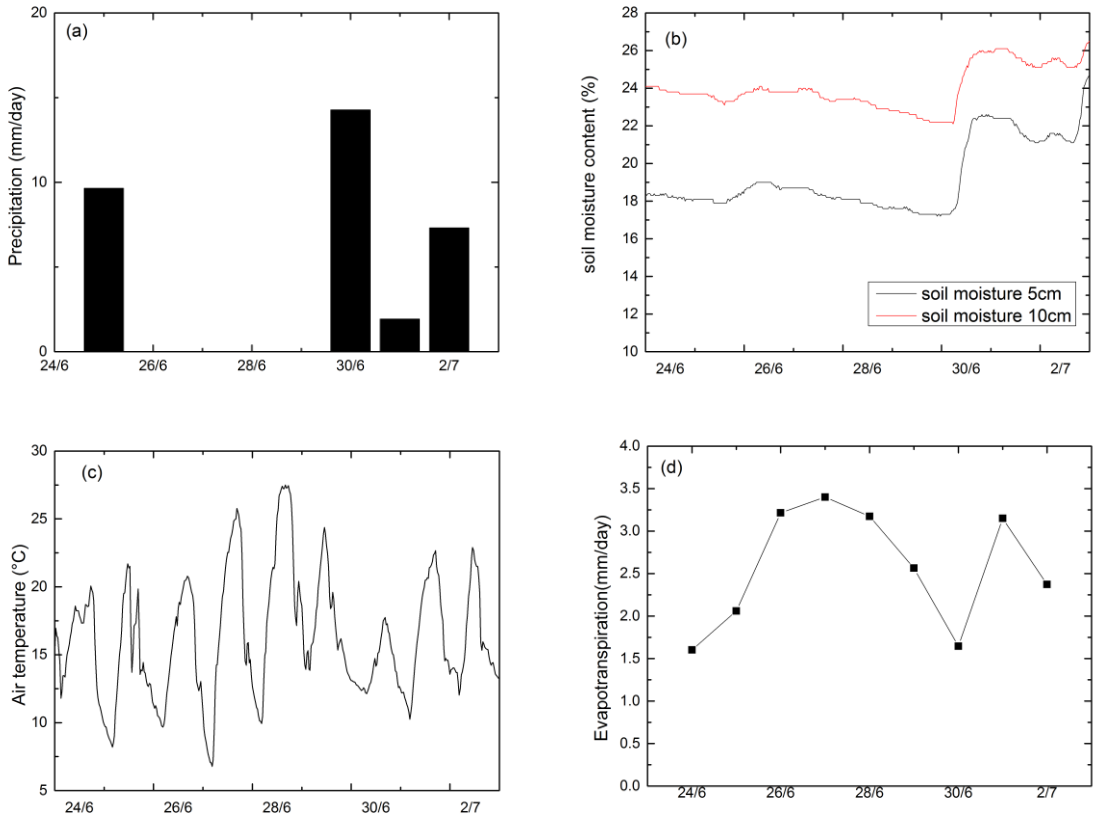

Figure 3.4: Half hourly plots of (a) precipitation, (b) soil moisture at 5 and 10 cm, (c) air temperature and (d) daily values of evapotranspiration measured using the eddy covariance system for the period June 24th - July 2nd, 2014.

experiment, with the highest daily values occurring during the dry period from the 26th – 28th. Figure 3.5 shows the friction velocity and the virtual stability measured using the eddy covariance system. The friction velocity was in general quite low at this site, following a diurnal pattern during the period of high solar radiation from the 26th – 29th. The atmospheric stability was generally unstable during the

Die approbierte gedruckte Originalversion dieser Dissertation ist an der TU Wien Bibliothek verfügbar.
The approved original version of this doctoral thesis is available in print at TU Wien Bibliothek.
TU Bibliothek Your knowledge hub WIEN

daytimes except for the period during the passage of the frontal system, where the stability was very close to neutral.

3.6.2 Evapotranspiration partitioning

The steady state assumption for the stable isotope analysis does not hold in the morning, however it is usually met in the afternoon (Yepez et al., 2005). The analysis in this paper is hence limited to the time from 10:00 – 17:00, as this corresponds to the time periods with the largest amounts of solar

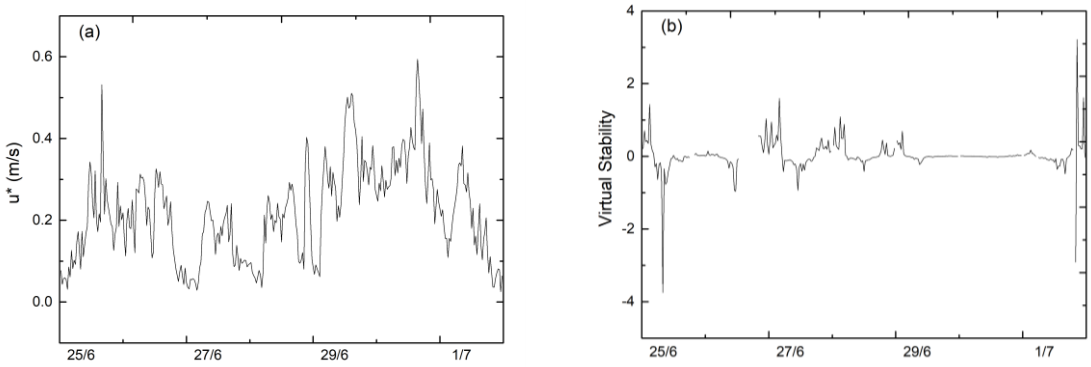

Figure 3.5: Half hourly plots of (a) u^* and (b) virtual stability over the period June 25th - July 2nd, 2014.

radiation and hence evapotranspiration, there will only be a limited effect on the results. Data from the 30th and during and directly after precipitation events are also excluded, due to the strong neutral stability and change in the atmospheric water vapor resulting from the passage of the frontal system or interception, resulting in values of *Ft* in excess of 100%. However, due to the very strong concentration gradients near the surface when soil evaporation is very close to zero, the inversion matrix can become ill-conditioned resulting in values over 100% for the LNF method. Therefore, in general values of *Ft* higher than 110 % and lower than –20 % were excluded from the results, allowing for some uncertainty (Wei et al., 2015). For purposes of averaging *Ft* was capped at 100 %.

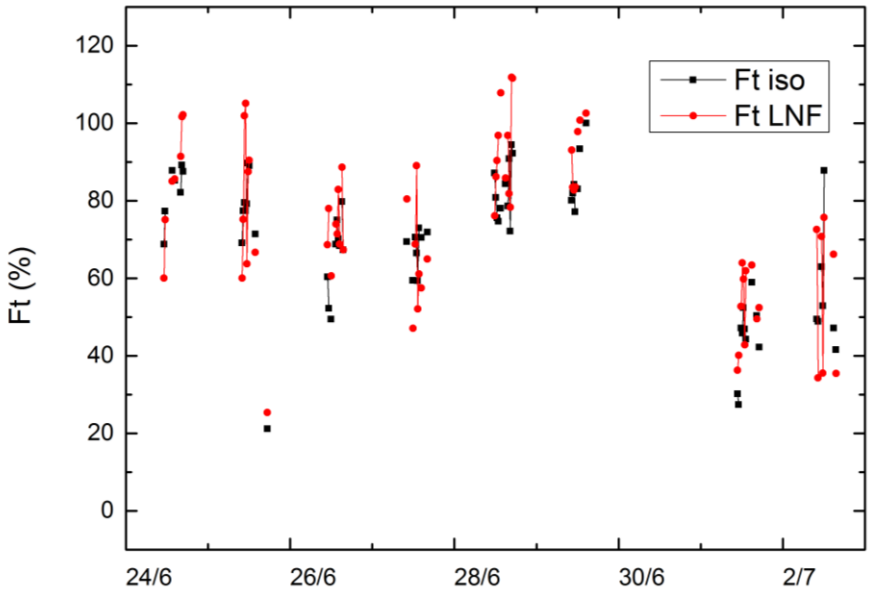

Figure 3.6: Twenty-minute values of *Ft* using the LNF (red circles) and isotope (black squares) methods over the entire experimental period.

Using the stable isotope method, the daily averages of Ft_{ISO} ranged from 43.0 – 88.5 %, with an average value of 67.5 % following a pattern of decreasing after precipitation events and steadily increasing over

Die approbierte gedruckte Originalversion dieser Dissertation ist an der TU Wien Bibliothek verfügbar.
The approved original version of this doctoral thesis is available in print at TU Wien Bibliothek.
TU Bibliothek Your knowledge hub WIEN

the following days. Using the LNF method, *Ft* (Ft_{LNF}) was found to range from 52.3 – 91.5 % with an average value of 73.5 %. Figure 3.6 shows a comparison of the two methods for the entire experimental period. While the two methods show a high level of agreement on average, on the 29th and 1st July the LNF method estimates much higher values of *Ft*, on the 29th 91.5 % versus 81.7 % and on the 1st 52.3 % versus 44.5 %. Ft_{LNF} however shows much greater variance on these days than Ft_{ISO}, with Ft_{LNF} also estimating values of *Ft* over 100 % on the 28th.

Daily *ET* is strongly dependent on solar radiation and temperature, with the highest values of *ET* measured from the 26th – afternoon of the 29th. Both Ft_{LNF} and Ft_{ISO} show a similar pattern, with increasing values estimated during this time period. Conversely the soil moisture content in the upper level of the soil at 5 cm was measured decreasing from 19.0 % to 17.2 %. Following the precipitation event on the 29th - 30th the soil moisture content was recharged up to 22.6 %, leading to a marked decrease in Ft_{LNF} from 92.0 % to 52.3 %.

3.6.3 Method comparison

Figure 3.7 shows a comparison of the two methods on the 26th of June during the daytime period. The uncertainty on the Ft_{iso} estimates was calculated using the single isotope, two source mixing model of Phillips and Gregg (2001). In the late morning period, Ft_{LNF} consistently makes higher estimates of *Ft*, with a difference of up to 25.8 % at 11:00, although closer agreement is noted during the afternoon period, following a gap in the results of Ft_{LNF} from 12:00 – 13:30 due to overestimation of *Ft*. During this period Ft_{ISO} continued to give realistic estimates of *Ft*. Throughout the early afternoon Ft_{ISO} and Ft_{LNF} steadily increase with *ET*, with Ft_{LNF} increasing at a much faster rate to 80 – 90 % by 15:00 while Ft_{ISO} exhibits a slower rate of increase, reaching a maximum of 80 %.

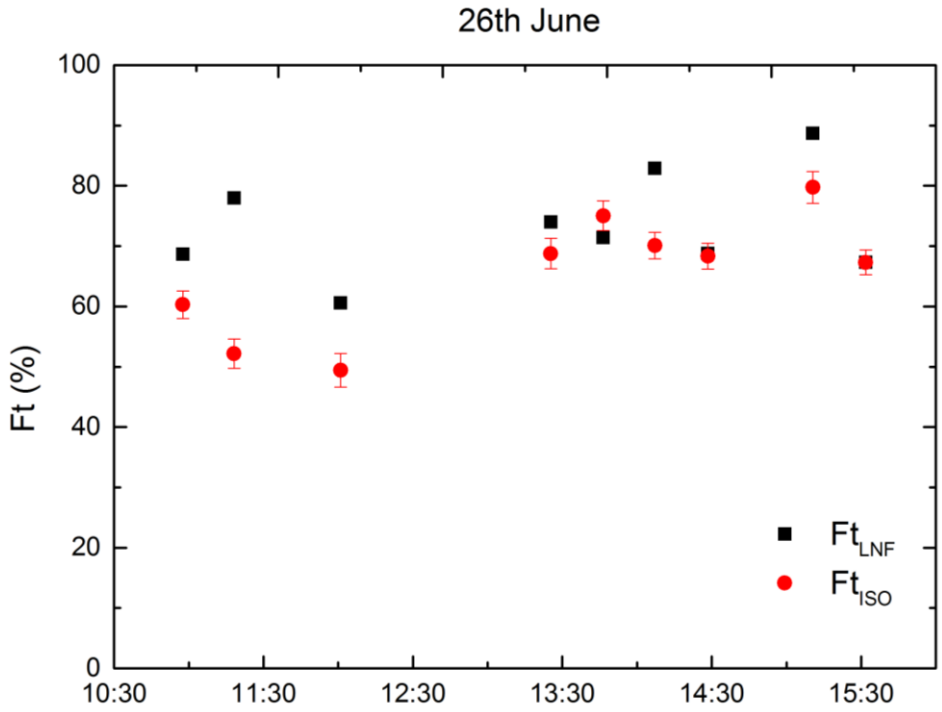

Figure 3.7: Comparison of the two methods on the 26th of June during the daytime period.

Ft was also estimated using the Leuning set of parameterizations for u^* and T_L. In this case Ft_{LNF} varied from 50.1 – 91.4 % with an average of 75.0 %. Figure 3.8 shows a scatterplot of 20 minute values of *Ft* using the isotope and (a) LNF Raupach and (b) LNF Leuning methods. Both methods give similar R^2 values, 0.65 and 0.63 respectively with the Raupach parameterisations performing slightly better.

Die approbierte gedruckte Originalversion dieser Dissertation ist an der TU Wien Bibliothek verfügbar.
The approved original version of this doctoral thesis is available in print at TU Wien Bibliothek.

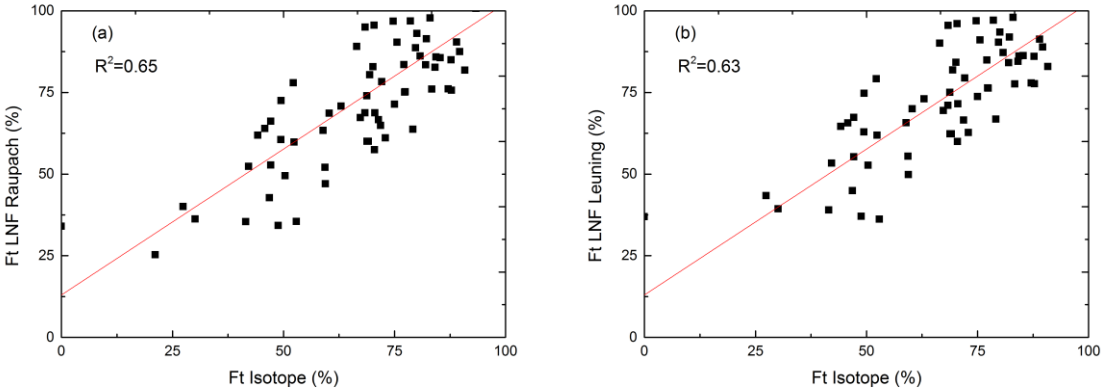

Figure 3.8: Scatterplots of 20 minute values of *Ft* using the isotope and (a) LNF Raupach and (b) LNF Leuning methods for the entire experimental period.

3.7 Discussion

In this study we utilize the LNF and ISO methods to partition evapotranspiration. Both methods use water vapor concentration measurements from inside the plant canopy, however the stable isotope method requires much more additional data as well as equipment and labour for measuring and analysing the isotope samples.

The average *Ft* estimated by the LNF method was 74.0 % and using the stable isotopes 67.5 %. The correlation between the two methods was 0.65. These compare well with measurements using lysimeters which gave a range of 71 – 75 % (Liu et al., 2002, Kang et al., 2003) for maize, 69 – 87 % for olive trees (Williams et al.,2004), and 20 – 100% over the course of the entire season for rice (Wei et al., 2015). Using chamber-based measurements to directly measure the isotopic values, Wu et al. (2016) estimated *Ft* for the entire vegetative growing section to be ~55 %, and ~70 % using the Craig-Gordon based model approach, with the difference attributed to deviation in measuring δE using the chamber method. Using isotope tracers Ma et al. (2018) found that for a winter wheat field the value of *Ft* over the entire crop season did not vary significantly with the type of irrigation treatment, however the value of *Ft* for each stage of the growing season did. While an average value for *Ft* of 65 % in line with similar experiments using 5 different irrigation methods was found, between these methods a difference of up 25 % in *Ft* was noted. In non-irrigated catchments the precipitation amounts and intervals must be analyzed in order to apply the results from year to year. During the course of this experiment, both a short but intense (~10 mm/hr) and a less intense but longer duration (~1 mm/hr) precipitation event were recorded, allowing for the changes in *Ft* to be seen. The response of the soil moisture at 5 cm to the intense event was much less than for the longer event, with a large amount of runoff recorded. This results in a much smaller decrease in *Ft* on the following day, 73.4 % versus 52.3 %.

Over the course of the experiment the LNF method shows a pattern of slightly larger estimates of *Ft*, particularly on the 29th and 1st of July. On the 1st this exceptionally large difference is possibly due to the higher levels of soil evaporation after the large precipitation event on the previous day, resulting in reduced water vapor concentration gradients near the surface, which will have a greater effect on the LNF method as it uses less additional data. On the 29th Ft_{LNF} estimated *Ft* to be over 100 %, however this can be explained due to measurement errors as *Ft* approached 100 %, with Wei et al. (2015) reporting similar values while using the stable isotope method. The only slight change in the performance of the LNF method depending on the parameterisation for the turbulent statistics, would suggest either parameterisation can be used. Comparing LNF modelled and eddy covariance measured latent heat flux estimates, Santos ett al. (2011) also noted only slight changes to the results.

Die approbierte gedruckte Originalversion dieser Dissertation ist an der TU Wien Bibliothek verfügbar.
The approved original version of this doctoral thesis is available in print at TU Wien Bibliothek.

Over the course of the experiment the isotope method proved to be less affected by the environmental conditions, excepting the steady state condition that limits the method to the daytime periods. During these periods the LNF method gives 45.2 % less data than the isotope method, with a lot less useable data on days where there is less coupling between the canopy and the atmosphere (25th and 29th) due to the changing conditions and precipitation. This reduction in results is offset however by the lower requirements of additional data, with the isotope method needing isotope measurements of the air, plants and soil. An advantage of using the LNF method which gives a high temporal resolution is that the response of the fraction of transpiration to rain events can be seen in Figures 3.6 and 3.8 and used for adjusting transpiration estimates measured using the eddy covariance method. Isotope methods that use only weekly sampling of the soil water (Santos et al., 2012) will not be able to capture changes in δ_E, however even the daily sampling of the soil and plant isotopes in this experiment is limited due to sudden short precipitation events and the isotopic steady state assumption. While the air sampling can be performed at a high resolution using the Picarro device, the sampling of the plants and soil had to be done manually in this experiment, resulting in a much higher workload and limiting the overall length of the measurement campaign. Measurement devices such as leaf and soil flux chambers which allow for automatic sampling of soil and plant isotope values have been developed in recent years (Wu et al., 2016), however they are still limited by the heterogeneity of field conditions, requiring a number of different devices of considerable expense.

With an estimate for *Ft* during the growing season, where *ET* and *Ft* change in response to not only the environmental conditions but due to the changing physical properties of the plant, compared to the more stable initial and mid-season stages of plant development (FAO-56). As it is difficult and expensive to make full season measurements at a high temporal resolution,

An alternative approach is to use our estimate for *Ft* and an evapotranspiration model. Using a modified version of the FAO-56 method, where the crop coefficient is separated into a crop basal coefficient and an evaporation coefficient, Ding et al. (2013) was able to partition the *ET* by modifying the crop basal coefficient according to crop leaf cover. The model was then validated using soil heat flux and lysimeter measurements. During the vegetative season however the heterogenous canopy cover and rapid growth of the maize plants can lead to errors when upscaling the individual measurements to the field scale, to avoid this the LNF method which is based on vapor measurements allowing for an averaging through the canopy could be used.

3.8 Conclusions

In this experiment the fraction of evapotranspiration that was due to transpiration was estimated for a maize field using two methods, the isotope measurement based stable isotope method, and the Localised Near Field theory of Raupach based on an inverse Lagrangian modelling approach. Both methods are based on measurements of the water vapour concentration within a plant canopy, however they vary greatly in experimental procedure, required assumptions, and data analysis. The two methods overall gave similar results, with the fraction of transpiration ranging from 43.0 – 88.5 %, with an average of 67.5 % for the isotope method, while the fraction of evaporation was found to range from 52.3 – 91.9 % with an average value of 74.8 % for the Localised Near Field method. These values were found to be in line with results from similar experiments for this stage of maize development. However, the stable isotope method was found to return a much larger amount of useable data, as well as having a lower variance. This is offset by the need for more additional measurements and analysis, as well the uncertainty due to the need for the Isotopic Steady State assumption. Future experiments should be conducted using chamber methods when possible to account for this. The parameterizations used for the turbulent wind statistics for the Localised Near Field method were found to vary only slightly. Care must also be taken when applying the results over larger time periods or year to year, to account for different precipitation regimes if the field is not irrigated, with different precipitation events giving different soil moisture and hence soil evaporation responses.

Die approbierte gedruckte Originalversion dieser Dissertation ist an der TU Wien Bibliothek verfügbar.
The approved original version of this doctoral thesis is available in print at TU Wien Bibliothek.
TU Bibliothek Your knowledge hub WIEN

4. Spatial patterns of evaporation in a small catchment

4.1 General

The objective of this study is to obtain long term spatial measurements of the evaporation in a small agricultural catchment and to analyse the distribution and the controls of the patterns of evaporation. To capture the spatial variability of the entire catchment, this project will use a number of mobile eddy covariance devices including a fixed tower located in the centre of the catchment, as well the catchment and subcatchment water balances.

The present chapter is based on the following scientific publication:

Hogan, P., Szeles, B., Rab, G., Oismueller, M., Pavlin, L., Parajka, J., Strauss, P., & Blöschl, G. (2022). *Hydrological Sciences Journal*. Under review

4.2 Key Points

Spatial differences can be seen between subcatchments at different timescales. Seasonal patterns can be seen between the eddy covariance stations due to changes in land cover resulting from the agricultural land use cycle due to the variations in leaf and root area density during the growing season. At the subcatchments, annual differences in evaporation connected to the presence of vegetation with roots connected to the groundwater result in higher evaporation estimates than at wetland subcatchments, which tended to dry out in drier years.

Year to year variability in monthly evaporation measured by the eddy covariance stations was driven primarily by net radiation and temperature. Precipitation was the main driver of annual water balance-based evaporation estimate, versus net radiation for the annual eddy covariance-based estimate method.

Year to year variability of the catchment evaporation methods is consistent when storage and leakage are estimated during years with above average precipitation.

4.3 Abstract

The measurement and modelling of evaporation (E) poses several challenges at all scales due to the heterogeneity of surface and atmospheric conditions. At the small catchment scale E is usually estimated by modelling or upscaling measurements made at a single point which may not be representative for the entire catchment, because the spatial patterns of evaporation and their drivers are rarely known.

In this study distributed evaporation measurements are made and combined with solar radiation, precipitation, discharge and soil moisture data to study the patterns of E in the 66 ha Hydrological Open Air Laboratory (HOAL) in Petzenkirchen, Austria. A network of three meteorological stations equipped with eddy covariance devices, consisting of two semi-mobile tripods and a fixed tower, are used to measure E at a number of different locations within the catchment for 8 years. Discharge measurements at the tributaries and outlet of the main catchment allow for E to be estimated for 6 subcatchments using the water balance method.

Year to year variability in monthly E measured by the eddy covariance stations is found to be driven primarily by net radiation (R^2 = 0.91 and 0.85 for the central weather station and mobile stations respectively) and temperature (R^2 = 0.77 and 0.74) and annual E by net radiation (R^2 = 0.50). Year to year variability in water balance-based E estimate (R^2 = 0.81) was driven by precipitation. The two methods are found to be consistent when the storage and leakage are accounted for with R^2 = 0.80, while R^2 = 0.37 if storage and leakage are not considered.

Spatial differences can be seen between subcatchments at different timescales and are consistent between the methods. The largest differences (up to 50 mm/3 months between the eddy correlation stations) occur during the adult stages of crop development and during periods of low soil cover due to

Die approbierte gedruckte Originalversion dieser Dissertation ist an der TU Wien Bibliothek verfügbar.
The approved original version of this doctoral thesis is available in print at TU Wien Bibliothek.
TU Bibliothek Your knowledge hub WIEN

agricultural land use. In the agricultural and forested subcatchments E is higher than in wetland subcatchments because of the presence of vegetation with roots connected to the groundwater resulting in higher E estimates while the top soil layer of the wetlands tends to dry out more quickly in dry years and becomes disconnected from the atmosphere.

Die approbierte gedruckte Originalversion dieser Dissertation ist an der TU Wien Bibliothek verfügbar.
The approved original version of this doctoral thesis is available in print at TU Wien Bibliothek.

4.4 Introduction

Evaporation (*E*) is one of the most important processes in describing the land surface- atmosphere interactions as it connects the energy and water balances. Knowledge of the spatial variations in *E* is important for agricultural water use and conservation at a local level and for improving estimates of regional water balances at larger scales (Bastiaanssen et al., 2005).

Research on *E* can be roughly divided into five spatial scales of study: global and continental scales, regional scales, meso-scale (~20-500km^2), field/canopy scales and leaf scale. Each scale requires different methodology in order to estimate *E*, with significant differences in the spatial and temporal limitations and accuracy between the methods. At the field scale *E* can be measured directly providing increased temporal resolution, however the heterogeneity of the terrain and vegetation imposes a spatial limitation on the estimates (Shimzu et al., 2015). In order to bridge the gap between the meso-scale and the field scale this heterogeneity must be accounted for. A combination of ground-based measurement systems and remote sensing imagery or upscaling has frequently been used. The SMACEX and BEAREX08 experiments used eddy covariance towers and remote sensing temperature and vegetation products to investigate *E* in agricultural catchments over short term periods, finding spatial and temporal differences between the different crop types (Kustas et al. 2005; Anderson et al., 2012). Prueger et al. (2005) measured spatial and temporal variations due to differences in canopy cover and soil moisture between maize and soy crops, with the Bowen Ratio of maize being twice that of soy at the start of the experiment before converging due to increased precipitation (*P*) and leaf area as the crops approached maturity. Hssaine et al., (2021) estimated large spatial variations in latent heat flux (*LE*) using soil moisture remote sensing products in combination with Landsat imagery, with differences of up to 500 Wm^{-2} between vegetated and bare fields. Armstrong et al. (2019) used thermal and visible images from an unmanned aerial vehicle and eddy covariance measurements to estimate *E* according to net radiation (*Rn*) across a mixed wetland/agricultural area for one day, reporting lower rates of mean daily *E* where vegetation was less dense and higher rates were associated with densely vegetated areas and wetland fringes. Long term studies of the spatial differences in *E* at the small catchment scale are however lacking.

The catchment water balance method can also be used to estimate interannual spatial and temporal variability in *E* at various scales. While good convergence of the catchment water balance and eddy covariance methods in smaller catchments has been reported (Wilson et al., 2001; Denager (2020), considerable variability may be found on a year-to-year basis with Scott et al. (2010) reporting a range of -10 to 17%. In addition, storage and leakage might become non-negligible in smaller catchments with Tie et al. (2018) reporting water balance-based estimates of *E* over 100 mm higher compared to eddy covariance-based, which they postulated might be due to subsurface runoff. At this scale the water balance is evaluated over the entire catchment area, however, the gauging of tributaries could be used to provide spatial information on the variability of *E* on a subcatchment basis.

To utilise information on the spatial patterns of *E* the spatial and temporal drivers must also be known. These can vary between climate and ecosystem. At regional scales in arid and semi-arid areas landuse (Bouwer et al., 2008) and *P* (Valayamkunnath et al., 2018) are identified as key spatial and temporal drivers, while in humid areas the drivers of the variability are more complex, with wind speed, humidity, precipitation, soil moisture, temperature, solar radiation and landuse (Xu et al., 2006; Zhang et al., 2010; Jiang et al., 2018) all being variously reported as responsible for variations in evaporation. Less is known about drivers at the small catchment scale, as intensive measurement campaigns tend to be of short duration. Hatfield et al. (2011) found that short term spatial variation among different crop fields could be attributed to variations in solar radiation due to cloud cover, precipitation, and soil water availability due to soil type and rooting depth.

Most studies investigating the spatial patterns of *E* tend to be of limited duration or temporal resolution due to the high instrumentation requirements or limited to regions with good climatic conditions for

Die approbierte gedruckte Originalversion dieser Dissertation ist an der TU Wien Bibliothek verfügbar.
The approved original version of this doctoral thesis is available in print at TU Wien Bibliothek.
TU Bibliothek Your knowledge hub WIEN

remote sensing imagery with few long-term studies available. Accordingly, the objectives of this paper are to investigate (1) the spatial patterns of evaporation and (2) their drivers, in a small agricultural catchment at monthly to yearly timescales. The work is based on 8 years of eddy covariance and water balance measurements at the Hydrological Open Air Laboratory (HOAL) in Petzenkirchen in Lower Austria, Austria.

4.5 Materials and Methods

4.5.1 Experimental Site

The HOAL is located in the western part of Lower Austria (15° 9' E, 48° 8' N) (Blöschl et al., 2016). It is an agricultural catchment, 66 ha in size with the majority of the land being used for crops (87%), with a smaller amount being used for forest (6%) and the remainder consisting of meadow (5%) and paved surfaces (2%). The catchment altitude ranges from 268m to 323m with a mean slope of 8%. There is a large degree of variation in the soil composition throughout the catchment with clay content varying from 6-39%. The main catchment area, which is drained at the outlet MW, can be divided up into a set of subcatchments with different runoff generation mechanisms. The stream at the riparian section of the catchment is fed by the inlet Sys4, which drains the upper part of the catchment. Sys4 receives contributions from two tile drainage systems, resulting in it displaying similar characteristics to the two perennial tile drainage subcatchment Sys2. Sys3 has the characteristics of a mixed tile drain/wetland area while A2 is a perennial system with quick event runoff from wetlands. Sys1 is identified as a deep aquifer spring located on the east side of the stream bank. Frau2 is a tile drainage system with ephemeral flow characteristics which drains a part of the agricultural field west of the stream. A part of this network south of Frau2 stopped functioning in 2014 and is not included in this analysis (Figure 4.1).

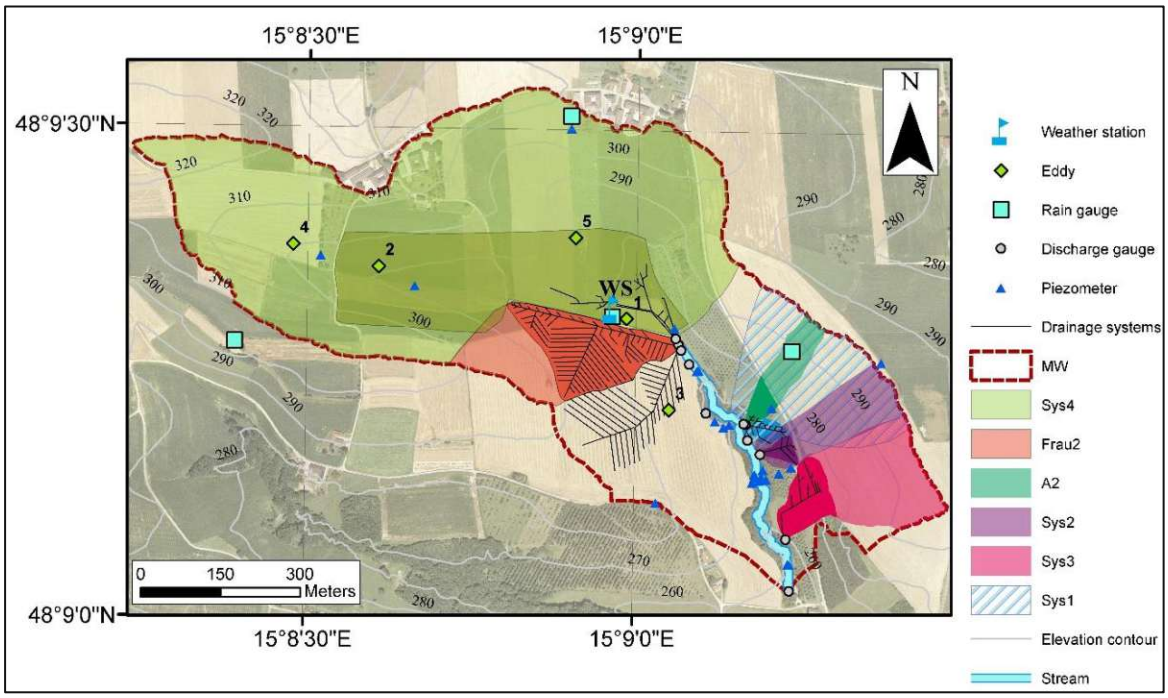

Figure 4.1: Map of the catchment and instrumentation network. The locations of the temporary eddy covariance stations are numbered 1 - 5 according to Table 4.1, while the central weather station is marked as WS. Subcatchment areas are displayed as shaded areas, with maximum and minimum areas shown for each subcatchment. Minimum areas are highlighted as a darker shade. Maximum subcatchment areas are delineated according to topography, while minimum areas exclude areas which may be affected by local drainage networks.

Die approbierte gedruckte Originalversion dieser Dissertation ist an der TU Wien Bibliothek verfügbar.
The approved original version of this doctoral thesis is available in print at TU Wien Bibliothek.

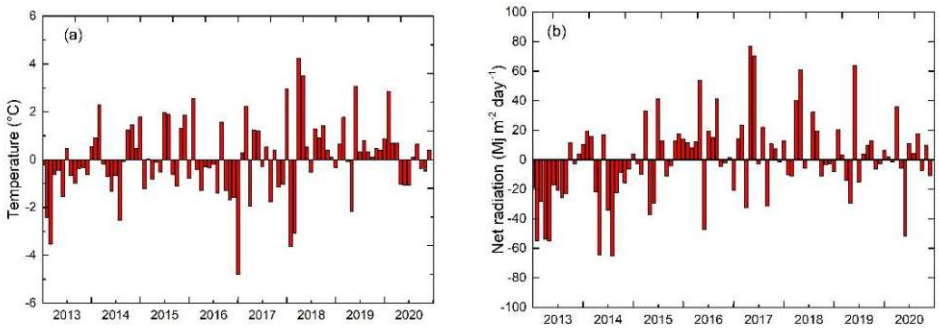

Figure 4.2: Monthly values of the (a) deviation from the average monthly temperature, and (b) deviation from the average monthly net radiation sum.

The mean annual temperature (*T*) at the catchment ranged from 9.4 - 10.7 °C over the course of the experiment with an average of 10.1 °C. Annual *Rn* varied from 1.01 - 1.23 MW/m^2 with an average of 1.14 MW/m^2. Figure 4.2 shows the deviation from (a) the average monthly *T* and (b) *Rn*. 2013 and 2014 recorded below average values for the summer months, with 2018 and 2019 having the warmest growing seasons.

4.5.2 Instrumentation and measurements

The weather station at the centre of the catchment is equipped with three temperature and humidity sensors (HMP - 155, Vaisala) at 2 m, 5 m, and 10 m heights, three wind sensors (Windsonic 232, Gill) at 2 m, 5 m, and 10 m heights, a 4 - component net radiation sensors (CNR-4 Kipp and Zonen) and from 2012-2013 and 2015 - 2020 two soil heat flux plates (HMP01, Huskeflux). The meteorological data is measured at 1 - 5 second frequency and 1 - and 30-minute averages are calculated and stored on CR3000 datalogger (Campbell Scientific).

E is measured at the catchment using a network of 3 eddy covariance devices, two open-path systems (IRGASON, Campbell Scientific) and one closed-path (EC-155, Campbell Scientific), from September 2012 to present. At the weather station an IRGASON (Campbell Scientific) open path eddy covariance sensor was installed on a 10 m tower at a height of 2.7 m and an orientation of 270° on the 1/8/2012. This was then replaced on the 26/8/2015 by the closed path eddy covariance sensor. The two other eddy covariance devices were installed at various locations on tripods (Figure 4.3) within the catchment according to the agricultural crop rotation (see Table 4.1). In 2014 and the first half of 2015 the soil heat flux plates were installed alongside the closed path device at locations 2 and 3. The installation heights of the devices were adjusted in relation to the surrounding vegetation, to control the footprint size.

Table 4.1: Installation details of eddy covariance sensors (see Figure 4.1 for locations)

From	To	Location	Device type	Installation height (m)	Direction (°)
1/8/2012	26/8/2015	1	IRGASON	2.7	270
26/8/2015	ongoing	1	EC155	2.7	270
1/1/2014	1/1/2015	2	EC155	2.7	270
1/1/2015	26/8/2015	3	EC155	2.2	270
26/8/2015	4/8/2016	3	IRGASON	2.2	270
1/6/2015	ongoing	4	IRGASON	3.5	270
4/8/2016	ongoing	5	IRGASON	4.5	180

Die approbierte gedruckte Originalversion dieser Dissertation ist an der TU Wien Bibliothek verfügbar.
The approved original version of this doctoral thesis is available in print at TU Wien Bibliothek.
TU Bibliothek Your knowledge hub WIEN

Measurements of the three-dimensional wind speed and water vapor density (IRGASON) /water vapor mixing ratio (EC155) were made at 10 Hz and saved on a CR3000 datalogger (Campbell Scientific). The raw measurements were then processed to sensible and latent heat fluxes online and the raw data and fluxes from the weather station are transferred directly to a desktop computer across a fiber optic network cable.

Figure 4.3: Eddy covariance system (IRGASON) mounted on a 2.5 m tripod at a mobile station.

From 2013 - September 2015 fluxes were processed offline using the Eddy-Covariance Software TK3 from Bayreuth University (Mauder and Foken, 2011). After September 2015 the fluxes were calculated online at the dataloggers using the EasyFlux software from Campbell Scientific. This was done to reduce data loss due to problems with the CF storage cards malfunctioning at the dataloggers; as the processed fluxes have a much lower storage space requirement than the raw data, they could be stored locally in the logger memory. Measurements with a low signal strength or spikes as flagged by the device are removed by the softwares before calculating the covariances. The covariances are calculated for a 30-minute averaging period. During the processing of the fluxes a number of corrections are applied to the calculated covariances:

(1) A double rotation of the coordinate system

(2) The Moore correction for low-frequency response (Moore, 1986)

(3) The sonic air temperature correction for the sensible heat flux (*H*) (Schotanus et. al 1983)

(4) The WPL correction for air density fluctuations (Webb et al. 1980)

The *LE* data from the closed-path sensor was found to be unreliable, as the optical lenses of the infrared gas sensor are quickly obscured by dust particles not filtered by the device intake, resulting in a non-linear decrease in signal strength of the water vapor mixing ratio which cannot be later corrected. The *LE* at this location is instead calculated from the energy balance using *H, Rn,* and the soil heat flux *G*.

$$\boldsymbol{Rn - G = LE + H} \tag{4.1}$$

In Eq (4.1) storage of energy in the air and vegetation is neglected on account of the low measuring and vegetation heights. In addition, lateral advective fluxes are not considered here, as there is no irrigation taking place in the catchment which could result in large temperature gradients between fields during dry conditions. To take into account the lack of energy balance closure (see 4.6.1), all components of the energy balance were measured at the site in 2013 (Section 3.1) and the measured closure (26%) is

Die approbierte gedruckte Originalversion dieser Dissertation ist an der TU Wien Bibliothek verfügbar.
The approved original version of this doctoral thesis is available in print at TU Wien Bibliothek.
TU Bibliothek Your knowledge hub WIEN

subtracted from the available energy (*Rn* - *G*). The processed fluxes are then controlled for implausible values (-30 > *LE* > 500, -100 > *H* > 700) and the *LE* is converted to evaporation rates.

When no data was available due to a failure of the device, 30-minute daytime gaps were filled using *Rn* when available. From the last good quality *LE* value, the *LE/Rn* ratio was calculated and used to fill *LE*. Daily gaps were filled using the FAO-56 Penman Monteith method (Allen, 1998).

The measurements from the individual eddy covariance stations are upscaled to the catchment area according to the landuse corresponding to each sensor; assuming that local differences in soil moisture between the different fields were small so that *E* measured at one landuse was valid for all similar fields in the catchment, and that the riparian zone had a *E* rate of 1.1 times the grassland meadow at the weather station, due to its predominantly forested vegetation with wet understory cover, estimated from a modified crop coefficient for tree plantations from Fischer et al. (2011) and the crop coefficient for small-vegetation-wetland from Allen et al. (1998).

In this study precipitation time series *(P)* observed by four weighing rain gauges distributed throughout the catchment for the period 2013 - 2020 were used. For the water balance calculations, the one-minute observations of the four sensors were averaged and then summed for every hour. As this is a lowland catchment, relatively small amounts of snowfall occur each year with less than 5 days of snow cover reported in 2014, 2015, 2016 and 2020. In the remaining years, an average of 15 days snow cover was observed, with an average snowfall of ~10 cm occurring 2 times per year. As these are relatively small amounts, a further analysis of snow cover was not considered in this study. Runoff time series were observed at the catchment outlet and at 6 tributaries (Figure 4.1). Runoff was monitored at the outlet of the catchment (MW) by a calibrated H-flume with a pressure transducer, while at the inlet (Sys4), the tile drainage systems (Frau1 and Sys2), the deep aquifer tile drain (Sys1), the tile drain/wetland (Sys3) and at a wetland (A2) H-flumes and pressure transducers are used to monitor the flow. In 2019 the flumes at the tributaries were upgraded. Details on the sensors are found in Blöschl et al. (2016), while the runoff generation mechanisms are described by Exner-Kittridge et al. (2016) and Szeles et al. (2018). For the water balance calculations, the one-minute observations were averaged for every hour and scaled by the (sub)catchment area. The subcatchment areas were delineated according to topography. However, there is some uncertainty regarding the true size of certain subcatchments as the local drainage networks may divert water from the outer fields out of the subcatchment. For this reason, minimum and maximum areas, referred to as *min* and *max*, have been used in this study for these subcatchments.

Soil moisture (*SM*) was measured using a soil moisture sensor (Spade TDT, Jülich) located at the weather station with sensors located at 5, 10, 20 and 50 cm depths below the ground surface. The groundwater level in the riparian zone along the stream is monitored using 19 piezometers, with a temporal resolution of five minutes. As the groundwater levels in the riparian zone close to the stream are generally higher compared to the catchment average groundwater levels which might introduce a bias, 8 piezometers were installed in deep boreholes further away from the stream on the hillslopes and valley bottom of the catchment in 2017. A good agreement was found between the dynamics of these boreholes and the riparian zone piezometers, indicating that any potential bias in previous years would be small. The storage change at the catchment was estimated by first calculating the mean January ground water level at each station. The change in level from year to year was then calculated and multiplied by a specific yield value of 0.025 to get the yearly storage change value. These values were then interpolated using Thiessen Polygons and the mean change was then calculated over the entire catchment. Ordinary Kriging was also used delivering similar results for most years, however since there are very few points on the edges of the catchment area, which might affect the kriging method, the Thiessen method was preferred for the full analysis.

Die approbierte gedruckte Originalversion dieser Dissertation ist an der TU Wien Bibliothek verfügbar.
The approved original version of this doctoral thesis is available in print at TU Wien Bibliothek.
TU Bibliothek Your knowledge hub WIEN

4.5.3 Crops and growing seasons

The crops grown are predominantly corn, winter wheat and rapeseed. Figure 4.4 shows the landuse in each field from 2013-2020 and the locations of the eddy covariance stations. Winter crops are generally planted in late October/ November and harvested in July. Maize crops are sown in April and harvested in September/ early October depending on the weather conditions and the resulting moisture content of the plants. Table 4.2 shows the planting and harvesting dates for fields in the immediate locality of the eddy covariance stations.

Table 4.2: Planting and harvesting dates for the winter and summer crops at mobile eddy covariance device locations.

Year	Winter crop harvest	Summer crop sowing date	Summer crop harvest date
2013	18th Jul.	10th May	1st Oct.
2014	1st Jul.	4th Apr.	30 Sep.
2015	10th Jul.	15 - 24th Apr.	7 - 15th Sep.
2016	23rd Jul.	25 - 27th Apr.	30th Sep. - 14th Oct.
2017	14th Jul.	22nd Apr.	25th Oct.
2018	-	20th Apr.	1st Oct./25th Sep.
2019	30th Jun.	16th Apr.	27th Sep.
2020	7th Jul.	11th Apr.	24th Sep.

Die approbierte gedruckte Originalversion dieser Dissertation ist an der TU Wien Bibliothek verfügbar.
The approved original version of this doctoral thesis is available in print at TU Wien Bibliothek.

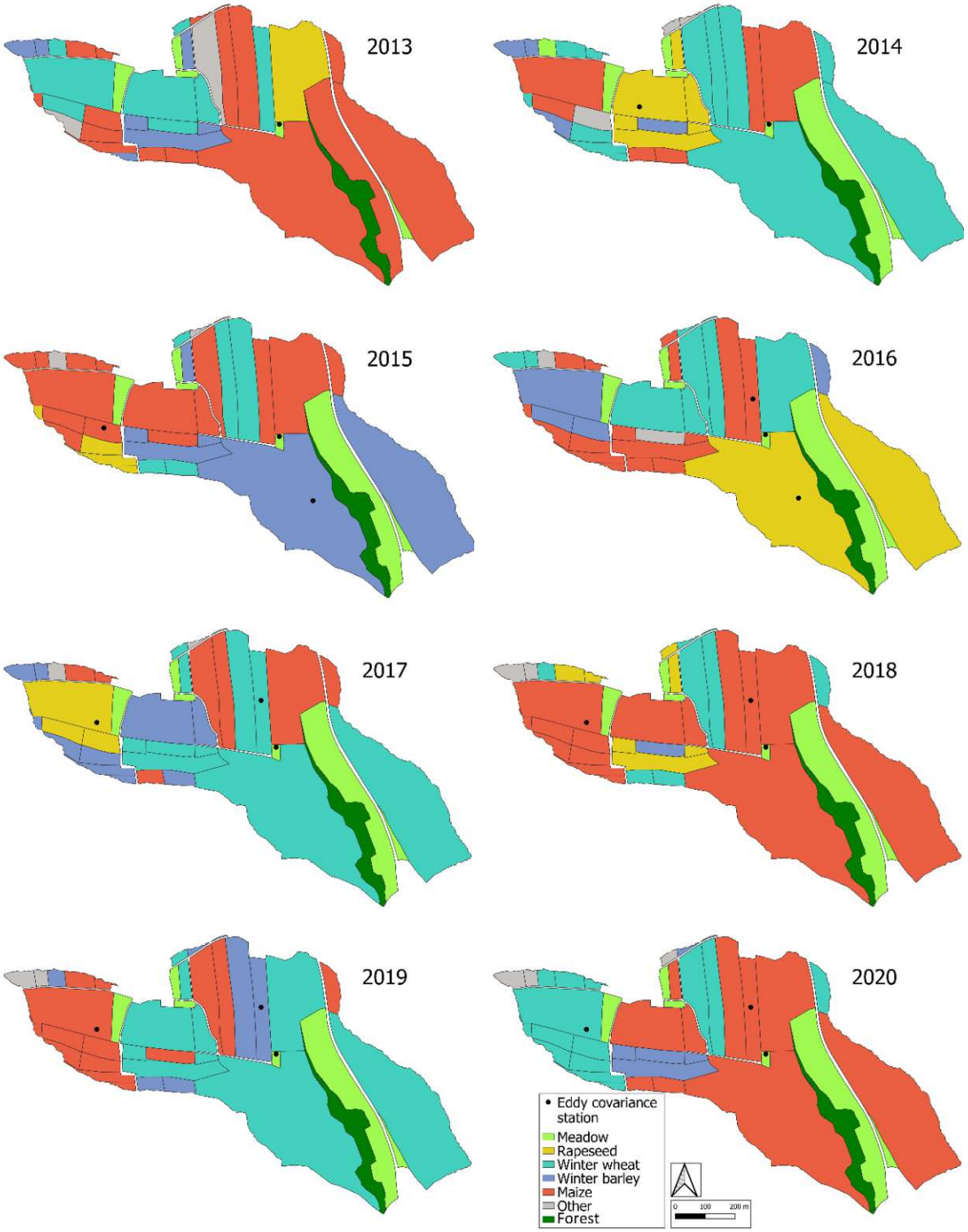

Figure 4.4: Main crop type for each field from 2013 - 2020. Locations of eddy covariance stations marked with black diamonds.

Die approbierte gedruckte Originalversion dieser Dissertation ist an der TU Wien Bibliothek verfügbar.
The approved original version of this doctoral thesis is available in print at TU Wien Bibliothek.

4.6 Results

4.6.1 Energy balance closure

To estimate the reliability of the eddy covariance measurements the energy balance closure is analysed. By measuring all the components of Eq. (4.1) and performing a linear regression of the fluxes measured by the eddy covariance device ($LE + H$) against the available energy ($Rn - G$) the extent of the closure of the energy balance can be estimated.

Using the most complete data set the energy balance was calculated at the central tower for the year 2013 and is shown in Figure 4.5. The regression line slope of 0.74 ($R^2 = 0.93$) falls within the commonly reported range of 10 – 30 % missing energy (Eshonkulov et al., 2019; Leuning et al., 2012; Wilson et al., 2002). The analysis was performed for one entire year to avoid a seasonal bias, however, the possibility of differences on an inter-annual scale cannot be excluded. As the soil heat flux plates were removed in 2014 it was not possible to extend the analysis for longer than one year. Various reasons for the commonly reported imbalance have been put forward (Foken 2008; Leuning et al., 2012; Mauder et al., 2020) e.g., errors in the eddy covariance measurements and flux corrections, neglection of the heat storage in the air, underestimation of the soil heat flux as the storage in the final centimetres cannot be accurately measured, or secondary circulations. Imukova (2016) found for an agricultural catchment at a similar latitude and climatological conditions (Mean annual temperature between 9 and

10 °C and precipitation between 730 and 830 mm) that the latent heat flux is not a major component of the energy balance gap. It is possible to force the energy balance closed by attributing the missing energy to the sensible and latent heat fluxes; however considerable uncertainty remains as to the suitability of the various closure models. As it is not possible to attribute the lack of closure at the catchment to any definite cause and considering the results of Imukova, the latent and sensible heat fluxes were not corrected to close the energy balance in this study, as in other similar studies (Tie et al., 2018; Zhang et al., 2014).

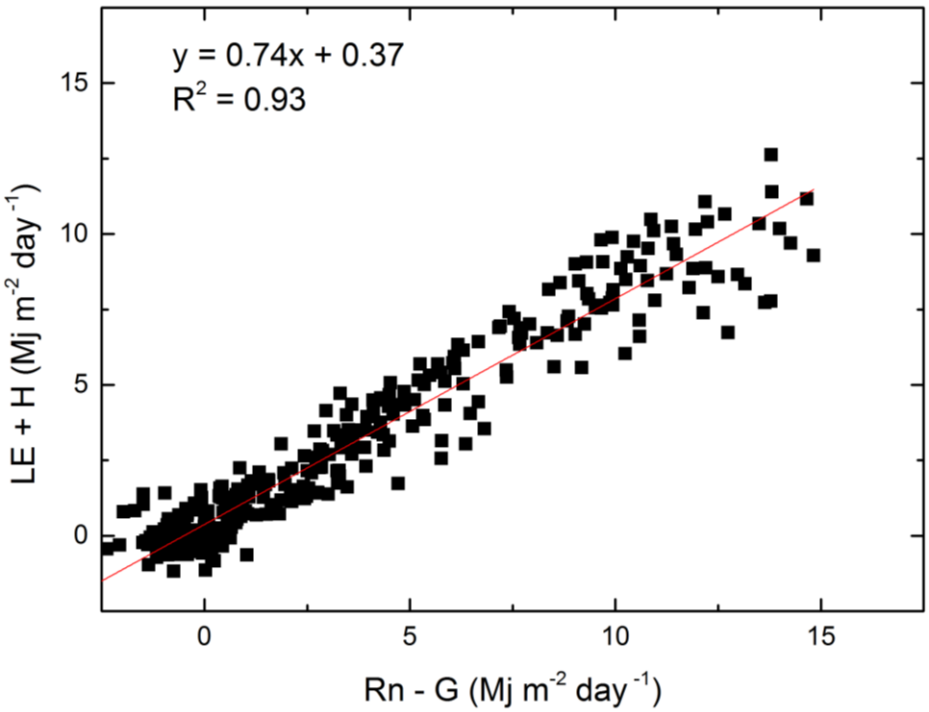

Figure 4.5: The sum of the turbulent fluxes (i.e., the sum of the latent heat flux and the sensible heat flux, $LE + H$) versus the available energy (net radiation minus the soil heat flux, $Rn - G$) for the year 2013.

Die approbierte gedruckte Originalversion dieser Dissertation ist an der TU Wien Bibliothek verfügbar.
The approved original version of this doctoral thesis is available in print at TU Wien Bibliothek.

To check the appropriateness of using the energy balance to calculate *LE* using *H* and a closure factor, the *LE* measured at the eddy covariance device installed at the central tower was compared with the *LE* calculated using *H* measured at the same device for 2013. The two methods compare well with yearly totals of *E* of 391 mm and 374 mm for the measured and calculated *LE* respectively. The difference between the monthly totals of *E* varied between -13.2 and 13.4 %, and -8.6 and 9.1 mm for the period April - September. To determine differences between the different types of eddy covariance device, an open-path and the closed-path device were installed together at the tower for one week in March 2015 and the calculated sensible heat fluxes compared. Minimal difference was found between the two devices, with a scatterplot comparison giving a R^2 coefficient of 0.97 and a slope of 0.974.

4.6.2 Evaporation

Annual *E* at the weather station ranged from 575.3 – 380.3 mm/ year with an average of 505.5 mm/ year. Maximum daily rates of *E* varied from 3.1 mm/ day in 2014 to 5.6 mm/ day in 2015. The relationships between monthly E and the environmental conditions at the catchment are shown in Figure 4.6. Excluding months with a large percentage of gap-filled values, net *Rn* (R^2 = 0.91) and air temperature (*Ta*) (R^2 = 0.77) are the best correlated with monthly *E* measured by the eddy covariance station, with almost no correlation with *P* (R^2 = 0.08) and a limited correlation with *SM* (R^2 = 0.34). At the annual timescale, the highest correlation was found for *Rn* (R^2 = 0.50, not shown in figures).

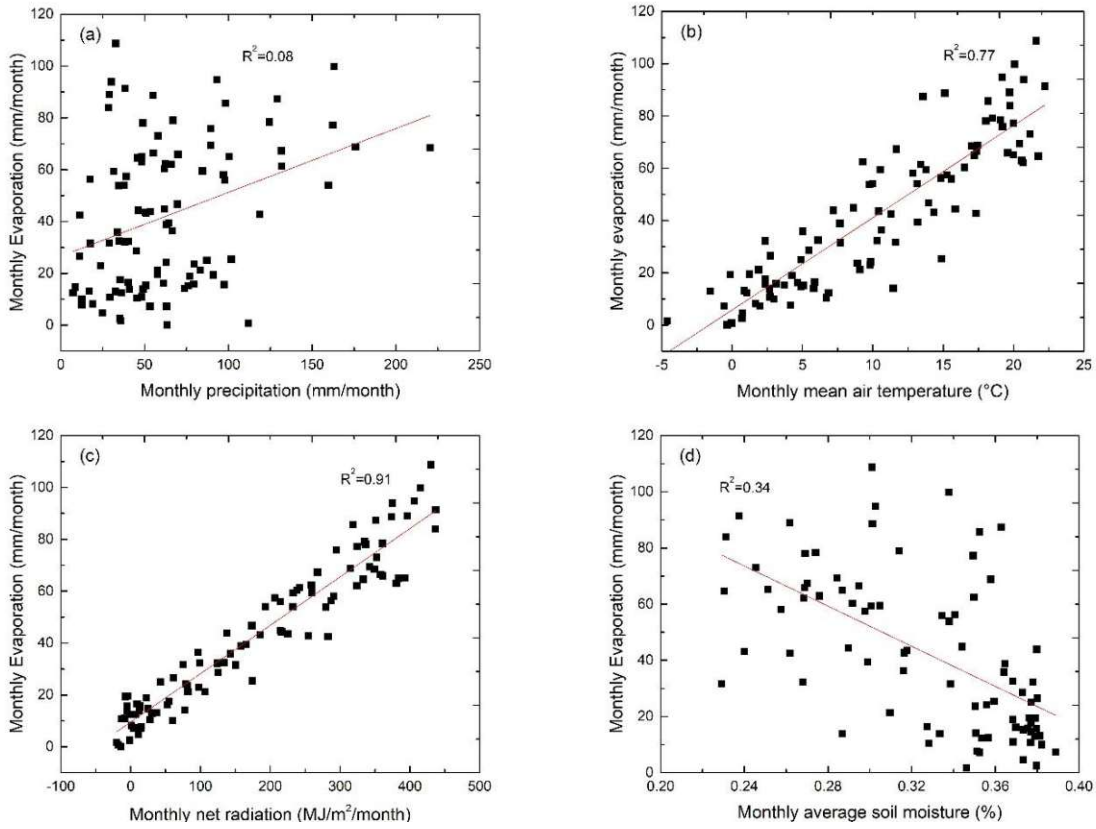

Figure 4.6: Scatterplots of (a) monthly sum of precipitation, (b) monthly mean temperature (c) monthly sum of net radiation and (d) monthly mean soil moisture versus the monthly sum of evaporation at the weather station.

Die approbierte gedruckte Originalversion dieser Dissertation ist an der TU Wien Bibliothek verfügbar.
The approved original version of this doctoral thesis is available in print at TU Wien Bibliothek.

Figure 4.7 shows the daily *E* rates at each eddy covariance station for the years 2014 - 2020. From January - March *E* rates are low with only small differences between the stations. From April onwards the station located at the winter wheat field starts to measure much higher *E* rates as the crop starts to grow, while the grassland weather station also shows an increase in *E*. From April to May the maize field is bare, resulting in low levels of *E* as soil moisture decreases with only a small increase in response to a precipitation event in the middle of April. *E* rates continue to increase at all stations from May onwards with the highest rates being measured at the maize field until the winter wheat crop is harvested at the beginning of July. From July - September the highest rates are measured at the fully grown maize field until it is harvested at the beginning of October, with much reduced rates measured at the bare winter wheat field. From October onwards a catch crop is grown at the winter wheat field to provide soil cover and fertiliser, resulting in slightly higher *E* values than at the other locations.

Seasonal differences can be seen between the different measurement locations in most years. In 2015 and from 2017 - 2020 daily differences of up to 2 mm/ day of *E* were measured between locations adjacent to fields containing winter season crops and grassland and bare soil locations, while in 2017, 2018 and 2019 differences of up to 3.1 mm/ day were recorded between fields containing summer crops. In 2014 and 2016 much smaller or no significant differences were seen between the locations, due to the low evaporative demand in 2014 and the high soil moisture during the summer months in 2016. Comparing the tripod stations locations to the grassland weather station, *Rn* (R^2 = 0.85) and *Ta* (R^2 = 0.74) are again the environmental variables best correlated with monthly *E*, however, *SM* now shows a much stronger correlation with *E*, R^2 = 0.47 compared to 0.33 at the weather station while *P* also shows increased correlation, it still remains much weaker than the other variables (R^2 = 0.15).

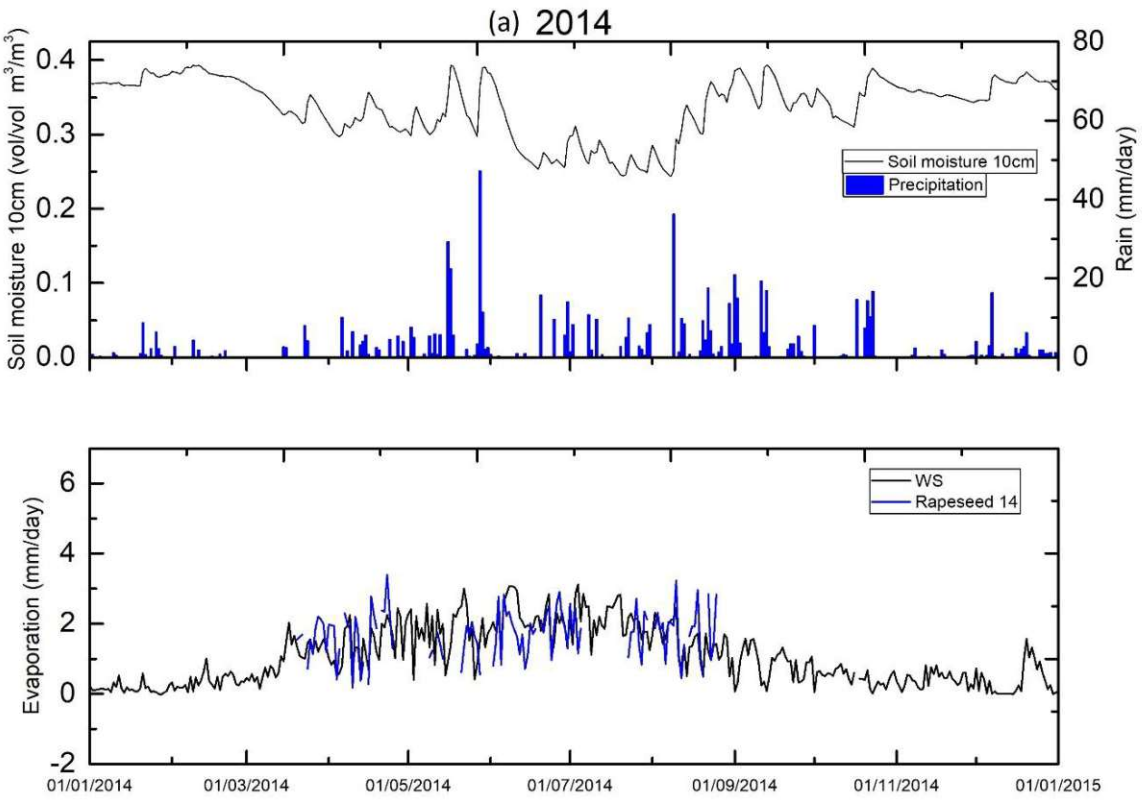

Die approbierte gedruckte Originalversion dieser Dissertation ist an der TU Wien Bibliothek verfügbar.
The approved original version of this doctoral thesis is available in print at TU Wien Bibliothek.

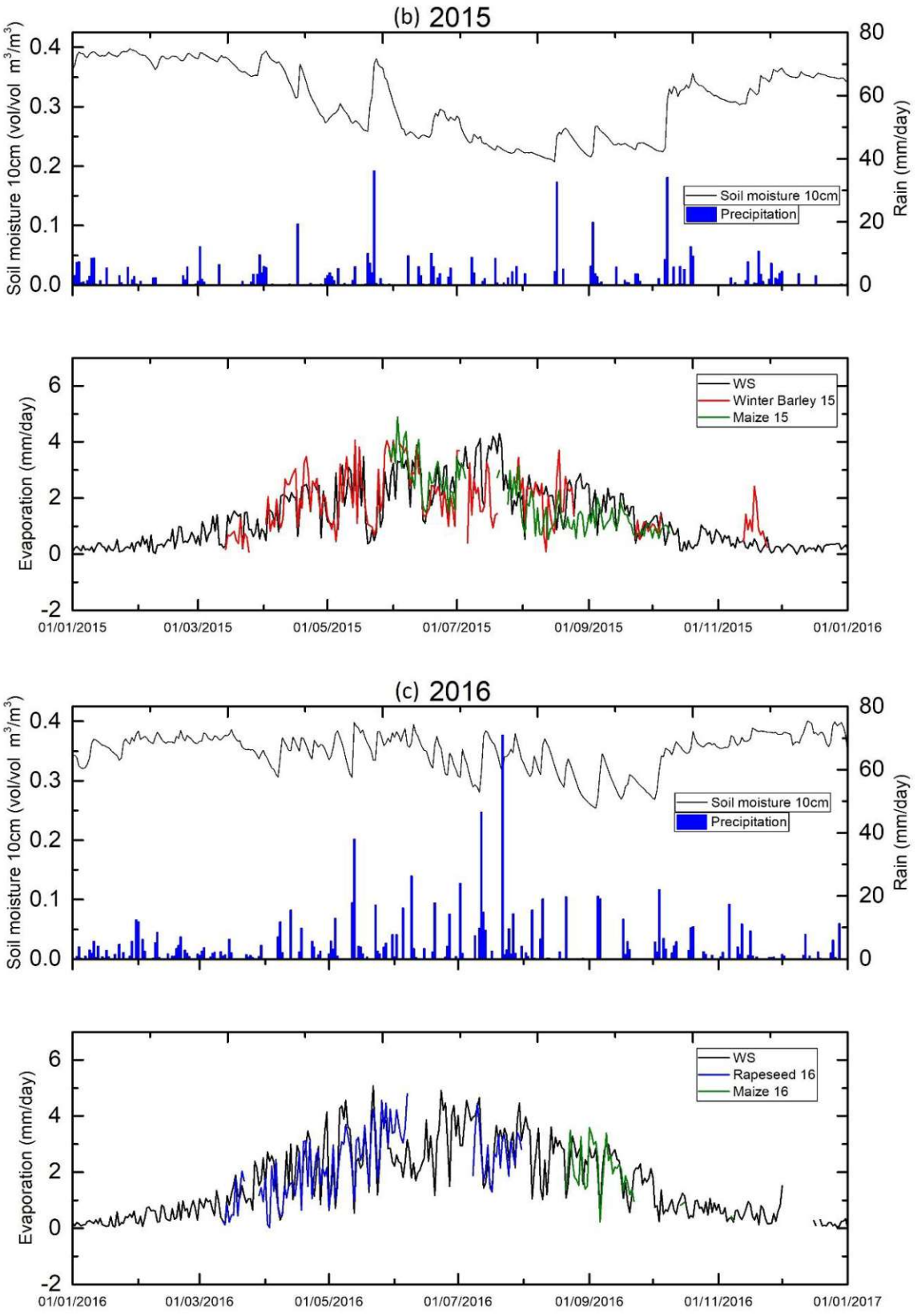

Die approbierte gedruckte Originalversion dieser Dissertation ist an der TU Wien Bibliothek verfügbar.
The approved original version of this doctoral thesis is available in print at TU Wien Bibliothek.

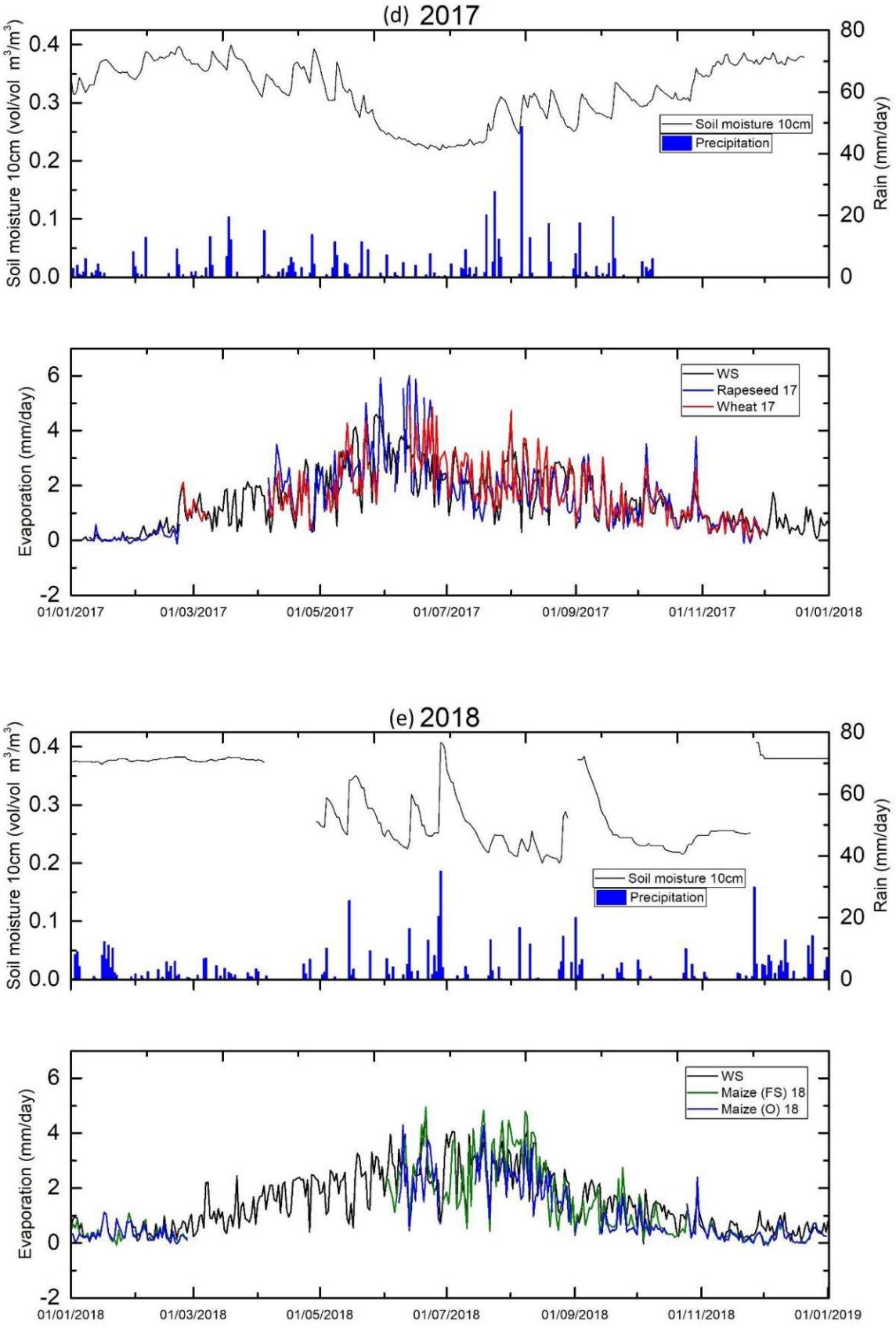

Die approbierte gedruckte Originalversion dieser Dissertation ist an der TU Wien Bibliothek verfügbar.
The approved original version of this doctoral thesis is available in print at TU Wien Bibliothek.

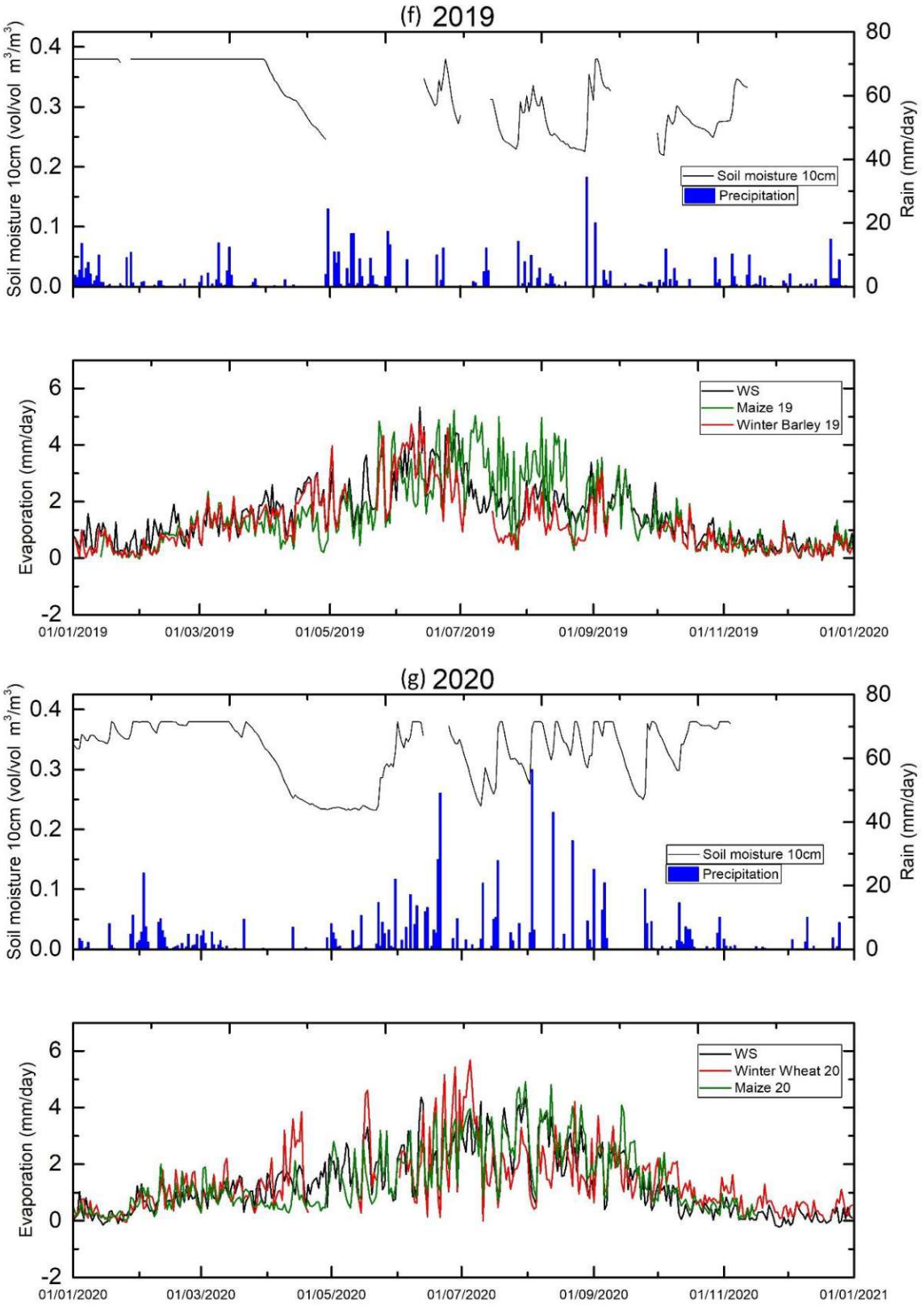

Figure 4.7: Daily sums of evaporation at each eddy covariance station (*WS* indicates weather station, the other locations are indicated by the predominant crop type), precipitation (blue bars) and soil moisture (black line) for the years 2014 - 2020.

Die approbierte gedruckte Originalversion dieser Dissertation ist an der TU Wien Bibliothek verfügbar.
The approved original version of this doctoral thesis is available in print at TU Wien Bibliothek.

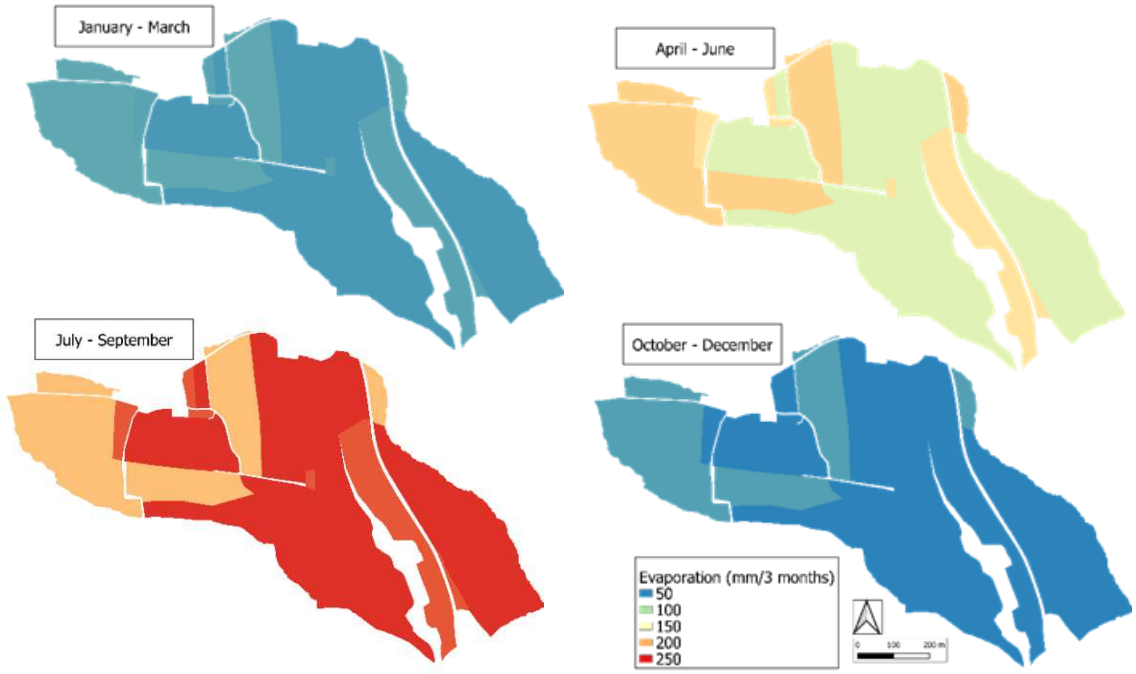

Figure 4.8: Tri-monthly maps of evaporation upscaled from each eddy covariance sensor by landuse (mm /3 months) for the year 2020.

Based on this analysis the measurements from the eddy covariance network were then upscaled to the entire catchment as outlined in section 4.5.2. Figure 4.8 shows tri-monthly maps of *E* at the catchment for the year 2020. The winter months show little variation across the catchment, with the largest differences of ~50 mm measured in the July - September period.

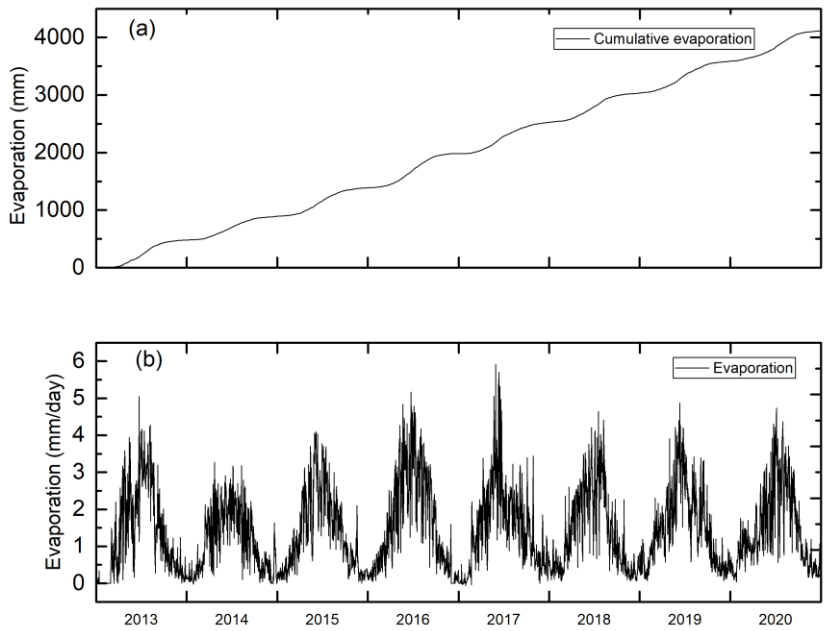

Figure 4.9: (a) Cumulative evaporation (mm) and (b) daily values of eddy covariance based catchment averaged evaporation (mm /day) from 2013 - 2020

Die approbierte gedruckte Originalversion dieser Dissertation ist an der TU Wien Bibliothek verfügbar.
The approved original version of this doctoral thesis is available in print at TU Wien Bibliothek.

The upscaled E values were then averaged over the entire catchment. Figure 4.9 shows the cumulative and the daily values of upscaled E (E_{eddy}) over the course of the study. Annual values of E_{eddy} ranged from 586.2 – 420.0 mm/ year with an average of 514.5 mm/ year.

4.6.3 Catchment Water Balance

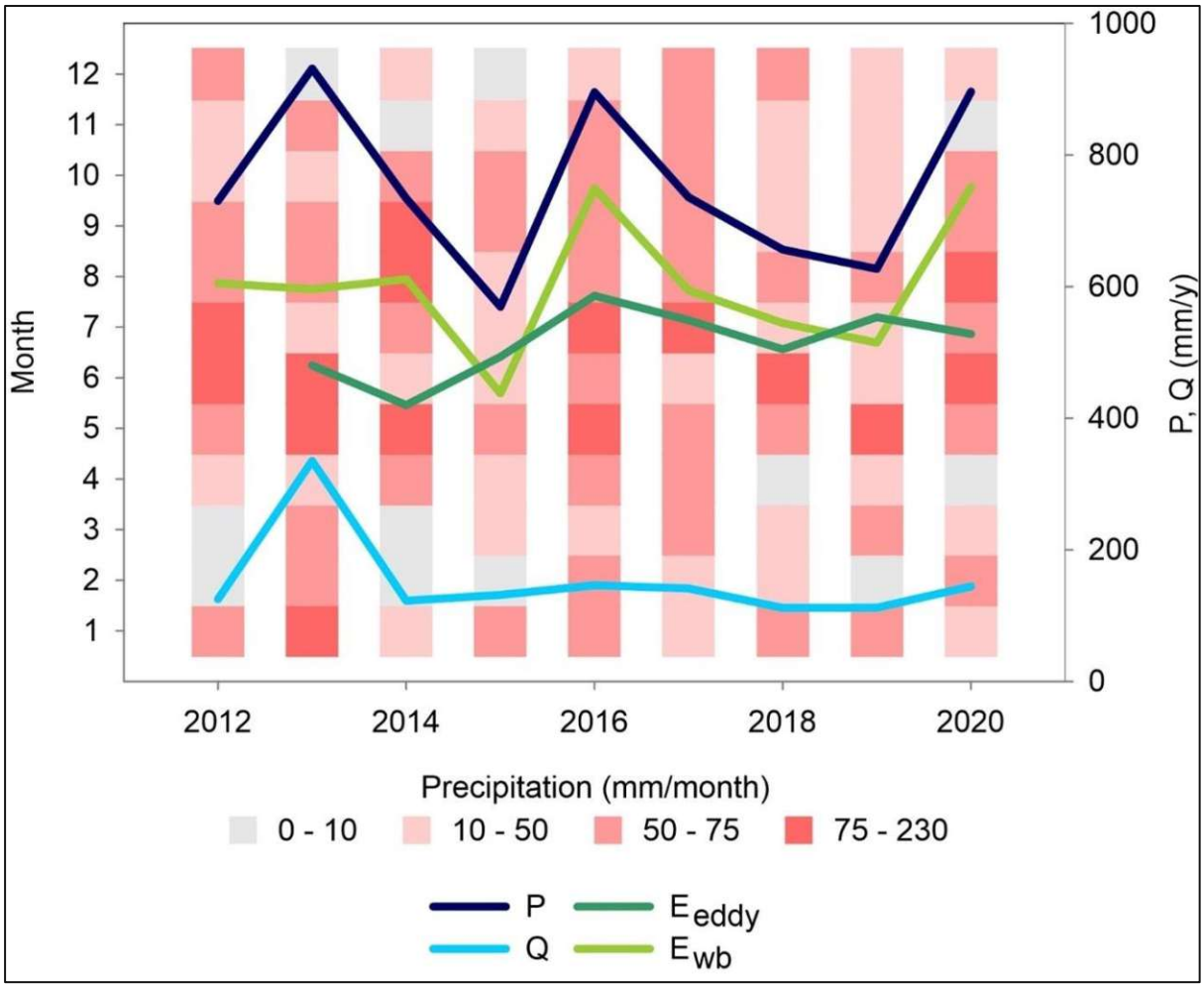

Figure 4.10: The components of the catchment water balance displayed over the monthly distribution of precipitation for the years 2012 - 2020. The red vertical bars show the monthly distribution of P for each year. On the right axis the yearly sums of: eddy covariance evaporation E_{eddy} (dark green line), water balance evaporation E_{wb} (light green line), outlet discharge Q (light blue line) and P (dark blue line) for the entire catchment area are displayed for each year.

Figure 4.10 shows the yearly values of E_{eddy} and the components of the catchment water balance from 2012 - 2020, with water balance evaporation, E_{wb}, calculated as the difference between precipitation and discharge. Discharge was relatively constant throughout this period except for a very large increase in 2013 resulting from a series of large P events in May and June, and a slight decrease in 2018 and 2019 due to lower P amounts. It can be seen that in years with low P amounts there is good agreement between the two estimates, while in years with high P amounts there is a clear difference between the E_{wb} and E_{eddy}. To investigate the possible causes for this difference the groundwater level and storage in the catchment were studied. First the water balance was also calculated according to the hydrologic year (1st Oct. - 30th Sep.) to minimise the storage changes. While this leads to improvements in the closure from ~16 - 50 mm in 2014, 2017 and 2019, in the remaining years the closure is decreased by similar amounts. Figure 4.11 shows the E_{wb} - E_{eddy} difference between the evaporation estimates against the depth to groundwater level during the summer months. In the years with the smallest E_{wb} - E_{eddy} values the depth to the groundwater level was deepest, while in the years with the largest values of E_{wb}

Die approbierte gedruckte Originalversion dieser Dissertation ist an der TU Wien Bibliothek verfügbar.
The approved original version of this doctoral thesis is available in print at TU Wien Bibliothek.
TU Bibliothek Your knowledge hub WIEN

- E_{eddy} the groundwater level was highest, indicating that some of the water was being stored in the groundwater. The storage change was estimated and plotted against E_{wb} - E_{eddy} in Figure 4.12. The results suggest that in 2015, 2018, 2019 and 2020 the change in storage can account for the difference between the E estimates. With the exception of 2020, this corresponds to the years with lower P amounts. In the years 2017, 2016 and 2014 however, where higher P amounts were measured, the storage change can account for only 41 %, 19 % and 13 % of the discrepancy, while in 2013 the storage change is positive.

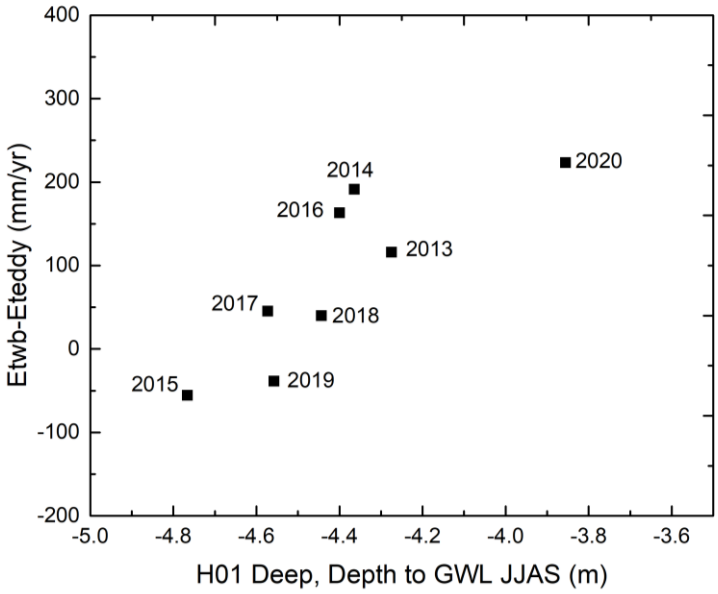

Figure 4.11: The yearly gap between the water balance based and the eddy covariance based evaporation estimates plotted against the summer/ early autumn average (June - September) depth to groundwater level measured at a deeper riparian piezometer (H01).

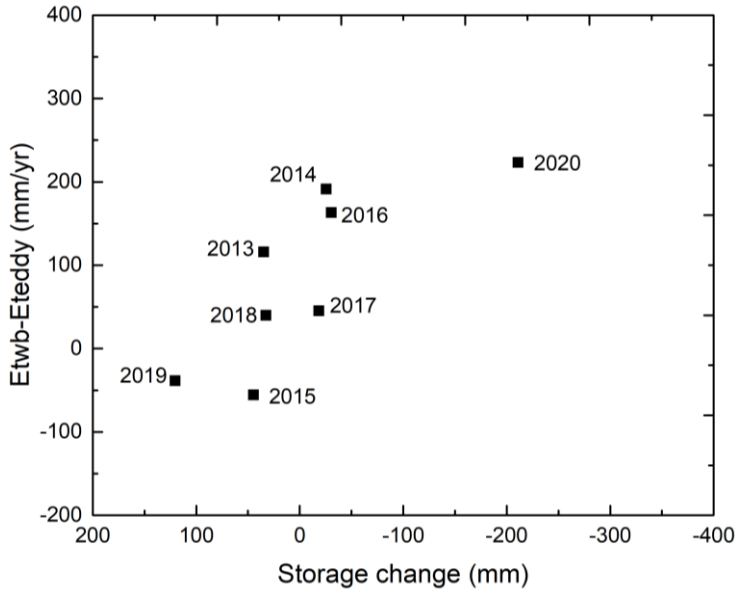

Figure 4.12: The yearly gap between the water balance based and the eddy covariance based evaporation estimates plotted against the yearly catchment averaged storage change.

Die approbierte gedruckte Originalversion dieser Dissertation ist an der TU Wien Bibliothek verfügbar.
The approved original version of this doctoral thesis is available in print at TU Wien Bibliothek.

4.6.4 Subcatchment Water Balances

The evaporation was also estimated for each subcatchment using the water balance method. Figure 4.13 shows the average E for each subcatchment from 2014 - 2019. Due to the change in measurement flume in 2019, most of the subcatchments did not give plausible E estimates in 2020 and are not included in the calculation. The largest estimates are from the subcatchments corresponding to agricultural (Sys4-Max, Frau2) and mixed forest-agriculture (Sys3-Max) landuse.

The yearly values of E estimated using the subcatchments/ water balance (E_{sub}), and by the eddy covariance measurements/ landuse (E_{lu}) are compared in Figure 4.14. With the exception of Sys4-Max which gives consistently higher estimates of E, the two methods give reasonably similar results. The spatial distribution of E_{wb} is quite homogenous in the eastern side of the catchment along the riparian zone, with only small differences between the subcatchments (A2, Sys2, Sys3-Max) in most years. E ranges between 509 - 521 mm in 2017 and 505 - 536 mm in 2018, while in 2015 the A2 catchment dried out over the course of the summer due to the low amounts of P resulting in a lower E estimate of 450 mm compared to 526 and 506 mm for the Sys2 and Sys3-Max catchments.

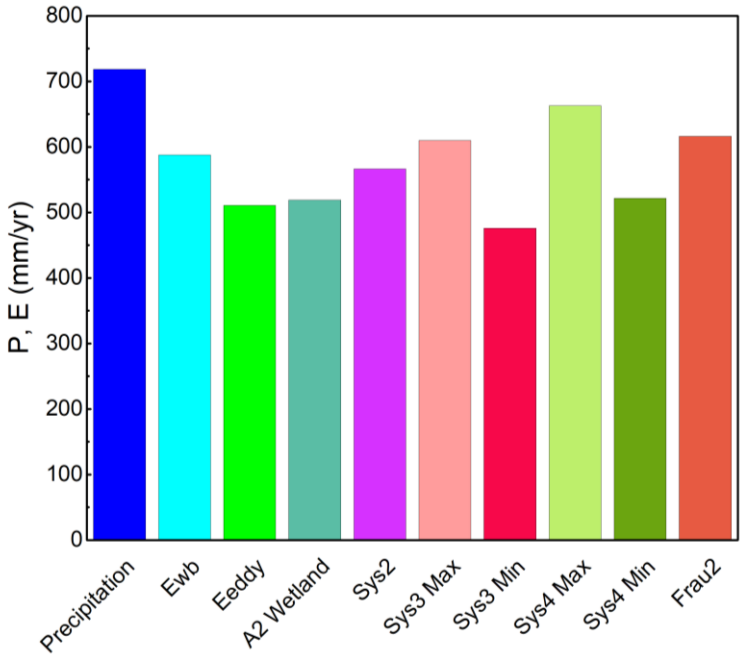

Figure 4.13: Average yearly precipitation and evaporation E (2014 - 2019), calculated from the catchment water balance for the entire catchment (E_{wb}), for each subcatchment, and the catchment averaged eddy covariance based estimate (E_{eddy}).

Die approbierte gedruckte Originalversion dieser Dissertation ist an der TU Wien Bibliothek verfügbar.
The approved original version of this doctoral thesis is available in print at TU Wien Bibliothek.

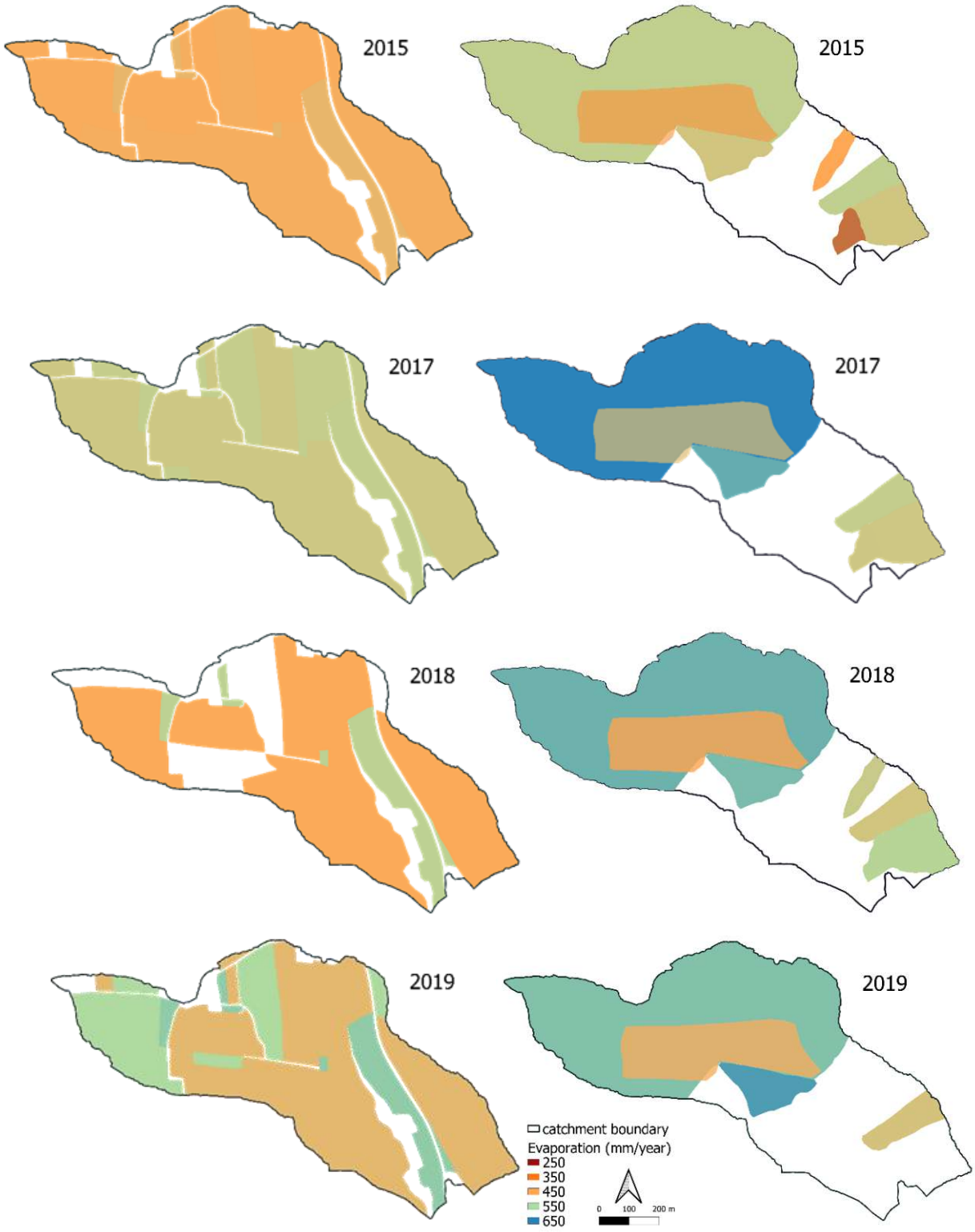

Figure 4.14: Yearly maps of (left) evaporation upscaled from each eddy covariance sensor by landuse and (right) subcatchment water balance method-based evaporation for each tributary, for years where the catchment water balance residual < 100 mm.

Die approbierte gedruckte Originalversion dieser Dissertation ist an der TU Wien Bibliothek verfügbar.
The approved original version of this doctoral thesis is available in print at TU Wien Bibliothek.

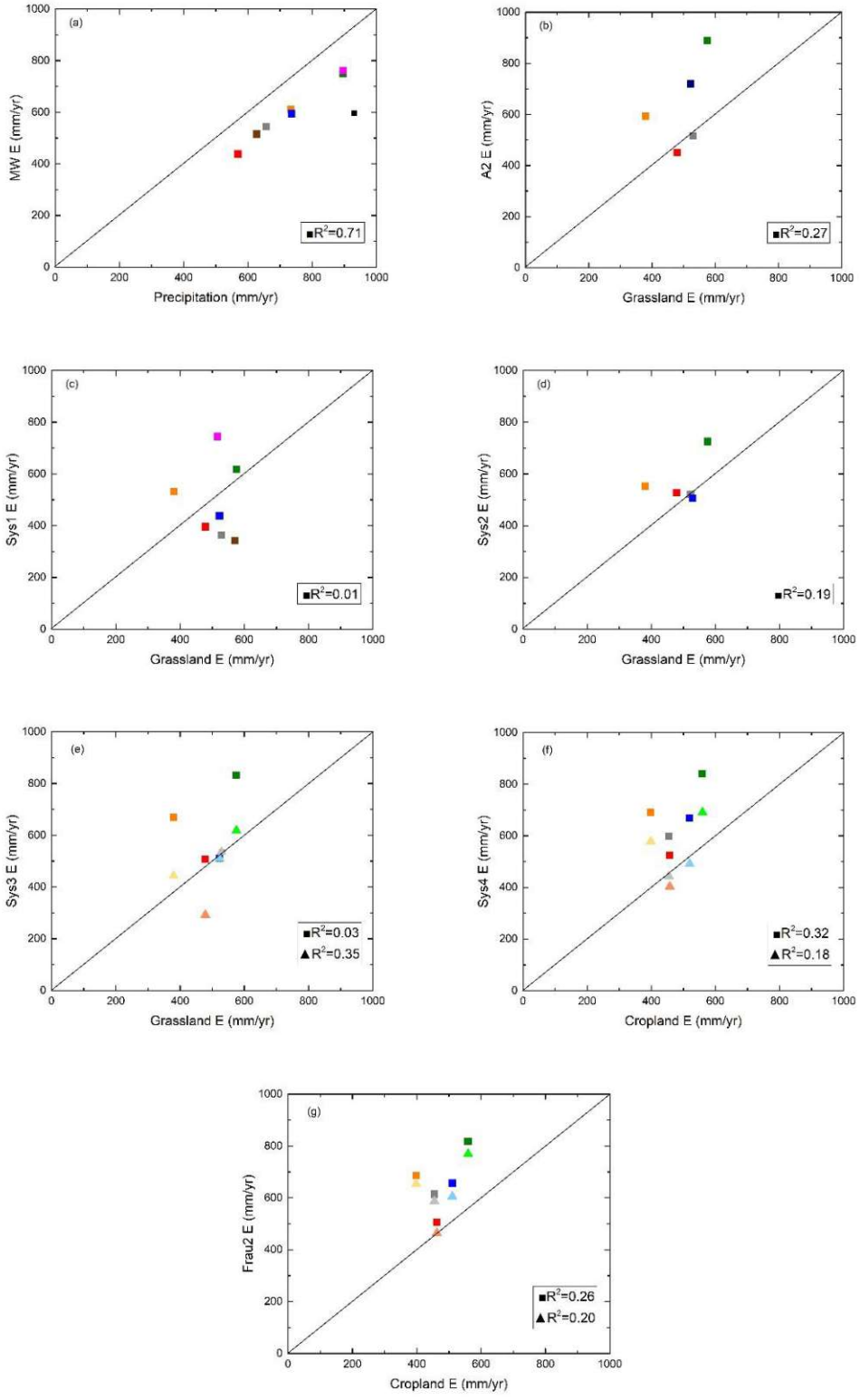

Figure 4.15: Scatterplots of subcatchment water balance ET versus (a) precipitation and (b-g) evaporation *E* measured at the most representative eddy covariance station. Squares represent maximum catchment area estimates and triangles minimum catchment area estimates, with individual years coloured according to: 2013 (black, for the catchment outlet MW only), 2014 (yellow), 2015 (red), 2016 (green), blue (2017), grey (2018), 2019 (brown, MW only), 2020 (purple, MW and Sys1 only).

Die approbierte gedruckte Originalversion dieser Dissertation ist an der TU Wien Bibliothek verfügbar.
The approved original version of this doctoral thesis is available in print at TU Wien Bibliothek.

Each subcatchment is compared with the most representative eddy covariance landuse estimate in Figure 4.15. A2 shows a slight correlation with measured *E* from the grassland area ($R^2 = 0.27$). In 2016 and 2017 only very small amounts of runoff were measured. Sys 1 shows no correlation with measured *E*. There is also a gradual decrease in the ratio of precipitation to runoff from 2013 - 2018. Sys3-Min showed a much higher correlation with measured *E* than Sys2 and Sys3-Max ($R^2 = 0.35$ versus $R^2 = 0.19$ and $R^2 = 0.03$). Sys3-Min also estimates similar levels of *E* on a yearly basis compared to the catchment average *E*, with Sys2 and Sys3-Max only providing similar estimates for 2015, 2017 and 2018. There is a large uncertainty in the catchment area for Sys4. The maximum catchment area was more strongly correlated with *E* measured over the crop fields compared to the minimum area ($R^2 = 0.32$ versus $R^2 = 0.18$), however Sys4-Min shows much better agreement in yearly *E*. This might indicate that the minimum catchment area is more representative for the subcatchment than the maximum area, with the higher *E* estimates being a product of the larger surface area. Frau 2 is a tile drainage system within a crop field. As it is mainly activated during rainfall events with only a small base flow, it results in low amounts of measured runoff and hence high *E* estimates.

4.7 Discussion

At the daily and monthly timescales, spatial patterns can be seen between the eddy covariance stations. These are due to changes in land cover resulting from the agricultural land use cycle, and resulting variations in leaf and root area density. The largest differences, up to 3 mm/ day (Figure 4.7), are seen between bare fields and fully grown crops during dry summer months (July- September). This is consistent with other studies conducted over shorter time periods, with Hsseine (2021) reporting differences of greater than 4 mm/ day between harvested and irrigated fields in a semi-arid climate. From late autumn to early spring, E rates tend to be low due to the reduced temperature and incoming solar radiation and only small spatial differences are measured between the stations, as the low amounts of evaporation results in a homogeneous soil moisture distribution across the catchment. Zhang et al. (2010) reported similar differences between seasons in reference evapotranspiration when modelled at the basin scale, with low variation from Dec - February and highest from May - August. At the annual scale, reduced patterns of E are found between fields, as the higher E rates during the vegetated periods tend to be balanced out by the reduced rates during the non-vegetated periods.

At the subcatchments located primarily within the riparian zone (Sys2, Sys3 and A2) annual differences in E connected to the presence of permanent vegetation with roots able to access the groundwater result in higher E estimates than at the grassland-wetland subcatchment (A2), which tended to dry out in drier years, as in 2015. In the following years the larger precipitations amount of 2016, 2017 and 2018 gradually recharged the subsurface aquifers, resulting in runoff occurring here again in 2018. Sys 1 shows no correlation with measured ET. There is also a gradual decrease in the ratio of *P* to runoff from 2013 - 2018. Following this and the findings of Exner-Kittridge et al., (2016) and the chemical composition analysis Sys1 can be characterised as a deep aquifer system. There is a large groundwater component to the runoff which is independent of the dryness of the unsaturated zone, resulting in Sys1 being unaffected by the meteorological drivers of evaporation. This is in contrast to the nearby A2 where the contributing flowpaths run closer to the surface. The large level of disagreement between the two catchment areas for Sys3, with Sys3-Min providing a more similar *E* estimate to eddy covariance *E* in certain years and Sys3-Max in others, would suggest that the catchment area is changing from year to year. Szeles et al. (2018) found that the vegetation influence on streamflow during rainless periods is higher at Sys3 compared to Sys2. This was explained by the difference in soil types and dominant trees species; at Sys3 the soil is well watered, and the roots of the trees are well connected to the groundwater levels. Sys4 runs through the entire year with a comparatively high base flow component, while the catchment area is covered predominantly by crop fields. Sys4-Max gives considerably higher estimates of *E* than Sys4-Min. As the crop fields have a larger influence on the subcatchment water balance than at the other subcatchments, there is good agreement between the catchment average and water balance estimates for years with relatively low *P* and high *E* (2015, 2017, 2018 and 2019). Combined with the large groundwater component, this results in this tributary behaving similarly to the

Die approbierte gedruckte Originalversion dieser Dissertation ist an der TU Wien Bibliothek verfügbar.
The approved original version of this doctoral thesis is available in print at TU Wien Bibliothek.
TU Bibliothek Your knowledge hub WIEN

main catchment. Due to the low but permanent runoff during the entire year, Frau2 is partly influenced by evapotranspiration from the crops, which are the dominant landuse type for this subcatchment, showing a lower correlation to measured *E* compared to Sys4.

Interannual differences of -13 – 27% were measured between the upscaled eddy covariance and water balance methods, which falls outside the -10 to 17% range reported by Scott (2010) over a 5-year period and -7 – 11% estimated by Denager et al. (2020) over a 3-year period. In these catchments however no significant groundwater flow or storage was reported. Tie et al. (2018) found differences 20% which were attributed to groundwater flow. When storage and leakage are estimated during years with above average *P*, year to year variability of the catchment evaporation methods is consistent ($R^2 = 0.80$ when accounted for versus $R^2 = 0.37$ when not).

In this study E was upscaled according to landuse and crop type, assuming that the *E* measured at an eddy covariance station in a certain crop type is valid for other fields within the catchment with the same crop. Net radiation and temperature were found to be the main drivers of monthly *E* measured by the weather station and mobile eddy covariance stations, with almost no correlation with *P*. The biggest difference between the stations was found to be due to soil moisture, with the mobile stations showing a larger correlation than the weather station. The landuse at the weather station is meadow which is subjected to minimal management. This results in a lower dependency on soil moisture for evaporation compared to the mobile stations where the crops are regularly harvested, resulting in bare surfaces where the evaporation is limited by the soil moisture near the surface. At the field scale global radiation was also found to be the main environmental driver of crop transpiration by Gao et al. (2010) and Zhao (2016). At the annual timescale, *Rn* was also the main driver for the eddy covariance-based estimate method ($R^2 = 0.50$), however *P* was the main driver of the water balance-based E estimate ($R^2 = 0.81$). At the field scale Mo et al. (2004) and Hatfield et al. (2007) observed that spatial variation in *Rn* and *P* due to cumulus clouds and the resulting variation in energy and soil moisture lead to patterns in *E* between fields of the same crop type across a small watershed. Due to the much smaller size of our catchment (66 vs 5,400 Ha) and with cumulus clouds having a typical linear dimension of 3-10 km (Weisman and Klemp, 1986), it is unlikely that such variation could affect the upscaling. This assumption also assumes that there is only minimal variation in soil moisture within each field. While a soil moisture network is installed within the catchment the number of stations located within the agricultural fields is limited, and in addition these sensors must be removed and reinstalled before and after land management practices.

4.8 Conclusions

In this study the spatial patterns of evaporation and their drivers in a small agricultural catchment were investigated at monthly to yearly timescales. Spatial differences can be seen between subcatchments at different timescales and are consistent between the methods. Seasonal patterns can be seen between the eddy covariance stations due to changes in land cover resulting from the agricultural land use cycle due to the variations in leaf and root area density during the growing season. At the subcatchments annual differences in E connected to the presence of vegetation with roots connected to the groundwater result in higher E estimates than at wetland subcatchments, which tended to dry out in drier years.

Year to year variability in monthly E measured by the eddy covariance stations was driven primarily by net radiation and temperature. Precipitation was the main driver of annual water balance-based E estimate, versus net radiation for the annual eddy covariance-based estimate method. Year to year variability of the catchment evaporation methods is consistent when storage and leakage are estimated during years with above average precipitation.

The results indicate that at daily and monthly timescales information on land cover and soil moisture is important in order to correctly estimate E in catchments with agricultural vegetation, particularly when E is sampled infrequently such as during satellite overpasses, as changes in landuse result in large variations in E.

Die approbierte gedruckte Originalversion dieser Dissertation ist an der TU Wien Bibliothek verfügbar.
The approved original version of this doctoral thesis is available in print at TU Wien Bibliothek.
TU Bibliothek Your knowledge hub WIEN

5. Summary and conclusions

The objective of this thesis was to investigate the spatial patterns of evaporation in a small agricultural catchment, focusing on how these patterns are formed and what their environmental drivers are, how they change in time, and if we can further our understanding of these patterns by partitioning the evaporation into transpiration and soil evaporation.

Chapter 2 tested if the stable isotope method can be used to partition evaporation in a maize field and how the ratio of evaporation to transpiration changes in response to the environmental conditions on a daily time scale. While the method had previously been shown to work well for crops with simpler canopy structures such as rice and wheat, this experiment was the first to focus on using the stable isotope for the more complex canopy structure of maize during the growth stage between seedling and adult, where the canopy closes as the plant grows. Using sap flow sensors installed concurrently in the field as a control, the method was shown to also be appropriate for maize. This study also provides information for when the soil in a maize crop field has been wetted, which is the case for irrigated fields, particularly as while the experiment was only of a short duration (nine days) there was a change in conditions from dry to wetted followed by a drying out period. The amount of soil evaporation and transpiration was dependent on the availability of soil water in the upper layer of the soil, with a general pattern of a large decrease in the transpiration fraction following a precipitation event followed by a period of increase, due to the drying out of the upper layer of the soil. Daily average values of transpiration fraction varied considerably indicating that there was a large effect due to the precipitation events. The temporal patterns of both evaporation and transpiration were much better correlated with solar radiation than with vapor pressure deficit over the course of the experiment for the analysed sub-daily time period (~10:00 - 17:30).

Chapter 3 went further into evaporation partitioning, comparing the different methods of Lagrangian dispersion analysis and stable isotopes. While most partitioning methods require some sampling of the soil or plants, and are therefore less reliable in heterogenous conditions, the Lagrangian dispersion analysis method offers the possibility of partitioning evaporation using just sampling of the water vapour within the canopy. The study showed that the two methods gave similar results, however, the stable isotope method was found to return a much larger amount of usable data, as well as having a lower variance. This is offset by the need for more additional measurements and analysis, as well as the uncertainty due to the need for the Isotopic Steady State assumption. Different levels of precipitation intensity give different soil evaporation responses, due to the different runoff levels and resulting changes in soil moisture.

In Chapter 4 the spatial patterns of evaporation in the Hydrological Open Air Laboratory (HOAL) were studied using spatially distributed eddy covariance evaporation measurements and subcatchment water balances. Previous research has tended to be of a short duration, this study however was conducted over eight years. The results show that the daily and seasonal patterns of evaporation in the agricultural area of the catchment are strongly linked to the crop cycle, while at the yearly timescale the patterns of evaporation tend to be averaged out, as each field goes through a complete cycle from fallow to crop and back. However, when the riparian zone is included the influence of permanent vegetation results in yearly patterns between the hydrological subcatchments in dry years (2015 and 2018). The meteorological drivers of evaporation were also investigated, showing that year to year variability in monthly evaporation measured by the eddy covariance stations was driven primarily by net radiation and temperature. At the annual timescale, precipitation was the main driver of evaporation for the water balance method, while net radiation was best correlated with the eddy covariance method. Year to year variability of the catchment evaporation methods was found to be consistent during years with above average precipitation, only when storage and leakage were included.

This thesis has advanced our knowledge of evaporation, its role in the water cycle, its spatial patterns and its components, in small agricultural catchments. This work has provided an analysis of spatial

Die approbierte gedruckte Originalversion dieser Dissertation ist an der TU Wien Bibliothek verfügbar.
The approved original version of this doctoral thesis is available in print at TU Wien Bibliothek.
TU Bibliothek Your knowledge hub WIEN

evaporation using a unique long-term dataset, showing the importance of detailed landuse information when small catchments are to be studied or modelled, with evaporation patterns forming according to the crop cycle in the agricultural areas and the vegetation in the riparian zone. The results also show the importance of, and provide a method for testing the water balance method for non-closure and leakage, by measuring and upscaling the evaporation using the eddy covariance method and vegetation. Two different methods of evaporation partitioning have been evaluated, providing direct insight into how the transpiration ratio changes in a response to the environmental conditions and how detailed knowledge of the crop growing stage, soil moisture and precipitation intensities are needed when estimating the transpiration through modelling in order to correctly capture its dynamics. These studies provide a basis for how the spatial patterns of transpiration and soil evaporation could be measured in a future study.

The findings of this study have many implications for hydrological and atmospheric modelling of evaporation. At daily to seasonal timescales, singular measurements made over non-permanent vegetation should be combined with model estimates of actual evaporation (e.g., calibrated Penman-Monteith equation) and upscaled to the catchment scale in order to be representative. The importance of detailed and updated landuse information is emphasised; outside of dedicated research areas landuse data tends to be static, which in patchwork agricultural landscapes can result in incorrect evaporation model estimates. Particularly in the case where the spatial landuse patterns combine with temporal patterns of the main meteorological drivers, suggested from the results of this study as: net radiation, temperature and precipitation. In the case of atmospheric simulations, particularly those with a spatial scale appropriate for small catchments such as Large Eddy Simulation (LES), although the atmosphere tends to smooth out surface properties, at the small catchment scale without detailed landuse information the surface energy balance will be incorrectly partitioned leading to the generation of different local atmospheric conditions. The results of Chapter 2 confirm the importance of global radiation in controlling transpiration, while the Chapter 3 results suggest when modelling soil evaporation and transpiration over short time periods, not only the total precipitation but also the precipitation intensity or runoff data should be used to give the correct soil moisture and hence soil evaporation response.

The findings also have implications from a practical viewpoint for evaporation measurement. At long-term observation sites, measurement devices are frequently located at areas of permanent vegetation so to ensure a continuous measurement record and so they may be easily maintained. When planning short-term to seasonal length experiments however, the influence of patterns generated by the landuse cycle, particularly non-permanent vegetation such as crops, needs to be taken into account when choosing an installation site for the devices. For long-term observations in catchments consisting of different types of permanent vegetation and/ or different runoff generation mechanism, singular measurements of evaporation with a limited footprint, such as eddy covariance, should be used to support distributed measurements, such as subcatchment gauging, by providing a control for evaporation for subcatchments where the surface vegetation tends to become disconnected from the groundwater. Additionally, evaporation estimated using water balance measurements should be controlled with alternative evaporation measurements or model estimates in years with high amounts of precipitation. In areas with pronounced topographical or soil texture differences, differences in the soil moisture content may result in short term evaporation patterns following precipitation events when leaf area is low, either during the early growing stages of densely planted crops or for crops with a wide row spacing. This could best be measured at the seasonal time scale using Lagrangian dispersion analysis to investigate long term patterns due to the lower sampling and technical requirements of the method, while for investigating specific conditions at shorter timescales the stable isotope method is preferable.

The results of this study could be furthered by performing a similar measurement campaign in a non-agricultural catchment with permanent vegetation, as the results of the subcatchment water balances indicate that yearly patterns of evaporation can be seen between the subcatchments surrounding the riparian zone. In agricultural catchments, further research could focus on sub-field scale pattern analysis

Die approbierte gedruckte Originalversion dieser Dissertation ist an der TU Wien Bibliothek verfügbar.
The approved original version of this doctoral thesis is available in print at TU Wien Bibliothek.
TU Bibliothek Your knowledge hub WIEN

using evaporation partitioning methods combined with a spatial analysis of soil moisture. By expanding the experimental set-up of the stable isotope measurement system with additional intake ports and a rainwater sampler the interception could be also estimated. Interception is highly variable within complex canopies and difficult to measure. The integrated measurement footprint of the stable isotope method would allow for more accurate quantification of the interception, enabling rigorous testing of complex soil-vegetation-atmosphere models as well as improving the accuracy of the other partitioning components. In both agricultural and non-agricultural catchments lysimeters could be included as part of the measurement campaign as a complementary method for measuring evaporation. As lysimeters have a small footprint in comparison to the eddy covariance method and have been shown to have good agreement with catchment scale water balance estimates in small homogenous catchments, they could be used for measuring evaporation in subcatchments where the eddy covariance method cannot be easily applied, for example areas of high vegetation or where the eddy covariance footprint will not match the subcatchment area due to wind direction or different composite landuse types.

Die approbierte gedruckte Originalversion dieser Dissertation ist an der TU Wien Bibliothek verfügbar.
The approved original version of this doctoral thesis is available in print at TU Wien Bibliothek.
TU Bibliothek Your knowledge hub WIEN

6. References

Agam, N., Evett, S.R., Tolk, J.A., Kustas, W.P., Colaizzi, P.D., Alfieri, J.G., McKee, L.G., Copeland, K.S., Howell, T.A., & Chávez, J.L. (2012). Evaporative loss from irrigated interrows in a highly advective semi-arid agricultural area. *Advances in Water Resources*, 50, 20-30.

Allen, R.G., Pereira, L.S., Raes, D., & Smith, M. (1998). *Crop Evapotranspiration—Guidelines for Computing Crop Water Requirements*. FAO Irrigation and drainage paper 56. Food and Agriculture Organization of the United Nations, Rome, Italy.

Anderson, M.C., Kustas, W.P., Alfieri, J.G., Gao, F.N., Hain, C., Prueger, J.H., Evett, S.R., Colaizzi, P.D., Howell, T.A., & Chavez, J. (2012). Mapping daily evapotranspiration at Landsat spatial scales during the BEAREX'08 field campaign. *Advances in Water Resources*, 50,162-177.

Armstrong, R.N., Pomeroy, J.W., & Martz, L.W. (2019). Spatial variability of mean daily estimates of actual evaporation from remotely sensed imagery and surface reference data. *Hydrology and Earth System Sciences*, 23, 4891–4907. https://doi.org/10.5194/hess-23-4891-2019

Aubinet, M., Vesala, T. & Papale, D. (2012). *Eddy Covariance. A Practical Guide to Measurements and Data Analysis*, Springer: Dorndrecht, Germany, p. 325.

Baldocchi, D.D. (2003). Assessing the eddy covariance technique for evaluating carbon dioxide exchange rates of ecosystems: past, present and future. *Global Change Biology*, 9, 479–492. https://doi.org/10.1046/j.1365-2486.2003.00629.x

Bastiaanssen, W.G.M., Pelgrum, H., Wang, J., Ma, Y., Moreno, J.F., Roerink, G.J., & van der, W.T. (1998). A Surface Energy Balance Algorithm for Land (SEBAL). Part 2 validation. *Journal of Hydrology*, 212, 213–229.

Bastiaanssen, W.G.M., Noordman, E.J.M., Pelgrum, H., Davids, G., Thoreson, B.P., & Allen, R.G. (2005). SEBAL model with remotely sensed data to improve water-resources management under actual field conditions. *Journal of Irrigation and Drainage Engineering*, 131 (1), 85–93.

Blöschl, G., Blaschke, A. P., Broer, M., Bucher, C., Carr, G., Chen, X., Eder, A., Exner-Kittridge, M., Farnleitner, A., Flores-Orozco, A., Haas, P., Hogan, P., Kazemi Amiri, A., Oismüller, M., Parajka, J., Silasari, R., Stadler, P., Strauss, P., Vreugdenhil, M., Wagner, W., & Zessner, M. (2016). The Hydrological Open Air Laboratory (HOAL) in Petzenkirchen: a hypothesis-driven observatory. *Hydrology and Earth System Sciences*, 20.1, 227-255.

Blöschl, G., Bierkens, M.F.P., Chambel, A., Cudennec, C., Destouni, G., Fiori, A., Kirchner, J.W., McDonnell, J.J., Savenije, H.H.G., Sivapalan, M., Stumpp, C., Toth, E., Volpi, E., Carr, G., Lupton, C., Salinas, J., Széles, B., Viglione, A., et al. (2019). Twenty-three unsolved problems in hydrology (UPH) – a community perspective. *Hydrological Sciences Journal*, 64, 1141–1158. https://doi.org/10.1080/02626667.2019.1620507

Brutsaert, W., Cheng, L., & Zhang, L. (2020). Spatial Distribution of Global Landscape Evaporation in the Early Twenty-First Century by Means of a Generalized Complementary Approach. *Journal of Hydrometeorology*, 21, 287–298. https://doi.org/10.1175/JHM-D-19-0208.1

Bouwer, L.M., Biggs, T.W., & Aerts, J.C.J.H. (2008). Estimates of spatial variation in evaporation using satellite-derived surface temperature and a water balance model. *Hydrological Processes*, 22, 670-682. https://doi.org/10.1002/hyp.6636

Castelli, M., Anderson, M.C., Yang, Y., Wohlfahrt, G., Bertoldi, G., Niedrist, G., Hammerle, A., Zhao, P., Zebisch, M., Notarnicola, C. (2018). Two-source energy balance modeling of evapotranspiration in Alpine grasslands. *Remote Sensing of Environment* 209, 327–342. https://doi.org/10.1016/j.rse.2018.02.062

Die approbierte gedruckte Originalversion dieser Dissertation ist an der TU Wien Bibliothek verfügbar.
The approved original version of this doctoral thesis is available in print at TU Wien Bibliothek.
TU Bibliothek Your knowledge hub WIEN

Čermák, J., Kučera, J., & Nadezhdina, N. (2004). Sap flow measurements with some thermodynamic methods, flow integration within trees and scaling up from sample trees to entire forest stands. *Trees*, *18*, 529–546.

Craig, H. & Gordon, L. (1965). In *Deuterium and Oxygen-18 variations in the Ocean and Marine Atmosphere, Proceedings of the Conference on Stable Isotopes in Oceanographic Studies and Paleotemperatures.* Tongiorgi, E. Ed., Laboratory of Geology and Nuclear Science: Pisa, Italy, 9–130.

Dai, A. Increasing drought under global warming in observations and models (2013). *Nat. Clim. Change*, 3, 52–58.

Dai, A., Zhao, T., & Chen, J. (2018). Climate Change and Drought: a Precipitation and Evaporation Perspective, *Current Climate Change Reports*, 4, 301–312.

Denager, T., Looms, M.C., Sonnenborg, T.O., & Jensen, K.H. (2020). Comparison of evapotranspiration estimates using the water balance and the eddy covariance methods. *Vadose Zone Journal*, 19. https://doi.org/10.1002/vzj2.20032

Denmead O.T., & Bradley E.F. (1985). Flux-gradient relationships in a forest canopy. B.A. Hutchison, B.B. Hicks (Eds.), *The Forest–Atmosphere Interaction*. D. Reidel Publishing Co., Dordrecht, pp. 421-442.

Ding, R., Kang, S., Zhang, Y., Hao, X., Tong, L., & Du, T. (2013). Partitioning evapotranspiration into soil evaporation and transpiration using a modified dual crop coefficient model in irrigated maize field with ground-mulching. *Agricultural Water Management*, 127, 85–96.

Dubbert, M., Cuntz, M., Piayda, A., Maguas, C., & Werner, C. (2013). Partitioning evapotranspiration: Testing the Craig and Gordon model with field measurements of oxygen isotope ratios of evaporative fluxes. *Journal of Hydrology*, 496, 142–153.

Ehleringer, J.R. & Dawson, T.E. (1992). Water uptake by plants: Perspectives from stable isotope composition. *Plant Cell Environment*, 15, 1073–1082.

Ehleringer, J. & Field, C. (1993). *Scaling Physiological Processes: Leaf to Globe,* Physiological Ecology Academic Press: San Diego, CA, USA, p. 388.

Eshonkulov, R., Poyda, A., Ingwersen, J., Wizemann, H.-D., Weber, T.K.D., Kremer, P., Högy, P., Pulatov, A., & Streck, T. (2019). Evaluating multi-year, multi-site data on the energy balance closure of eddy-covariance flux measurements at cropland sites in southwestern Germany. *Biogeosciences*, 16, 521–540. https://doi.org/10.5194/bg-16-521-2019

Eswar, R., Sekhar, M., & Bhattacharya, B.K. (2017). Comparison of three remote-sensing-based models for the estimation of latent heat flux over India. *Hydrological Sciences Journal*, 62, 2705–2719. https://doi.org/10.1080/02626667.2017.1404067

Exner-Kittridge, M., Strauss, P., Blöschl, G., Eder, A., Saracevic, E., & Zessner, M. (2016). The seasonal dynamics of the stream sources and input flow paths of water and nitrogen of an Austrian headwater agricultural catchment. *Science of The Total Environment* 542, Part A, 935–945. https://doi.org/10.1016/j.scitotenv.2015.10.151

Fischer, M., Trnka, M., Hlavinka, P., Orság, M., Kučera, J., & Žalud, Z. (2011). Identifying the Fao-56 crop coefficient for high density poplar Plantation: the role of interception in estimation of Evapotranspiration. In *Bioclimate: Source and Limit of Social Development International Scientific Conference. Topol'čianky, Slovakia*.

Die approbierte gedruckte Originalversion dieser Dissertation ist an der TU Wien Bibliothek verfügbar.
The approved original version of this doctoral thesis is available in print at TU Wien Bibliothek.
TU Bibliothek Your knowledge hub WIEN

Flanagan, L.B., Comstock, J.P., & Ehleringer, J.R. (1991). Comparison of modelled and observed environmental influences on the stable oxygen and hydrogen isotope composition of leaf water in *Phaseolus vulgaris* L. *Plant Physiology*, 96, 588–596.

Foken, T. (2008). The Energy Balance Closure Problem: An Overview. *Ecological Applications*, 18, 1351–1367. https://doi.org/10.1890/06-0922.1

Forstner, V., Groh, J., Vremec, M., Herndl, M., Vereecken, H., Gerke, H.H., Birk, S., Pütz, T. (2021). Response of water fluxes and biomass production to climate change in permanent grassland soil ecosystems. *Hydrology and Earth System Sciences* 25, 6087–6106. https://doi.org/10.5194/hess-25-6087-2021

Gao, Y., Duan, A.W., Qiu, X., Zhang, J., Sun, J., & Wang, H. (2010). Plant transpiration in a maize/soybean intercropping system measured with heat balance method. *Chinese Journal of Applied Ecology*, 21, 1283.

Granier, A. (1985). Une nouvelle méthode pour la mesure du flux de sève brute dansle tronc des arbres (A new method of sap flow measurement in tree stems). *Annals of Forest Science*, 42, 193–200.

Groh, J., Slawitsch, V., Herndl, M., Graf, A., Vereecken, H., Pütz, T. (2018). Determining dew and hoar frost formation for a low mountain range and alpine grassland site by weighable lysimeter. *Journal of Hydrology* 563, 372–381. https://doi.org/10.1016/j.jhydrol.2018.06.009

Guerra, L.C., Bhuiyan, S.I., Tuong, T.P., & Barker, R. (1998). *SWIM Paper 5: Producing More Rice with Less Water from Irrigated Systems*. International Water Management Institute, Colombo, Sri Lanka.

Good, S.P., Soderberg, K., Guan, K.G., King, E., Scanlon, T.M., & Caylor, K.K. (2014). δ^2H isotopic flux partitioning of evapotranspiration over a grass field following a water pulse and subsequent dry down. *Water Resources Research*, 50, 1410–1432.

Grayson, R.B. & Bloschl, G. (2000). *Spatial Patterns in Catchment Hydrology: Observations and Modelling*, UK: Cambridge: Univ. Press. https://doi.org/10.1002/hyp.5215

Gribovszki, Z., Kalicz, P., Szilagyi, J., & Kucsara, M. (2008). Riparian zone evapotranspiration estimation from diurnal groundwater-level fluctuations. *Journal of Hydrology*, 349, 6-17.

Haddeland, I., Heinke, J., Biemans, H., Eisner, S., Flörke, M., Hanasaki, N., Konzmann, M., Ludwig, F., Masaki, Y., Schewe, J., Stacke, T., Tessler, Z.D., Wada, Y., & Wisser, D. (2014). Global water resources affected by human interventions and climate change. *Proceedings of the National Academy of Science*, 111, 3251–3256. https://doi.org/10.1073/pnas.1222475110

Hatfield, J.L. & Prueger, J.H. (2011). Spatial and Temporal Variation in Evapotranspiration. *Evapotranspiration - From Measurements to Agricultural and Environmental Applications*. IntechOpen, Rijeka, Croatia, ch. 1. https://doi.org/10.5772/17852

Haverd, V., Leuning, R., Griffith, D., van Gorsel, E., & Cuntz, M. (2009). The turbulent Lagrangian time scale in forest canopies constrained by fluxes, concentrations and source distributions. *Boundary Layer Meteorology*, 130, 209–228.

Haverd, V., Cuntz, M., Griffith, D., Keitel, C., Tadros, C., & Twining, J. (2011). Measured deuterium in water vapour concentration does not improve the constraint on the partitioning of evapotranspiration in a tall forest canopy, as estimated using a soil vegetation atmosphere transfer model. *Agricultural and Forest Meteorology*, 151, 645-654.

Die approbierte gedruckte Originalversion dieser Dissertation ist an der TU Wien Bibliothek verfügbar.
The approved original version of this doctoral thesis is available in print at TU Wien Bibliothek.
TU Bibliothek Your knowledge hub WIEN

Heinlein, F., Biernath, C., Klein, C., Thieme, C., & Priesack, E. (2017). Evaluation of Simulated Transpiration from Maize Plants on Lysimeters. *Vadose Zone Journal*, 16, 1-16.

Herbst, M., Kappen, L., Thamm, F., & Vanselow, R. (1996). Simultaneous measurements of transpiration, soil evaporation and total evaporation in a maize field in northern Germany. *Journal of Experimental Botany*, 47, 1957–1962.

Hirschi, M. and Michel, D. and Lehner, I. & Seneviratne, S. I. (2017). A site-level comparison of lysimeter and eddy covariance flux measurements of evapotranspiration. *Hydrology and Earth System Sciences*, 21,4, 1809 - 1825. https://doi:10.5194/hess-21-1809-2017

Hollinger, D. & Richardson, A. (2005). Uncertainty in eddy covariance measurements and its application to physiological models. *Tree Physiology*, 25, 873–885.

Hossain, M., Rumi, M., & Nahar, B.M.A. (2014). Radiation use efficiency in different row orientation of maize (*Zeas* L.). *Journal of Environmental Science and Natural Resources,* 7, 41–46.

Hssaine, B., Chehbouni, A., Er-Raki, S., Khabba, S., Ezzahar, J., Ouaadi, N., Ojha, N., Rivalland, V., & Merlin, O. (2021). On the Utility of High-Resolution Soil Moisture Data for Better Constraining Thermal-Based Energy Balance over Three Semi-Arid Agricultural Areas. *Remote Sensing*, 13, 727. https://doi.org/10.3390/rs13040727

Hu, Z., Wen, X., Sun, X., Li, L., Yu, G., Lee, X., & Li, S. (2014). Partitioning of evapotranspiration through oxygen isotopic measurements of water pools and fluxes in a temperate grassland. *Journal of Geophysical Research: Biogeosciences*, 119, 358–372.

Huang, S., Gao, Y., Li, Y., Xu, L., Tao, H. & Wang, P. (2017). Influence of plant architecture on maize physiology and yield in the Heilonggang River valley. *The Crop Journal*, 5, 52–62.

Hupet, F., & Vanclooster, M. (2005). Micro-variability of hydrological processes at the maize row scale: Implications for soil water content measurements and evapotranspiration estimates. *Journal of Hydrology*, 303, 247–270.

Imukova, K., Ingwersen, J., Hevart, M., & Streck, T. (2016). Energy balance closure on a winter wheat stand: comparing the eddy covariance technique with the soil water balance method. *Biogeosciences* 13, 63–75. https://doi.org/10.5194/bg-13-63-2016

Jara, J., Stockle, C.O., & Kjelgaard, J. (1998). Measurement of evapotranspiration and its components in a corn (*Zea Mays*, L.) field. *Agricultural and Forest Meteorology*, 92, 131–145.

Jiang, Z.-Y., Yang, Z.-G., Zhang, S.-Y., Liao, C.-M., Hu, Z.-M., Cao, R.-C., & Wu, H.-W. (2020). Revealing the spatio-temporal variability of evapotranspiration and its components based on an improved Shuttleworth-Wallace model in the Yellow River Basin. *Journal of Environmental Management*, 262, 110310. https://doi.org/10.1016/j.jenvman.2020.110310

Kang, S., Gu, B., Du, T., & Zhang., J. (2003). Crop coefficient and ratio of transpiration to evapotranspiration of winter wheat and maize in a semi-humid region. *Agricultural Water Management*, 59, 239–254.

Keeling, C. D. (1958). The concentration and isotopic abundances of atmospheric Carbon dioxide in rural areas, *Geochimica et Cosmochimica Acta*, 13, 322–334.

Kelliher, F.M., Köstner, B.M.M., Hollinger, D.Y., Byers, J.N., Hunt, J.E., McSeveny, T.M., Meserth, R., Weir, P.L., & Schulze, E.D. (1992). Evaporation, xylem sap flow, and tree transpiration in a New Zealand broad-leaved forest. *Agricultural and Forest Meteorology*, 62, 53–73.

Die approbierte gedruckte Originalversion dieser Dissertation ist an der TU Wien Bibliothek verfügbar.
The approved original version of this doctoral thesis is available in print at TU Wien Bibliothek.

Klimešová, J., Středová, H., & Středa, T. (2014). Maize transpiration in response to meteorological conditions. *Contributions to Geophysics and Geodesy*, 43, 225–236.

Kustas, W.P. & Norman, J.M. (1996). Use of remote sensing for evapotranspiration monitoring over land surfaces. *Hydrological Sciences Journal*, 41, 495–516. https://doi.org/10.1080/02626669609491522

Kustas, W.P., Hatfield, J.L., & Prueger, J.H. (2005). The soil moisture-atmosphere coupling experiment (SMACEX): background, hydrometeorological conditions, and preliminary findings. *Journal of Hydrometeorology*, 6, 791–804.

Lai, C.T., Ehleringer, J.R., Bond, B.J., & Paw, U.K.T. (2006). Contributions of evaporation, isotopic non-steady state transpiration and atmospheric mixing on the δ18O of water vapour in Pacific Northwest coniferous forests. *Plant Cell Environment*, 29, 77–94.

Leuning, R. (2000). Estimation of scalar source/sink distributions in plant canopies using Lagrangian dispersion analysis: corrections for atmospheric stability and comparison with a multilayer canopy model. *Boundary Layer Meteorology*, 96, 293–314.

Leuning, R., van Gorsel, E., Massman, W.J., & Isaac, P.R. (2012). Reflections on the surface energy imbalance problem. *Agricultural and Forest Meteorology*, 156, 65–74.

Lian, X., Piao, S., Huntingford, C., Li, Y., Zeng, Z., Wang, X., Ciais, P., McVicar, T.R., Peng, S., Ottlé, C., Yang, H., Yang, Y., Zhang, Y., & Wang, T. (2018). Partitioning global land evapotranspiration using CMIP5 models constrained by observations. *Nature Climate Change*, 8, 640-646.

Lin, L. & Sternberg, L.,1993. Hydrogen Isotopic Fractionation by Plant Roots during Water Uptake in Coastal Wetland Plants, Stable Isotopes and Plant Carbon-water Relations, Academic Press, 497-510.

Lindroth, A., Cermák, J., Kučera, J., Cienciala, E., & Eckersten. H. (1995). Sap flow by heat balance method applied to small size Salix trees in a short-rotation forest. *Biomass and Bioenergy*, 8, 7–15.

Liu, C., Zhang, X., & Zhang, Y. (2002). Determination of daily evaporation and evapotranspiration of winter wheat and maize by large-scale weighing lysimeter and micro-lysimeter. *Agricultural and Forest Meteorology*, 111, 109–120.

Liu, S., Xu, Z., Song, L., Zhao, Q., Ge, Y., Xu, T., Ma, Y., Zhu, Z., Jia, Z., & Zhang, F. (2016). Upscaling evapotranspiration measurements from multi-site to the satellite pixel scale over heterogeneous land surfaces. *Agricultural and Forest Meteorology*, 230–231, 97–113. https://doi.org/10.1016/j.agrformet.2016.04.008

Ma, Y., Kumar, P., & Song, X. (2018). Seasonal variability in evapotranspiration partitioning and its relationship with crop development and water use efficiency of winter wheat, *Hydrological Earth Systems Science*, Discuss. [preprint], https://doi.org/10.5194/hess-2018-234, 2018.

Majoube, M. (1971). Fractionnement en oxygene-18 et en deuterium entre leau et sa vapaeur. *Journal de Chimie Physique*, 68, 1423–1436.

Mauder, M. & Foken, T. (2015). Eddy-Covariance Software TK3. In Documentation and Instruction Manual of the Eddy-Covariance Software Package TK3 (update) (p. 67). University of Bayreuth. https://doi.org/10.5281/zenodo.20349

Mauder, M., Foken, T. & Cuxart, J, (2020). Surface-Energy-Balance Closure over Land: A Review. *Boundary-Layer Meteoroogyl* **177,** 395–426. https://doi.org/10.1007/s10546-020-00529-6

Mayr, L., Aigner, M., & Heng, L. (2016). Supporting Sampling and Sample Preparation Tools for Isotope and Nuclear Analysis, Section 3.

Die approbierte gedruckte Originalversion dieser Dissertation ist an der TU Wien Bibliothek verfügbar.
The approved original version of this doctoral thesis is available in print at TU Wien Bibliothek.
TU Bibliothek Your knowledge hub WIEN

Miralles, D. G., Brutsaert, W., Dolman, A. J., & Gash, J. H. (2020). On the use of the term "evapotranspiration". *Water Resources Research*, 56, e2020WR028055. https://doi.org/10.1029/2020WR028055

Mo, X., Liu, S., Lin, Z., & Zhao, W. (2004). Simulating temporal and spatial variation of evapotranspiration over the Lushi basin. *Journal of Hydrology*, 285, 125–142. https://doi.org/10.1016/j.jhydrol.2003.08.013

Moore, C.J. (1986). Frequency response corrections for eddy correlation systems. *Boundary Layer Meteorol*ogy, 37, 17–35.

Moreira, M., Martinelli, L., Victoria, R., Barbosa, E., Bonates, L., & Nepstads, D. (1997). Contribution of transpiration to forest ambient vapour based on isotopic measurements. *Global Change Biology*, 3, 439–450.

Mu, Q., Zhao, M., Running, S.W., 2011. Improvements to a MODIS global terrestrial evapotranspiration algorithm. *Remote Sensing of Environment*, 115, 1781–1800. https://doi.org/10.1016/j.rse.2011.02.019

Overgaard, J., Rosbjerg, D., & Butts, M.B. (2005). Land-surface modelling in hydrological perspective. *Biogeosciences Discussions,* 2, 1815–1848.

Philips, D.L., & Gregg, J.W. (2001). Uncertainty in source partitioning using stable isotopes. *Oecologia*, 127, 171–179.

Prueger, J.H., Hatfield, J.L., Parkin, T.B., Kustas, W.P., Hipps, L.E., Neale, C.M.U., MacPherson, J.I., Eichinger, W.E., & Cooper, D.I. (2005). Tower and Aircraft Eddy Covariance Measurements of Water Vapor, Energy, and Carbon Dioxide Fluxes during SMACEX. *Journal of Hydrometeorology,* 6, 954–960. https://doi.org/10.1175/JHM457.1

Quade, M., Klosterhalfen, A., Graf, A., Brüggerman, N., Hermes, N., Vereecken, H., & Rothfuss, Y. (2019). In-situ monitoring of soil water isotopic composition for partitioning of evapotranspiration during one growing season of sugar beet (Beta vulgaris). *Agricultural and Forest Meteorology*, 266-267, 53-64.

Rafi, Z., Merlin, O., Le Dantec, V., Khabba, S., Mordelet, P., Er-Raki, S., Amazirh, A., Olivera-Guerra, L., Ait Hssaine, B., Simonneaux, V., Ezzahar, J., & Ferrer, F. (2019). Partitioning evapotranspiration of a drip-irrigated wheat crop: Inter-comparing eddy covariance-, sap flow-, lysimeter- and FAO-based methods. *Agricultural and Forest Meteorology*, 265, 310–326.

Rana, G. & Katerji, N. (2000). Measurement and Estimation of Actual Evapotranspiration in the Field under Mediterranean Climate: A Review. *European Journal of Agronomy*, 13, 125-153. http://dx.doi.org/10.1016/S1161-0301(00)00070-8

Raupach, M.R. (1989). Applying lagrangian fluid mechanics to infer scalar source distributions from concentration profiles in plant canopies. *Agricultural and Forest Meteorology*, 47, 85–108.

Raupach M. R., (1989b). A practical Lagrangian method for relating scalar concentrations to source distributions in vegetation canopies. *Quarterly Journal of the Royal Meteorological Society*, 115, 609–632.

Ritchie, J.T. (1972). Model for predicting evaporation from a row crop with incomplete cover. *Water Resources Research*, 8, 1204–1213.

Die approbierte gedruckte Originalversion dieser Dissertation ist an der TU Wien Bibliothek verfügbar.
The approved original version of this doctoral thesis is available in print at TU Wien Bibliothek.

Roden, J. & Ehleringer, J. (1999). Observations of hydrogen and oxygen isotopes in leaf water confirm the craig-gordon model under wide-ranging environmental conditions. *Plant Physiol*ogy, *120*, 1165–1174, https://doi.org/10.1104/pp.120.4.1165

Rothfuss, Y., Biron, P., Braud, I., Canale, L., Durand, J.L., Gaudet, J.P., Richard, P., Vauclin, M., & Bariac, T. (2010). Partitioning evapotranspiration fluxes into soil evaporation and plant transpiration using water stable isotopes under controlled conditions. *Hydrological Processes*, 24, 3177–3194.

Ruhoff, A.L., Paz, A.R., Aragao, L.E.O.C., Mu, Q., Malhi, Y., Collischonn, W., Rocha, H.R., & Running, S.W. (2013). Assessment of the MODIS global evapotranspiration algorithm using eddy covariance measurements and hydrological modelling in the Rio Grande basin. *Hydrological Sciences Journal*, 58, 1658–1676. https://doi.org/10.1080/02626667.2013.837578

Santos, E., Wagner-Riddle, C., Warland, J.S., & Brown, S. (2011). Applying a lagrangian dispersion analysis to infer carbon dioxide and latent heat fluxes in a corn canopy. *Agricultural and Forest Meteorology*, 151, 620–632.

Santos, E., Wagner-Riddle, C., Lee, X., Warland, J., Brown, S., Staebler, R., Bartlet, P., & Kim, K., (2012). Use of the isotope flux ratio approach to investigate the C18O16O and 13CO2 exchange near the floor of a temperate deciduous forest. *Biogeosciences*, 9, 2385-2399.

Schotanus, P., Nieuwstadt, F.T.M., & De Bruin, H.A.R. (1983). Temperature measurement with a sonic anemometer and its application to heat and moisture fluxes. *Boundary-Layer Meteorology*, 26, 81–93. https://doi.org/10.1007/BF00164332

Scott, R.L. (2010). Using watershed water balance to evaluate the accuracy of eddy covariance evaporation measurements for three semiarid ecosystems. *Agricultural and Forest Meteorology,* 150, 219–225. https://doi.org/10.1016/j.agrformet.2009.11.002

Seneviratne, S.I., Lehner, I., Gurtz, J., Teuling, A.J., Lang, H., Moser, U., Grebner, D., Menzel, L., Schroff, K., Vitvar, T., Zappa, M. (2012). Swiss prealpine Rietholzbach research catchment and lysimeter: 32 year time series and 2003 drought event. *Water Resources Research* 48. https://doi.org/10.1029/2011WR011749

Shiklomanov, I. A. (1998). World water resources: an appraisal for the 21st century. *IHP Report. International Hydrological Program, United Nations Educational, Scientific and Cultural Organization, Paris*.

Shimizu, T., Kumagai, T., Kobayashi, M., Tamai, K., Iida, S., Kabeya, N., Ikawa, R., Tateishi, M., Miyazawa, Y., & Shimizu, A. (2015). Estimation of annual forest evapotranspiration from a coniferous plantation watershed in Japan (2): Comparison of eddy covariance, water budget and sap-flow plus interception loss. *Journal of Hydrology,* 522, 250–264. https://doi.org/10.1016/j.jhydrol.2014.12.021

Stoy, P. C., El-Madany, T., Fisher, J. B., Gentine, P., Gerken, T., Good, S. P., Liu, S., Miralles, D. G., Perez-Priego, O., Skaggs, T. H., Wohlfahrt, G., Anderson, R. G., Jung, M., Maes, W. H., Mammarella, I., Mauder, M., Migliavacca, M., Nelson, J. A., Poyatos, R., Reichstein, M., Scott, R. L., & Wolf, S. (2019). Reviews and syntheses: Turning the challenges of partitioning ecosystem evaporation and transpiration into opportunities, *Biogeosciences*, 16, 3747–3775.

Styles, J.M., Raupach, M.R., Farquhar, G.D., Kolle, O., Lawton, K.A., Brand, W.A., Werner, R.A., Jordan, A., Schulze, E.D., Shibistova, O., & Lloyd, J. (2002). Soil and canopy CO2, (CO2)-C-13, H2O and sensible heat flux partitions in a forest canopy inferred from concentration measurements. *Tellus B: Chemical and Physical Meteorology,* 54, 655–676.

Die approbierte gedruckte Originalversion dieser Dissertation ist an der TU Wien Bibliothek verfügbar.
The approved original version of this doctoral thesis is available in print at TU Wien Bibliothek.

Sutanto, S.J., Wenninger, J., Coenders-Gerrits, A.M.J., & Uhlenbrook, S. (2012). Partitioning of evaporation into transpiration, soil evaporation and interception: A comparison between isotope measurements and a HYDRUS-1D model. *Hydrology and Earth System Sciences*, 16, 2605–2616.

Széles, B., Broer, M., Parajka, J., Hogan, P., Eder, A., Strauss, P., & Blöschl, G. (2018). Separation of Scales in Transpiration Effects on Low Flows: A Spatial Analysis in the Hydrological Open Air Laboratory. *Water Resources Research,* 54, 6168–6188. https://doi.org/10.1029/2017WR022037

Tasumi, M., Trezza, R., Allen, R.G., & Wright, J.L. (2005). Operational aspects of satellite-based energy balance models for irrigated crops in the semi-arid U.S. *Irrigation Drainage Systems*, 19, 355–376. https://doi.org/10.1007/s10795-005-8138-9

Tie, Q., Hu, H., Tian, F., & Holbrook, N.M. (2018). Comparing different methods for determining forest evapotranspiration and its components at multiple temporal scales. *Science of The Total Environment* 633, 12–29. https://doi.org/10.1016/j.scitotenv.2018.03.082

Tong, X., Li, J., Yu, Q., & Qin, Z. (2009). Ecosystem water use efficiency in an irrigated cropland in the North China Plain. *Journal of Hydrology*, 374 (3–4), 329–337.

Valayamkunnath, P., Sridhar, V., Zhao, W., & Allen, R.G. (2018). Intercomparison of surface energy fluxes, soil moisture, and evapotranspiration from eddy covariance, large-aperture scintillometer, and modeling across three ecosystems in a semiarid climate. *Agricultural and Forest Meteorology,* 248, 22–47. https://doi.org/10.1016/j.agrformet.2017.08.025

Vinukollu, R.K., Wood, E.F., Ferguson, C.R., & Fisher, J.B. (2011). Global estimates of evapotranspiration for climate studies using multi-sensor remote sensing data: evaluation of three process-based approaches. *Remote Sensing of Environment*, 115 (3), 801-823.

Walker, G.K. (1983). Measurement of evaporation from soil beneath crop canopies. *Canadian Journal of Soil Science.*, 63, 137–141.

Walker, E. & Venturini, V., (2019). Land surface evapotranspiration estimation combining soil texture information and global reanalysis datasets in Google Earth Engine. *Remote Sensing Letters*, 10, 929–938. https://doi.org/10.1080/2150704X.2019.1633487

Wang, X.F., & Yakir, D. (2000). Using stable isotopes of water in evapotranspiration studies. *Hydrological Processes*, 14, 1407-1421.

Wang, L., Niu, S., Good, S.P., Soderberg, K., McCabe, M.F., Sherry, R.A., Luo, Y., Zhou, X., Xia, J., & Caylor, K.K. (2013). The effect of warming on grassland evapotranspiration partitioning using laser-based isotope monitoring techniques. *Geochimica et Cosmochimica Acta*, 111, 28–38.

Warland, J.S., & Thurtell, G.W. (2000). A Lagrangian solution to the relationship between a distributed source and concentration profile. *Boundary-Layer Meteorology,* 96, 453–471.

Webb, E.K., Pearman, G.I., & Leuning, R. (1980). Correction of flux measurements for density effects due to heat and water vapour transfer. *Quarterly Journal of the Royal Meteorological Society,* 106, 85–100. https://doi.org/10.1002/qj.49710644707

Wei, Z., Yoshimura, K., Okazaki, A., Kim, W., Liu, Z., & Yokoi, M. (2015). Partitioning of evapotranspiration using high-frequency water vapour isotopic measurement over a rice paddy field: Partitioning of evapotranspiration. *Water Resources Research*, 51, 3716–3729.

Weisman M.L., & Klemp J.B. (1986). Characteristics of isolated convective storms. Ray PS (ed.) *Mesoscale Meteorology and Forecasting*, ch. 15, 331–358. Boston, MA: American Meteorological Society.

Die approbierte gedruckte Originalversion dieser Dissertation ist an der TU Wien Bibliothek verfügbar.
The approved original version of this doctoral thesis is available in print at TU Wien Bibliothek.

Welp, L.R., Lee, X., Kim, K., Gris, T.J., Billmark, K.A., & Baker, J.M. (2008). $\delta^{18}O$ of water vapor, evapotranspiration and the sites of leaf water evaporation in a soybean canopy. *Plant Cell Environment*, 31, 1214–1228.

Williams, D., Cable, W., Hultine, K., Hoedjes, J., Yepez, E., Simonneaux, V., Er-Raki, S., Boulet, G., de Bruin, H., Chehbouni, A. et al. (2004). Evapotranspiration components determined by stable isotope, sap flow and eddy covariance techniques. *Agricultural and Forest Meteorology*, 125, 241–258.

Wilson, K.B., Hanson, P.J., Mulholland, P.J., Baldocchi, D.D., & Wullschleger, S.D. (2001). A comparison of methods for determining forest evapotranspiration and its components: sap-flow, soil water budget, eddy covariance and catchment water balance. *Agricultural and Forest Meteorology,* 106, 153–168. https://doi.org/10.1016/S0168-1923(00)00199-4

Wilson, K., Goldstein, A., Falge, E., Aubinet, M., Baldocchi, D., Berbigier, P., Bernhofer, C., Ceulemans, R., Dolman, H., Field, C., Grelle, A., Ibrom, A., Law, B.E., Kowalski, A., Meyers, T., Moncrieff, J., Monson, R., Oechel, W., Tenhunen, J., Valentini, R., & Verma, S. (2002). Energy balance closure at FLUXNET sites. *Agricultural and Forest Meteorology*, 113, 223–243. https://doi.org/10.1016/S0168-1923(02)00109-0

Wu, Y., Du, T., Ding, R., Tong, L., Li, S., & Wang, L. (2016). Multiple Methods to Partition Evapotranspiration in a Maize Field. *Journal of Hydrometeorology*, 18(1), 139–149.

Xiao, W., Wei, Z., & Wen, X. (2018). Evapotranspiration partitioning at the ecosystem scale using the stable isotope method—A review. *Agricultural and Forest Meteorology,* 263, 346–361.

Xu, C., Gong, L., Jiang, T., Chen, D., & Singh, V.P. (2006). Analysis of spatial distribution and temporal trend of reference evapotranspiration and pan evaporation in Changjiang (Yangtze River) catchment. *Journal of Hydrology*, 327, 81–93. https://doi.org/10.1016/j.jhydrol.2005.11.029

Yakir, D. & Sternberg, L. (2000). The use of stable isotopes to study ecosystem gas exchange. *Oecologia*, 123, 297–311.

Yepez, E.A., Williams, D.G., Scott, R.L. & Lin, G. (2003). Partitioning overstory and understory evapotranspiration in a semiarid savanna woodland from the isotopic composition of water vapor. *Agricultural and Forest Meteorology*, 119, 53–68.

Yepez, E.A., Huxman, T.E., Ignace, D.D., English, N.B., Weltzin, J.F., Castellanos, A.E. & Williams, D.G. (2005). Dynamics of transpiration and evaporation following a moisture pulse in semiarid grassland: A chamber-based isotope method for partitioning flux components. *Agricultural and Forest Meteorology*, 132, 359–376.

Zhang, S., Wen, X., Wang, J., Yu, G. & Sun, X. (2010). The use of stable isotopes to partition evapotranspiration fluxes into evaporation and transpiration. *Acta Ecologica Sinica*, 30, 201–209.

Zhang, X., Kang, S., Zhang, L., & Liu, J. (2010). Spatial variation of climatology monthly crop reference evapotranspiration and sensitivity coefficients in Shiyang river basin of northwest China. *Agricultural Water Management*, 97, 1506–1516. https://doi.org/10.1016/j.agwat.2010.05.004

Zhang, Y., Shen, Y., Sun, H. & Gates, J. (2011). Evapotranspiration and its partitioning in an irrigated winter wheat field. A combined isotopic and micrometeorologic approach. *Journal of Hydrology*, 408, 203–211.

Zhang, Z., Tian, F., Hu, H., & Yang, P. (2014). A comparison of methods for determining field evapotranspiration: photosynthesis system, sap flow, and eddy covariance. *Hydrology and Earth System Sciences*, 18, 1053–1072. https://doi.org/10.5194/hess-18-1053-2014

Die approbierte gedruckte Originalversion dieser Dissertation ist an der TU Wien Bibliothek verfügbar.
The approved original version of this doctoral thesis is available in print at TU Wien Bibliothek.
TU Bibliothek Your knowledge hub WIEN

Zhao, L., He, Z., Zhao, W. & Yang, Q. (2016). Extensive investigation of the sap flow of maize plants in an oasis farmland in the middle reach of the Heihe River, Northwest China. *Journal of Plant Res*ources, 129, 841–851.

Zhou, L., Wang, Y., Jia, Q., Li, R., Zhou, M. & Zhou, G. (2019). Evapotranspiration over a rainfed maize field in northeast China: How are relationships between the environment and terrestrial evapotranspiration mediated by leaf area? *Agricultural Water Management*, 221, 538–546. https://doi.org/10.1016/j.agwat.2019.05.026

Zhou, S., Liu, W. & Lin, W. (2017). The ratio of transpiration to evapotranspiration in a rainfed maize field on the *Loess Plateau* of China. *Water Sciences & Technology Water Supply*, 17, 221–228.

Die approbierte gedruckte Originalversion dieser Dissertation ist an der TU Wien Bibliothek verfügbar.
The approved original version of this doctoral thesis is available in print at TU Wien Bibliothek.

TU Bibliothek Your knowledge hub
Die approbierte gedruckte Originalversion dieser Dissertation ist an der TU Wien Bibliothek verfügbar.
The approved original version of this doctoral thesis is available in print at TU Wien Bibliothek.